DATA DRIVEN MODEL DISCOVERY AND CONTROL OF LONGITUDINAL MISSILE DYNAMICS

A THESIS SUBMITTED TO
THE GRADUATE SCHOOL OF NATURAL AND APPLIED SCIENCES
OF
MIDDLE EAST TECHNICAL UNIVERSITY

BY

HASAN MATPAN

IN PARTIAL FULFILLMENT OF THE REQUIREMENTS
FOR
THE DEGREE OF MASTER OF SCIENCE
IN
MECHANICAL ENGINEERING

SEPTEMBER 2021

Approval of the thesis:

DATA DRIVEN MODEL DISCOVERY AND CONTROL OF LONGITUDINAL MISSILE DYNAMICS

submitted by **HASAN MATPAN** in partial fulfillment of the requirements for the degree of **Master of Science** i**n Mechanical Engineering, Middle East Technical University** by,

Prof. Dr. Halil Kalıpçılar
Dean, Graduate School of **Natural and Applied Sciences** _____

Prof. Dr. M. A. Sahir Arıkan
Head of the Department, **Mechanical Engineering** _____

Assoc. Prof. Dr. A. Buğra Koku
Supervisor, **Mechanical Engineering** _____

Examining Committee Members:

Assoc. Prof. Dr. Yiğit Yazıcıoğlu
Mechanical Engineering, METU _____

Assoc. Prof. Dr. A. Buğra Koku
Mechanical Engineering, METU _____

Assoc. Prof. Dr. Mehmet Bülent Özer
Mechanical Engineering, METU _____

Assist. Prof. Dr. Ali Emre Turgut
Mechanical Engineering, METU _____

Prof. Dr. Duygun Erol Barkana
Electrical and Electronics Eng., Yeditepe Uni. _____

Date: 07.09.2021

I hereby declare that all information in this document has been obtained and presented in accordance with academic rules and ethical conduct. I also declare that, as required by these rules and conduct, I have fully cited and referenced all material and results that are not original to this work.

Name, Surname: Hasan Matpan

Signature:

ABSTRACT

DATA DRIVEN MODEL DISCOVERY AND CONTROL OF LONGITUDINAL MISSILE DYNAMICS

Matpan, Hasan
Master of Science, Mechanical Engineering
Supervisor: Assoc. Prof. Dr. A. Buğra Koku

September 2021, 105 pages

Dynamical systems in nature are generally nonlinear and usually contains many hidden dynamics. Therefore, the need for data-driven model discovery and control methods continues. The most popular of these methods is neural networks-based methods nowadays. However, excessive data requirements, long training times and most importantly lack of interpretability of results are the main problems in neural networks-based system identification methods. Among the many other methods used for model discovery, SINDY (Sparce Identification of Non-linear Dynamical Systems) has recently attracted great attention with its simple and effective nature. SINDY, which has many extensions, also has various open problems.

The proposed extension in this study is called SINDY-SAIC and combines the methods from Stepwise Sparse Regression (SSR) and Akaike Information Criteria (AIC) model selection algorithm. The need for tuning threshold parameter in SINDY is relaxed using SSR and the robustness to noisy measurements is increased with a newly used state derivative calculation method in sparse regression. In addition, presence of model selection with AIC enables sparse solution by penalizing the number of terms and prevents the algorithm to converge collinear basis.

Studied dynamical systems are controlled by Model Predictive Control using discovered models. MPC is a control method that uses prediction models mostly discovered from data and try to minimize a given cost function subjected to the constraints. Both linear and nonlinear prediction models are generated using SINDY-SAIC and used in MPC as prediction models. The traditional state feedback (SF) controller is also presented for comparison.

The proposed SINDY-SAIC algorithm and the controllers (MPC and SF) are tested for linear and highly non-linear longitudinal missile dynamics under moderate and high level of noise conditions.

Keywords: SINDY, AIC, Model Discovery, System Identification, Sparse Regression, Model Selection, Model Predictive Control (MPC), State Feedback Control, Missile Dynamics

ÖZ

FÜZE DİNAMİK MODELİNİN VERİ TABANLI YÖNTEMLER İLE KESTİRİMİ VE KONTROLÜ

Matpan, Hasan
Yüksek Lisans, Makine Mühendisliği
Tez Danışmanı: Doç. Dr. A. Buğra Koku

Eylül 2021, 105 sayfa

Doğada bulunan dinamik sistemler genellikle doğrusal değildirler ve bazı gizli dinamikler içerirler. Bu nedenle veri tabanlı model kestirimi ve kontrol yöntemlerine olan ihtiyaç hala devam etmektedir. Bu yöntemler arasında günümüzde en tanınmış olanı yapay sinir ağı tabanlı sistem tanımlama yöntemleridir. Ancak aşırı miktarda veri ihtiyacı, uzun eğitim süreleri ve en önemlisi sonuçların yorumlanma zorluğu bu yöntemlerin temel problemlerindendir. Model dinamiğinin bulunması için kullanılan diğer birçok yöntem arasında SINDY, yalın ve verimli yapısı ile son zamanlarda büyük ilgi görmektedir. Birçok türeve sahip olan SINDY algoritmasının hala çözülmemiş bazı problemleri de bulunmaktadır.

Bu çalışmada önerilen algoritma SINDY-SAIC olarak adlandırılmıştır ve Adımsal Seyrek Regresyon (SSR) ile Akaike Bilgi Kriterleri (AIC) model seçiminden gelen yöntemleri birleştirmektedir. SSR kullanılarak eşik parametresinin ayarlanması ihtiyacı azaltılmıştır ve seyrek regresyonda ilk kez kullanılan bir durum türevi hesaplama yöntemi ile gürültülü ölçümlere karşı dayanım artırılmıştır. Ayrıca AIC ile model seçiminin varlığı, terim sayısını cezalandırarak seyrek çözüme olanak tanımakta ve algoritmanın eşdoğrusal çözümlere yakınmasını engellemektedir.

İncelenen dinamik sistemler, keşfedilen modeller kullanılarak Model Öngörülü Kontrol (MPC) ile kontrol edilmiştir. MPC, çoğunlukla veri tabanlı model kestirimi yöntemleri ile oluşturulan tahmin modellerini kullanan ve kısıtlamalara tabi belirli bir maliyet fonksiyonunu en aza indirmeye çalışan bir kontrol yöntemidir. Bu çalışmada hem doğrusal hem de doğrusal olmayan tahmin modelleri SINDY-SAIC kullanılarak oluşturulmuştur ve MPC algoritmasında tahmin modelleri olarak kullanılmıştır. Karşılaştırma yapabilmek için geleneksel Durum Geri Besleme (SF) kontrolcüsüne ait sonuçlar da sunulmuştur.

Önerilen SINDY-SAIC algoritması ve kontrol yöntemleri (MPC ve SF), orta ve yüksek seviyede gürültü koşulları altında doğrusal ve yüksek seviyede doğrusal olmayan füze dinamik modelleri ile test edilmiştir.

Anahtar Kelimeler: SINDY, AIC, Model Kestirimi, Sistem Tanımlama, Regresyon, Model Seçimi, Model Öngörülü Kontrol, Durum Geri Besleme Kontrolü, Füze Dinamiği

To my family

ACKNOWLEDGEMENTS

I would like to thank to my thesis supervisor Assoc. Prof. Dr. A. Buğra Koku for his advice and invaluable support all throughout the study. In addition to his academic guidance, I am also deeply grateful to him for constantly encouraging his students to think differently.

Next, I would like to thank to Assoc. Prof. Dr. Yiğit Yazıcıoğlu, Assoc. Prof. Dr. Mehmet Bülent Özer, Assist. Prof. Dr. Ali Emre Turgut and Prof. Dr. Duygun Erol Barkana who were my thesis committee members for their valuable support and feedbacks.

I would also like to thank to my colleagues and managers at ROKETSAN, who helped me gain experience and supported me in every way.

Finally, I would like to thank my mother, sister and brother who always believed and supported me.

TABLE OF CONTENTS

ABSTRACT v

ÖZ… vii

ACKNOWLEDGEMENTS x

TABLE OF CONTENTS xi

LIST OF TABLES xiv

LIST OF FIGURES xvi

LIST OF ABBREVIATIONS xx

CHAPTERS

1. INTRODUCTION 1

1.1. System Identification 1

1.2. Thesis Statement 5

2. SPARSE IDENTIFICATION OF DYNAMICAL SYSTEMS 7

2.1. Dynamical Systems and Measurement Data 7

2.2. Regression on Over Determined Systems 8

2.3. Sparsity Promoting Algorithms 9

2.4. Overfitting and Underfitting 11

2.5. Cross Validation 11

2.6. Model Selection 12

2.7. SINDY-SAIC Method for Nonlinear System Identification 15

3. MODEL PREDICTIVE CONTROL 21

3.1. Working Principle of MPC 21

3.2. MPC Design Parameters 22

3.2.1. Sample Time (Ts) 23
3.2.2. Prediction Horizon (Hp) 23
3.2.3. Control Horizon (Hm) 24
3.2.4. Constraints 24
3.2.5. Weights 24
3.3. Prediction Formulation and Solution of MPC Problems 25
3.3.1. Prediction Formulation 25
3.3.2. Solution of MPC Problem 28
3.4. MPC Framework with SINDY-SAIC Algorithm and Integral Action 30
4. MISSILE DYNAMIC MODEL AND STATE FEEDBACK CONTROL 33
4.1. Longitudinal Missile Dynamics 33
4.2. State Feedback Control 37
5. NUMERICAL RESULTS 41
5.1. Prediction Comparison 41
5.1.1. Linear Missile Dynamics - Longitudinal 41
5.1.1.1. Clean State (x) - Clean Derivative (dx) Case 44
5.1.1.2. Noisy State (x) - Derivative (dx) Calculated from Noisy Data 47
5.1.2. Highly Nonlinear Missile Dynamics – Longitudinal 56
5.1.2.1. Clean State (x) - Clean Derivative (dx) Case 58
5.1.2.2. Noisy State (x) - Derivative (dx) Calculated from Noisy Data 62
5.1.3. Comparison of SINDY-SAIC with Sequential Threshold Least Square SINDY (SINDY-T) Algorithm 69
5.2. Control Performance Comparison 72
5.2.1. Control Performance Comparison for Linear Missile Model 73

5.2.1.1. Control of Linear Missile Model Discovered from Clean Data.....75

5.2.1.2. Control of Linear Missile Model Discovered from Noisy Data 80

5.2.2. Control Performance Comparison for Non-Linear Missile Model.....86

5.2.2.1. Control of Non-Linear Missile Model Discovered from Clean Data 88

5.2.2.2. Control of Non-Linear Missile Model Discovered from Noisy Data 94

6. DISCUSSION.....101

REFERENCES.....103

LIST OF TABLES

TABLES

Table 4.1. Definitions for missile equations of motion 36
Table 5.1. Candidate models that SINDY generates. 44
Table 5.2. RMSE values for training and test data (clean measurements) 47
Table 5.3. Noise levels for Linear Missile Dynamics 48
Table 5.4. Candidate models that SINDY generates (moderate noise level) 49
Table 5.5. RMSE values for training and test data (moderate noise) 52
Table 5.6. True and discovered model for high level of noise 53
Table 5.7. RSME values for high level of noise 55
Table 5.8. Candidate models that SINDY generates for $x1$ (clean data) 59
Table 5.9. Candidate models that SINDY generates for $x2$ (clean data) 59
Table 5.10. RMSE values for training and test data 62
Table 5.11. Noise levels for Non-Linear Missile Dynamics 63
Table 5.12. Candidate models that SINDY generates for $x1$ (moderate noise level) 64
Table 5.13. Candidate models that SINDY generates for $x2$ (moderate noise level) 64
Table 5.14. RMSE values for training and test data (moderate noise level) 67
Table 5.15. True and discovered model for high level of noise 67
Table 5.16. RSME values for high level of noise 69
Table 5.17. Comparison of SINDY methods for $x1$ 70
Table 5.18. Comparison of SINDY methods for $x2$ 71
Table 5.19. RSME values of SINDY methods 71
Table 5.20. Discovered models using SINDY 73
Table 5.21. MPC design parameters for linear system 73
Table 5.22. SF design parameters 74
Table 5.23. Performance Metrics of MPC and SF for Different ICs 79

Table 5.24. Performance Metrics of MPC and SF for Different ICs 84
Table 5.25. Discovered models using SINDY 87
Table 5.26. MPC design parameters for linear system 87
Table 5.27. SF design parameters 88
Table 5.28. Performance Metrics for Different ICs 93
Table 5.29. Performance Metrics for Different ICs 99

LIST OF FIGURES

FIGURES

Figure 2.1. The shape of matrices for overdetermined system 9
Figure 2.2. Over-fitting and Under-fitting [25] 11
Figure 2.3. Procedure for k-fold cross validation [25] 12
Figure 2.4. Model error vs model complexity [26] 13
Figure 2.5. Sample AIC score with increasing model complexity 15
Figure 2.6. Schematic of SINDY-SAIC algorithm 16
Figure 3.1. MPC working principle [26] 22
Figure 3.2. Schematic of SINDY-SAIC and MPC framework 30
Figure 3.3. Schematic of integral action in MPC 31
Figure 3.4. Output of non-linear function for different gain values [34] 32
Figure 4.1. State Feedback Controller Structure [36] 37
Figure 5.1. Control Input (u) 42
Figure 5.2. Angle of Attack (x_1) 43
Figure 5.3. Pitch Rate (x_2) 43
Figure 5.4. AIC scores of the candidate models (the figure on the right is zoomed for better readability) 45
Figure 5.5. Prediction over **training data** of SINDY vs true model for clean measurements 45
Figure 5.6. Prediction over **test data** of SINDY for clean measurements of states .. 46
Figure 5.7. Control Input u for the Test Data 46
Figure 5.8. State measurements with and without noise 47
Figure 5.9. AIC scores of the candidate models (the figure on the right is zoomed for better readability) 50
Figure 5.10. Prediction over **training data** of SINDY vs true model for noisy measurements of states and calculated derivatives 51

Figure 5.11. Prediction over **test data** of SINDY vs true model for noisy measurements of states.....52
Figure 5.12. State measurements with different noise levels.....53
Figure 5.13. Prediction over **training data** of SINDY vs true model for high level of noise 54
Figure 5.14. Prediction over **test data** of SINDY vs true model for high level of noise 55
Figure 5.15. Control Input (u).....57
Figure 5.16. Angle of Attack (x_1) 57
Figure 5.17. Pitch Rate (x_2).....58
Figure 5.18. AIC scores of the candidate models (the figure on the right is zoomed for better readability) 60
Figure 5.19. Prediction over **training data** of SINDY vs true model for clean measurements of states and derivatives 61
Figure 5.20. Prediction over **test data** of SINDY for clean measurements of states 61
Figure 5.21. Control Input u for the Test Data.....62
Figure 5.22. State measurements with and without noise.....63
Figure 5.23. AIC scores of the candidate models (the figure on the right is zoomed for better readability) 65
Figure 5.24. Prediction over **training data** of SINDY vs true model for noisy measurements of states and calculated derivatives 66
Figure 5.25. Prediction over **test data** of SINDY vs true model for noisy measurements of states.....66
Figure 5.26. Prediction over **training data** of SINDY vs true model for high level of noise 68
Figure 5.27. Prediction over **test data** of SINDY vs true model for high level of noise 69
Figure 5.28. Open loop response for $x0 = [0\ 0]$ and $x0 = [5\ 15]$ 74
Figure 5.29. Angle of attack results for $x0 = [0\ 0]$.....75
Figure 5.30. Pitch rate results for $x0 = [0\ 0]$ 75

Figure 5.31. Delta results for $x0 = [0\ 0]$ 76
Figure 5.32. Delta dot results for $x0 = [0\ 0]$ 76
Figure 5.33. Angle of attack results for $x0 = [5\ 15]$ 77
Figure 5.34. Angle of attack results for $x0 = [5\ 15]$ 77
Figure 5.35. Angle of attack results for $x0 = [5\ 15]$ 78
Figure 5.36. Angle of attack results for $x0 = [5\ 15]$ 78
Figure 5.37. Angle of attack results for $x0 = [0\ 0]$ 80
Figure 5.38. Pitch rate results for $x0 = [0\ 0]$ 80
Figure 5.39. Delta results for $x0 = [0\ 0]$ 81
Figure 5.40. Delta dot results for $x0 = [0\ 0]$ 81
Figure 5.41. Angle of attack results for $x0 = [5\ 15]$ 82
Figure 5.42. Angle of attack results for $x0 = [5\ 15]$ 82
Figure 5.43. Angle of attack results for $x0 = [5\ 15]$ 83
Figure 5.44. Angle of attack results for $x0 = [5\ 15]$ 83
Figure 5.45. Angle of attack results for $x0 = [0\ 0]$ 85
Figure 5.46. Angle of attack results for $x0 = [5\ 15]$ 85
Figure 5.47. Angle of attack results for $x0 = [0\ 0]$ 88
Figure 5.48. Pitch rate results for $x0 = [0\ 0]$ 89
Figure 5.49. Delta results for $x0 = [0\ 0]$ 89
Figure 5.50. Delta dot results for $x0 = [0\ 0]$ 90
Figure 5.51. Angle of attack results for $x0 = [5\ 15]$ 91
Figure 5.52. Pitch rate results for $x0 = [5\ 15]$ 91
Figure 5.53. Delta results for $x0 = [5\ 15]$ 92
Figure 5.54. Delta dot results for $x0 = [5\ 15]$ 92
Figure 5.55. Angle of attack results for $x0 = [0\ 0]$ 94
Figure 5.56. Pitch rate results for $x0 = [0\ 0]$ 95
Figure 5.57. Delta results for $x0 = [0\ 0]$ 95
Figure 5.58. Delta dot results for $x0 = [0\ 0]$ 96
Figure 5.59. Angle of attack results for $x0 = [5\ 15]$ 97

Figure 5.60. Pitch rate results for $x0 = [5\ 15]$ 97
Figure 5.61. Delta results for $x0 = [5\ 15]$.....98
Figure 5.62. Delta dot results for $x0 = [5\ 15]$.....98

LIST OF ABBREVIATIONS

ABBREVIATIONS

AIC	Akaike Information Criteria
CE	Control Expenditure
CL	Closed Loop
CPU	Central Processing Unit
CRE	Control Rate Expenditure
DL	Deep Learning
DOF	Degree of Freedom
FPGA	Field Programmable Gate Array
GPU	Graphics Processing Unit
KL	Kullback-Leibler
LS	Least Square
MPC	Model Predictive Control
NN	Neural Networks
RSS	Residual Sum of Squares
SF	State Feedback
SINDY	Sparse Identification of Nonlinear Dynamical System
SSR	Stepwise Sparse Regression
TE	Tracking Error

CHAPTER 1

INTRODUCTION

This chapter will provide general information about system identification (SI) or model discovery. Commonly used SI methods will be described and compared in terms of data requirements, speed of convergence and interpretability. Finally, a brief introduction of the proposed model discovery method will be given.

1.1. System Identification

The identification of dynamical systems attracts great attention in many fields, such as engineering, biology, and finance. Obtaining the terms and coefficients in governing equation of a dynamic system is very important to predict the future behavior of this system. In addition to prediction, system identification plays an important role in understanding the nature of the system and detection of errors. It is also easier to control a system whose behavior is adequately determined. For these reasons, various methods have been studied to identify dynamical systems.

Studies in which the relationship between input and output is determined as a black box model frequently draw attention. The most common and popular of these methods is neural networks-based methods. System identification and control of an aerobatic helicopter are studied using fully connected neural networks in [1] and convolutional neural networks in [2]. Long execution times, need for large amount of data and lack of interpretability of results are the main issues in these studies. If enough data is available, in theory, it is possible to model any dynamical system with a deep neural network [3], [4]. These methods usually require large amount of data and training time. Therefore, they are usually used offline. Thanks to the rapid development of deep learning (DL) architectures, networks have a very high predictive capacity. However, since it is a black box method, it cannot give much information about the

inherent structure of the dynamic system. Another problem related to the DL system identification methods is lacking of any guarantees on convergence especially in low data limit [5].

Recently, physics informed neural networks are gaining attention in system identification community. This method attempts to reduce the problem of black box nature of neural network by incorporating physical law into the cost function formulation [5]. However, the need for long training periods remains. Another type of physics informed neural networks called structured neural network (SNN) [6], [7] are also proposed to deal with training issues in classic neural network architectures. The main idea of SNN is based on the divide-and-conquer approach. In other words, prior knowledge of the system is used to break down the identification problem into its basic components. Several small networks are then designed to solve these fundamental problems and are eventually combined to come up with a general solution. There are several approaches and still issues for improvement in this area.

Another method used in system identification is the newly popular Koopman based predictors. Koopman B. O. proposed his method in 1931 [8] . So far, many developments and applications are studied [9], [10]. The theory behind this method states that a nonlinear system appears linear in an infinite-dimensional space after passing through some observer functions [11]. In other words, some observer functions are tried to be found that will transform or lift the data into this high dimensional space in which systems becomes linear. With these observer functions and Koopman matrix, the system can be advanced over time with a linear model. In this way, both the system identification is performed, and the non-linear system is transformed to a linear model. Therefore, standard linear control theory can be applied to the identified linear model. The most important problem in Koopman based SI methods is that it is not known how to determine the observer functions. Polynomials [12], basis functions [13] and neural networks are mostly used to determine these functions. Although neural networks have great potential to find observer functions, a general solution for different dynamical systems has not been achieved yet. A lot of

work is still being done on this subject. In [14], very successful implementation of encoder-decoder type network for determining observer functions is performed, although the issue for generalizability still exists. Network structure requires lots of adaptation which is highly problem dependent. In general, since it is not very practical to determine observer functions in infinite dimensional space, the aim of Koopman based techniques is to find an accurate approximation in which the system behaves acceptably linear.

Another system identification method is called SINDY that is based on sparse regression. In this method, a non-linear function library is prepared, and sparse regression is performed to ensure that the system is represented with this library functions. In this way, the equations and coefficients governing the dynamic system are determined.

SINDY has some advantages over NN based system identification methods. SINDY is not a black box model like neural networks, so it is possible to study and interpret the system behavior in detail. Also compared to neural networks, SINDY is much faster to train and requires much less data [15]. The advantages of SINDY over Koopman-based SI methods can be expressed as that SINDY does not have hard-to-detect observer functions like Koopman. Also, SINDY finds a much more explicit and interpretable form of the dynamic system than Koopman [16]. The main issues in SINDY type SI techniques are as follows. At first, calculation of the state derivatives with enough precision is required for almost all extensions of SINDY. Secondly, an effective method of solving regression problem is crucial. Lastly, selecting the best model from among possible candidates is very important. So far, various studies are performed to overcome these problems.

In [17], L^1 regularized least-square minimization is used to discover unknown dynamics. The method gives accurate results under the assumption that state derivatives are measured accurately and then noise is added to the state derivatives after. However, in real life scenarios, generally states are measured with noise and

state derivatives are calculated from noisy state measurements. Therefore, a robust method to calculate state derivatives from noisy data is required.

The most popular SINDY implementation is given in [18] and abbreviated as SINDY-T throughout this thesis. In related work, “sequential thresholded least-square algorithm” is used to solve the regression problem. This is an iterative algorithm, that is, initially coefficients of the unknown dynamical system are found by standard least-square solution without any regularization. Then the coefficients smaller than some cut-off value are thresholded. Next, using the remaining active terms, new least-square solution is obtained for non-zero indices. This new solution is thresholded again. This procedure is repeated until all the coefficients are above the threshold value. Finally, the coefficients of the unknown dynamical system are obtained. The algorithm is more efficient and simpler than the previous regression type SI methods and convergences to a sparse solution rapidly. However, in cases where a suitable threshold value cannot be determined, it may be necessary to run the algorithm multiple times for different threshold values. This negatively affects the execution time.

Another extension of SINDY framework called SINDY-PI (SINDY Parallel Implicit) is in given in [19]. This approach is used to identify a dynamical system including partial derivatives and rational functions. The main difference from standard SINDY is that SINDY-PI considers every candidate function as a possible solution of regression equations and solve multiple optimization algorithms in parallel. Noise robustness of this extension is better than SINDY-I algorithm [20] which is developed to identify the dynamical systems including rational function.

The final SINDY extension examined is called Stepwise Sparse Regression (SSR) algorithm [21]. It is inspired by SINDY-T algorithm in the original SINDY study [18]. In SSR, thresholding approach is modified to remove only one coefficient per iteration to enforce sparsity. This modification eliminates the need of searching a threshold parameter and has the best accuracy and rate of convergence performance among the other SINDY applications. However, absence of model selection that penalizes the

number of terms result in solutions that are not sparse enough. Therefore, it is seen that algorithm may converge to non-sparse collinear basis depending on the library selection.

1.2. Thesis Statement

Many dynamical systems in nature are nonlinear and contain many uncertainties. Therefore, there is always a need for a data-driven model discovery and control methods for dynamic systems specialists. The most common and popular of these methods is neural networks-based methods. Long execution times, need for large amount of data and lack of interpretability of results are the main issues in neural networks-based SI methods. Among the many other methods used for system identification, SINDY has recently attracted great attention with its simple and effective nature. SINDY, which has many extensions, also has various open problems.

Instead of commonly used sequential thresholded SINDY-T, in this study an existing but rarely used sparsity promoting technique called “Stepwise Sparse Regression (SSR)” is used with AIC model selection algorithm. The proposed extension is called SINDY-SAIC and combines the methods from SSR [21] and AIC (Akaike information criteria) model selection [22], [23]. Shortly, in SINDY-SAIC, the safely determined expected number of terms (n) in the dynamical systems are used as threshold for regression to promote sparsity. Hence, SINDY-SAIC produces n candidate models that includes number of active terms ranging from 1 to n. Then, the best model is selected using AIC scores of the candidate models.

SINDY-SAIC does not require tuning of any threshold parameter as in the case of SINDY-T and state derivatives are estimated using a sliding window approach which improves the performance of model discovery over the traditional total variational regularization [24] . In addition, presence of model selection with AIC enables sparse solution by penalizing the number of terms and prevents the algorithm to converge to

collinear basis. Hence, SINDY-SAIC has speed and accuracy advantages over previously studied SINDY extensions.

In addition, the dynamical system is controlled by Model Predictive Control (MPC) using discovered models. MPC is a control method that uses short-term predictions using approximate system model to minimize a given cost function subjected to constraints. Both linear and nonlinear models are prepared for MPC. Traditional state feedback (SF) controller is also presented for comparison.

The proposed SINDY-SAIC algorithm and the controllers (MPC and SF) are tested for linear and highly non-linear longitudinal missile dynamics under moderate and high level of noise conditions.

CHAPTER 2

SPARSE IDENTIFICATION OF DYNAMICAL SYSTEMS

In this chapter, general form of the dynamical system equations and the type of regression methods used for model discovery will be presented. Cross validation and AIC algorithm that are used to select the best model among candidates will be explained. Finally, proposed SINDY extension will be presented.

2.1. Dynamical Systems and Measurement Data

$$\frac{d}{dt}x(t) = f(x(t), u) \tag{2-1}$$

Almost all the dynamical systems exist in nature have some degree of nonlinearity and can be defined as Eqn. (2-1) where x is the state, u is the control input of the system, and f is the non-linear function that possibly depends on x and u. The non-linearity in some dynamical systems may be quite low whereas, many other dynamical systems are highly nonlinear. However, the common feature of real dynamical systems is that their mathematical models usually have a simple and sparse form at least on an appropriate basis. Therefore, it may be possible to extract simple yet accurate mathematical models using a suitable system identification method.

The data required by the system identification methods are measured by means of various sensors on these systems. By using measurement data and the specified library functions, the system identification problem is transformed into a linear regression problem with the SINDY algorithm.

The measurement data is often not completely clean and contains some amount of noise. The amount of noise affects the system identification performance. Every system identification method has a noise upper limit at which it fails.

In the case of SINDY, noise affects system identification performance in two ways. First, noise complicates taking the derivative of measurements. Secondly, the solution of the regression problem becomes more difficult. For this reason, it is required to increase the noise robustness of the solution with various methods.

2.2. Regression on Over Determined Systems

Regression has long been used to solve a set of linear equations. However, in modern data science, this set of linear equations is generally over or under determined and has no analytical solution. Instead, various optimization methods are used to find an approximate solution.

The idea of regression can be stated as fitting a model to data using some parameters. Generally, regression is formulated as given in Eqn. (2-2) and is treated as a least square fitting problem.

$$Ax = b \tag{2-2}$$

As stated, lots of the system in nature is over or under-determined systems. In an over determined system, the number of equations is larger than the number of unknows (tall skinny system matrix A in Figure 2.1) and therefore the set of equations given in Eqn. (2-2) cannot be satisfied in general. Instead, it is tried to solve the optimization problem given in Eqn. (2-3). The error to be minimized to find an appropriate value of $\hat{x}$ is generally selected as the least square error (L_2) due to the inexpensive optimization cost [25].

$$\hat{x} = argmin_x \|Ax - b\|_2 \tag{2-3}$$

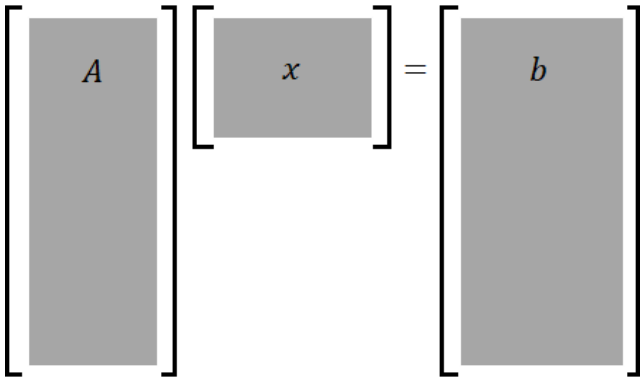

Figure 2.1. The shape of matrices for overdetermined system

In general, solution architecture given in Eqn. (2-3) does not give satisfactory results without any constraint on the solution of x. Therefore, optimization formulation is modified to enforce both minimizing the least square error and satisfying the constraint on the x. Parameters λ_1 and λ_2 given in Eqn. (2-4) are the penalization of the L_1 and L_2 norms, respectively.

$$\hat{x} = argmin_x(\|Ax - b\|_2 + \lambda_1\|x\|_1 + \lambda_2\|x\|_2) \tag{2-4}$$

The terms including $\lambda_{1,2}$ and $L_{1,2}$ norms are called regularization in machine learning literature. Some form of regularization is required and very important for model selection, which will be discussed in following section.

2.3. Sparsity Promoting Algorithms

In order to solve overdetermined regression problems, some form of regularization should be used to promote sparsity in the solution. The commonly used sparsity promoting methods are L_1 (Lasso), L_2 (Ridge) and Elastic Net regularizations.

In Ridge regression, the penalty term equivalent to square of the magnitude of coefficients is added to regression equation that is term λ_2 in Eqn. (2-4) becomes non-

zero and λ_1 is zero. On the other hand, in Lasso regression, λ_2 in Eqn. (2-4) are set to zero and λ_1 is non-zero. In Elastic Net regression, both λ_1 and λ_2 are non-zero in Eqn. (2-4).

Furthermore, "sequential threshold least square algorithm" proposed by [18] is another powerful sparsity promoting algorithm which is an extension of hard thresholded regression. Initially coefficients of the unknown dynamical system are found by ordinary least square (LS) solution without any regularization. Then the coefficients smaller than some cut-off value is hard thresholded that is forced to be zero. Next, using the remaining active terms, new ordinary LS solution is obtained for non-zero indices. This new solution is thresholded again. This procedure is repeated until all the coefficients are above the threshold value. Finally, the coefficients of the unknown dynamical system are obtained with promoting sparsity.

The final sparsity promoting algorithm is called Stepwise Sparse Regression (SSR) algorithm [21] and is inspired by previously mentioned sequential thresholded regression[18]. In SSR, thresholding approach is modified to remove only one coefficient per iteration to enforce sparsity. This modification eliminates the need of searching a threshold parameter and has the best accuracy and rate of convergence performance among the other applications. However, absence of model selection that penalizes the number of terms result in solutions that are not sparse enough. Therefore, it is seen that SSR algorithm may converge to non-sparse collinear basis depending on the library selection.

In this study, the SSR algorithm will be used to promote sparsity to the solution of regression equation whereas AIC model selection is included to solve the issues encountered during SSR implementation.

To sum up, all methods reduce the complexity of regression equation to prevent overfitting by means of penalizing the coefficients in the solution using different approaches.

2.4. Overfitting and Underfitting

Overfitting and underfitting are one of the most common problems encountered in data science applications. Overfitting results from having a model that is much more complex than necessary. As a result, model tries to memorize the data instead of learning the inherent structures. The major indicator of overfitting is that the error in the learning set is very small whereas the error in test set is relatively large.

On the other hand, underfitting is the lack of capacity of the model to accurately represent the data. In this case, the error in both training and test (withhold) sets are significantly large.

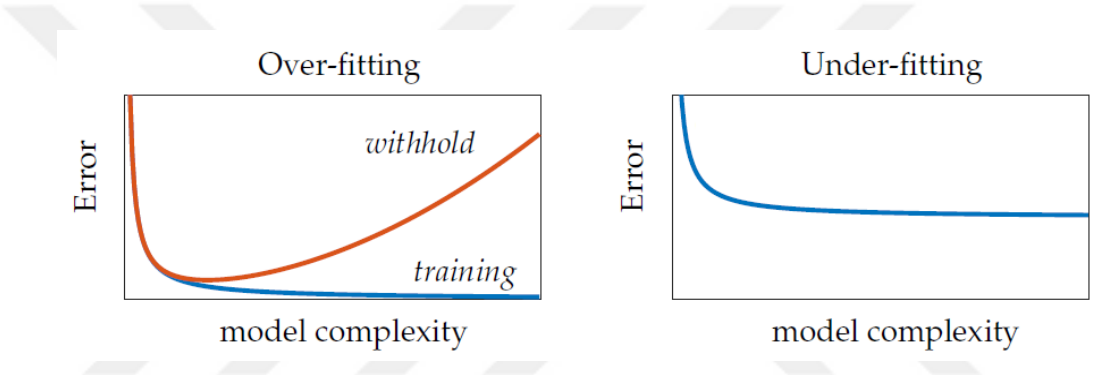

Figure 2.2. Over-fitting and Under-fitting [25]

As can be seen on the Figure 2.2 for overfitting, increasing the model complexity results in increasing the error in test data while error in training data continuously decreasing. In underfitting, on the other hand, error performance is limited because the model does not have enough number of free parameters required for the problem.

2.5. Cross Validation

Cross validation is one of the widely used techniques in almost all machine learning algorithms. Indeed, the model should not be trusted unless it is properly cross-validated. The procedure of cross-validation (Figure 2.3) can be given as follows:

1) Split the data as training and test sets.
2) Take a random portion of training data and build a model ($Y_k = f(X_k, \beta_k)$).
3) Repeat "step 2" k times and average values of the model parameters to obtain the final model ($Y = f(X, \bar{\beta})$).
4) Performs the model predictions on test data and evaluate the final model performance.

The reason behind splitting the training set into parts can be explained as follows: The common feature of the k sets is that they belong to the same real system. Random factor such as noise and outliers are not expected to be similar in these sets. In this way, system-specific features are learned by cross-validation and hence cross-validated models are expected to have high performance on test data.

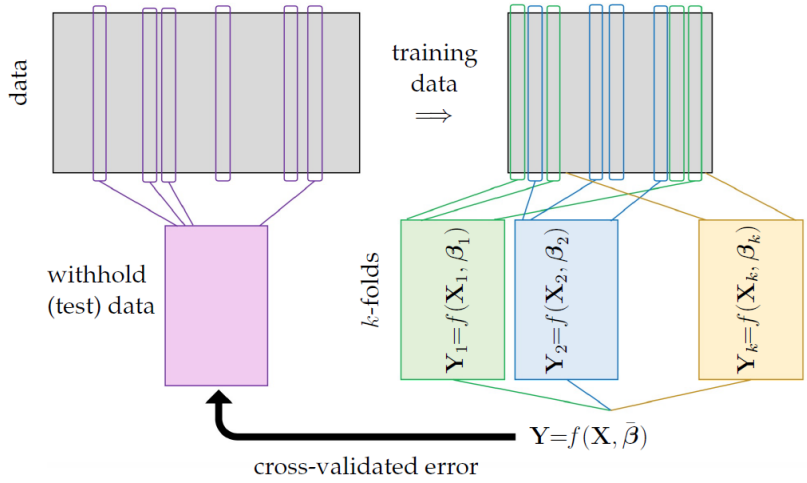

Figure 2.3. Procedure for k-fold cross validation [25]

2.6. Model Selection

The success of a model is closely related to the success of its generalization ability. In other words, a model is only as successful as its predictions in the extrapolation regime. However, given that the dominant behavior of real systems can be expressed in a limited number of terms, it is also important to choose the simplest model possible.

Therefore, selecting the appropriate model among many candidates is important for system identification. The solid line in Figure 2.4 represents the average behavior of the models having lowest error and least number of terms (magenta points) whereas models having high error are shown with green points. The aim of model selection is not only to discard the green models, but also to select the optimal model between candidates on the solid line.

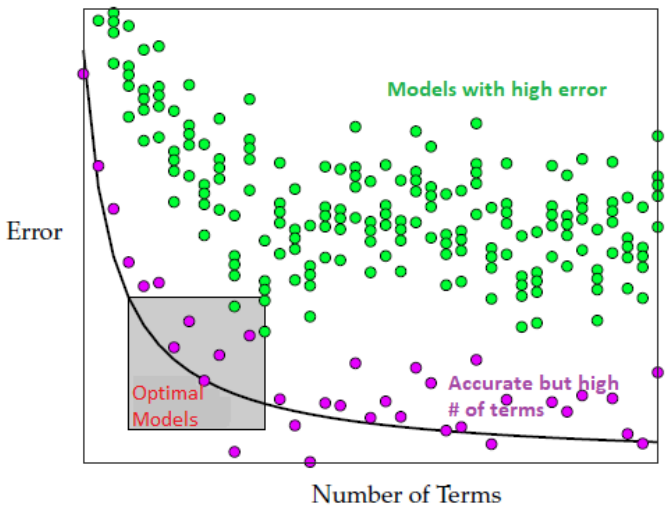

Figure 2.4. Model error vs model complexity [26]

Information theory provides an established statistical framework for model selection that has been studied for many years. Since the 1950s, the measure of information loss between the experimentally collected data and the model constructed from these data has been calculated using the Kullback-Leibler (KL) divergence [27],[28]. Based on this idea, Akaike then developed a method for estimating the relative loss of information between models and calculated a metric that balances model complexity with goodness of fit called Akaike Information Criteria, abbreviated as AIC [22].

AIC calculates estimates of the KL distance between the candidate models and the true measurements. Hence, selecting the model with minimum AIC score means choosing the one having the smallest KL distance to the true measurements. In other

words, AIC is used to compare and select candidate models. The AIC score for each candidate model j can be calculated using Eqn. (2-5).

$$AIC_j = 2k - 2ln(L(x, \hat{\mu})) \tag{2-5}$$

where k is the number of free parameters which corresponds to model complexity, $L(x, \hat{\mu}) = P(x|\mu)$ is the likelihood function of measurements x given candidate model parameters μ [22].

In general, for finite sample size AIC score formulation requires a correction [29] as given in Eqn. (2-6);

$$AIC_c = AIC \ + 2(k+1)(k+2)/(\ m - k - 2) \tag{2-6}$$

where m is the number of observations and AIC_c is the corrected AIC score.

If residual sum of squares (RSS) is used in likelihood function, AIC formulation becomes as given in Eqn. (2-7)

$$AIC = m \cdot ln(RSS/m) + 2k \tag{2-7}$$

where $RSS = \sum_{i=1}^{m}(y_i - g(x_i; \mu))^2$ and g is the candidate model and y_i , x_i are the observed outcomes and independent variables, respectively.

Note that Eqn. (2-7) penalizes models that have many free parameters and do not match with the observed outputs by increasing their AIC scores. An example AIC scores of the candidate models with increasing number of terms is given in Figure 2.5. As can be seen, if AIC model selection is applied to these candidate models, the model having 5 number of terms will be selected.

Note that AIC scores are stated as relative to each other. In other words, the minimum of the AIC score of the candidate models is found first and subtracted from all scores. Therefore, the minimum AIC score value is always equal to zero and does not always

indicate good performance. It only shows relative performance among candidate models.

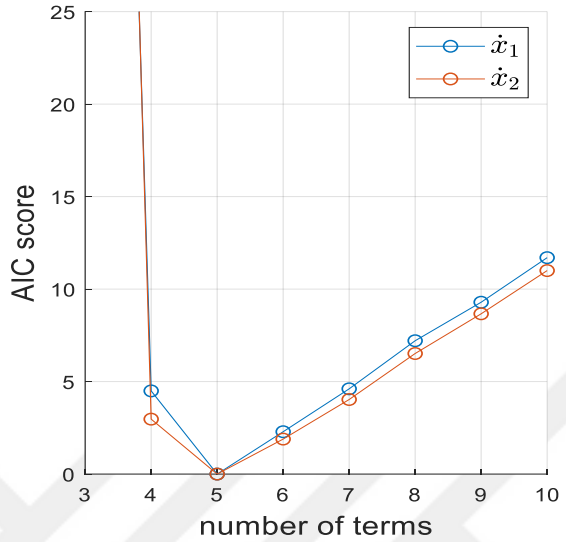

Figure 2.5. Sample AIC score with increasing model complexity

2.7. SINDY-SAIC Method for Nonlinear System Identification

SINDY (Sparse Identification of Nonlinear Dynamical System) is an algorithm that identifies nonlinear dynamical system from measurement data using special sparse regression techniques. Sparse regression with proper model selection algorithm can be very powerful yet simple for system identification. Sparsity comes from the assumption that many dynamical systems are governed by relatively few terms in their governing equations. This assumption is valid for many dynamical systems at least in an appropriate basis [18].

The proposed SINDY-SAIC algorithm which is an extension of SINDY is a sparse regression method with model selection and cross validation algorithm. It is used to identify the fewest terms in the governing equation that are required to accurately represent the data. Sparsity of the SINDY-SAIC algorithm establish the balance between accuracy and complexity that prevents overfitting. Model selection and cross-

validation allow the selection of the model with the fewest terms and at the same time having most representation capacity among the many candidate models. Therefore, SINDY-SAIC is not only a regression method, but it is a set of algorithms that are used to obtain a system model from measurement data.

In general, many system identification techniques such as neural networks result in black box models which are difficult to examine and control. On the other hand, SINDY-SAIC explicitly gives dominant terms in the governing equations.

The general flow of SINDY-SAIC algorithm is given in Figure 2.6.

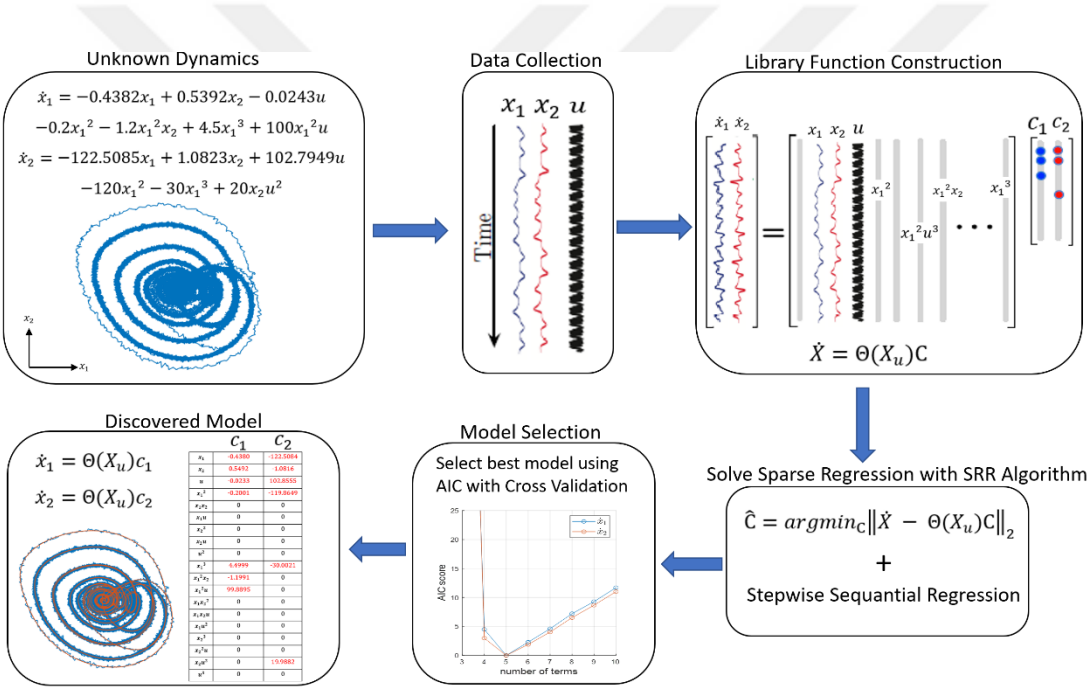

Figure 2.6. Schematic of SINDY-SAIC algorithm

To find unknown and possibly non-linear system of equations purely from data using SINDY-SAIC, following algorithm can be used.

Step 1. Measure $x_i(t_j)$

$x_i(t_j)$ is the measurement of the ith state of the system at time j. In other words, i is the subscript for states of the system ranging from 1 to the number of states n and j is the subscript for the measurements ranging from 1 to the number of measurements m. For example, a system can have 1000 measurements and 2 states such as position and velocity.

Step 2. Split measurement data into training and test sets and select number of folds *k* for cross validation. Selection of *k* mainly depends on the time response characteristics of the interested dynamical system and quality of measurement data. It is not recommended to select too large *k* value that will prevent the transient and steady state behavior to occur.

Step 3. Construct the measurement matrix X from training data.

$$X = \begin{bmatrix} x_1(t_1) & x_2(t_1) & \cdots & x_n(t_1) \\ x_1(t_2) & x_2(t_2) & \cdots & x_n(t_2) \\ \vdots & \vdots & \ddots & \vdots \\ x_1(t_m) & x_2(t_m) & \cdots & x_n(t_m) \end{bmatrix} \tag{2-8}$$

Step 4. Calculate derivative $\dot{x}_i(t_j)$ and construct the matrix $\dot{X}$

- $\dot{x}_i(t_j)$ is the derivative of measurement data. Derivative is calculated using proper methods. Note that in case of noisy data, using difference formulas to calculate derivative generally fails. Therefore, in this study local slope for a sequence of points is estimated using sliding window approach. In this approach, a polynomial of given model order is fitted to the noisy data of selected windows size. Then the polynomial derivative is taken.

$$\dot{X} = \begin{bmatrix} \dot{x}_1(t_1) & \dot{x}_2(t_1) & \cdots & \dot{x}_n(t_1) \\ \dot{x}_1(t_2) & \dot{x}_2(t_2) & \cdots & \dot{x}_n(t_2) \\ \vdots & \vdots & \ddots & \vdots \\ \dot{x}_1(t_m) & \dot{x}_2(t_m) & \cdots & \dot{x}_n(t_m) \end{bmatrix} \tag{2-9}$$

Step 5. Select the library of candidate functions and construct the matrix Θ

Proper choice of candidate function is crucial for success of SINDY algorithms. In general, polynomials up to order n and trigonometric functions are used as library functions. Note that it is better to choose library functions from a wide range and gradually reduce them. Also, already known terms in the equation of the dynamical system can be selected as library functions.

$$X_u = \begin{bmatrix} x_1(t_1) & x_2(t_1) & \cdots & x_n(t_1) \\ x_1(t_2) & x_2(t_2) & \cdots & x_n(t_2) \\ \vdots & \vdots & \ddots & \vdots \\ x_1(t_m) & x_2(t_m) & \cdots & x_n(t_m) \end{bmatrix} \Bigg| u \Bigg] \tag{2-10}$$

where X_u is the "augmented state-control matrix" formed by state X and control input u.

$$\Theta(X_u) = \begin{bmatrix} | & | & | & | & \cdots & | & | & | & | & \cdots \\ 1 & X_u & {X_u}^{P_2} & {X_u}^{P_3} & \cdots & sin(X_u) & cos(X_u) & sin(2X_u) & cos(2X_u) & \cdots \\ | & | & | & | & \cdots & | & | & | & | & \cdots \end{bmatrix} \tag{2-11}$$

$${X_u}^{P_2} = \begin{bmatrix} {x_1}^2(t_1) & x_1(t_1)x_2(t_1) & \cdots & x_1(t_1)u & {x_2}^2(t_1) & x_2(t_1)x_3(t_1) & x_2(t_1)u & \cdots & {x_n}^2(t_1) \\ {x_1}^2(t_2) & x_1(t_2)x_2(t_2) & \cdots & x_1(t_2)u & {x_2}^2(t_2) & x_2(t_2)x_3(t_2) & x_2(t_2)u & \cdots & x_n(t_2) \\ \vdots & \vdots & \vdots & \vdots & \vdots & \vdots & \vdots & \vdots & \vdots \\ \vdots & \vdots & \vdots & \vdots & \vdots & \vdots & \vdots & \vdots & \vdots \\ {x_1}^2(t_m) & x_1(t_m)x_2(t_m) & \cdots & x_1(t_m)u & {x_2}^2(t_m) & x_2(t_m)x_3(t_m) & x_2(t_m)u & \cdots & x_n(t_m) \end{bmatrix} \tag{2-12}$$

Step 6. Solve for coefficient matrix C using Stepwise Sparse Regression (SSR) technique [21] on training data.

Each column of C contains the sparse coefficient for every row of the governing equations. Sparsity is promoted during the calculation of C.

$$\dot{X} = \Theta(X_u)\mathrm{C} \tag{2-13}$$

$$C = [c_1\ c_2\ \dots\ c_n] \tag{2-14}$$

Step 7. Perform cross-validation on k folded test data and calculate the error in test data. Error is defined as residual sum of square (RSS) of the difference between the true and prediction value in the test data.

Step 8. Using the RSS error and the number of terms in the candidate models, apply Akaike Information Criteria (AIC) to select the appropriate model among many others using Eqn. (2-6).

The SINDY-SAIC algorithm provides a suitable environment for model discovery and selection. The discovered model will be more useful when used in conjunction with a data-driven control method such as Model Predictive Control. In the next chapter, the details about MPC will be given.

CHAPTER 3

MODEL PREDICTIVE CONTROL

MPC is a control strategy that uses a model to predict future plant output and solves an optimization problem with constraints to select the optimal control action. MPC is multi variable controller that can handle multi-input multi-output systems and can handle constraints that prevent the system from undesired consequences [30]. However, MPC requires a powerful, fast processing units and a large amount of memory because it solves an online optimization problem at each time step. In general, linear MPC solve the convex quadratic problem, thereby requires less computational power. On the other hand, nonlinear MPC solves non-convex optimization problem, thereby requires much more processing power, memory, and time [11]. Considering the rapid development of computational capacities, it is not difficult to predict that the use of nonlinear MPC will increase sharply in the near future.

3.1. Working Principle of MPC

MPC is formulated as an open-loop optimization problem. As with all optimization problems, MPC has a cost function to minimize and constraints to satisfy at each time step. The basic working principle of MPC is as follows: At current time t_0, future prediction up to $t_0 + H_p$ (prediction horizon) time is calculated using the approximate model of the real system and is called output prediction. Next, the cost function is calculated using the difference between the set point and the output prediction. By using a proper optimization routine, the cost function and constraints are tried to be satisfied and the control input u is calculated. Usually, the control input u is kept constant after time $t_0 + H_m$ (control horizon) during the calculation of the output prediction. Finally, only the first value of the control input is applied to the system and

the optimization is restarted using new measurements and repeated at each time step until the end of the trajectory as shown in Figure 3.1.

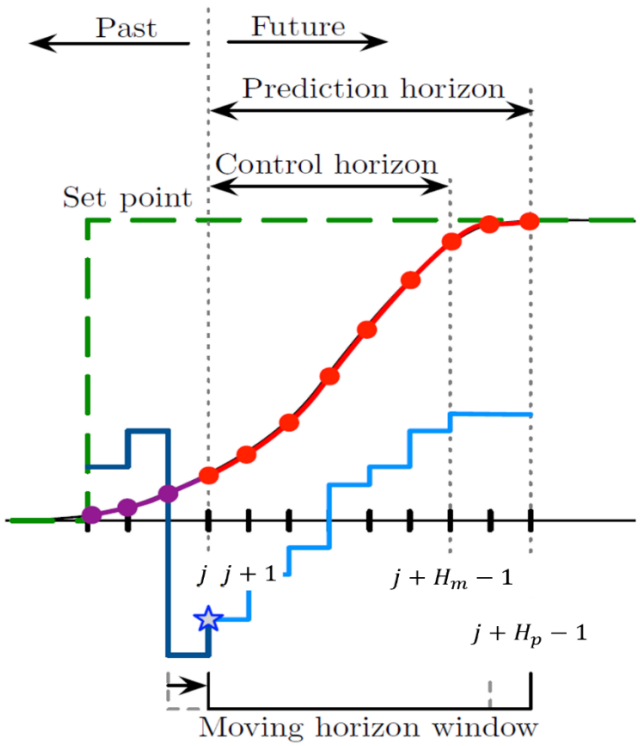

Figure 3.1. MPC working principle [26]

MPC requires a system model for its future predictions [31]. The higher the accuracy of this model, the higher the performance of the MPC. Therefore, MPC should be used in conjunction with a successful system identification method. The results obtained with SINDY-SAIC and MPC in the following sections will demonstrate the success of this combination in details.

3.2. MPC Design Parameters

Sample time, Prediction horizon, Control horizon, Constraints and Weights are the main design parameters of the MPC framework. The success of the results is closely

dependent on the appropriate selection of these design parameters. Therefore, in this section, some recommendations for the selection of these parameters will be given.

3.2.1. Sample Time (T_s)

T_s is the rate at which the controller executes the controller algorithm. The large sample time means that the controller cannot react fast enough to disturbances and changes in the reference input. On the other hand, in case of very small sample time controller can react much faster to disturbances and set point changes, but this introduces computational overloads. To balance the performance and the computational efforts, a general recommendation is to choose sample time between 5 -10 % of the rise time (T_r) of the open loop response.

$$0.05\, T_r \leq T_s \leq 0.1\, T_r$$

However, the designers should determine sampling time according to their performance expectations, available hardware, and other application specific requirements.

3.2.2. Prediction Horizon (H_p)

The number of predicted future time steps is called prediction horizon and determines how far the controller predicts into the future. In MPC, the model of the system is used for future predictions and as it is known, no model is perfect. In addition, unexpected situations may arise during long trajectories. Therefore, long-term predictions are not very accurate. Choosing a large prediction horizon does not offer much benefit, but also increases the computational burden. On the other hand, very small prediction horizon should not be chosen than the system dynamics allows. The general recommendation is to choose prediction horizon bigger than the settling time ($T_{settling}$) of the open loop response.

$$H_p \geq \frac{T_{settling}}{T_s}$$

3.2.3. Control Horizon (H_m)

The number of steps after which the control remains constant is called the control horizon. Control horizon determines the number of free variables to be chosen by the optimizer. So, the smaller the control horizon, the fewer the computations. Too small control horizon worsens the future predictions. The rule of thumb to choose control horizon is between 10-20% of the prediction horizon and having 2-3 steps at least.

$$0.1\, H_p \;\leq\; H_m \;\leq\; 0.2\, H_p$$

3.2.4. Constraints

In MPC, constraints on inputs, rate of change of inputs and outputs can be incorporated. These constraints can be soft and hard constraints. Hard constraints cannot be violated whereas soft constraints can be violated. Hard constraints generally come from the physical limits such as maximum allowable deflection of a missile canard, or the gas pedal limits of a car. On the other hand, soft limits are mostly due to performance requirements and measures taken to prevent the system from approaching operating limits of some of the subsystems. Setting hard constraints on both input and output at the same time should be avoided as these requirements may conflict and leading to an unfeasible solution for optimization.

3.2.5. Weights

In MPC, multiple goals are present, such as reference tracking and smooth control input. The importance of these goals relative to each other are specified with weights. In addition, reference tracking of the outputs can be weighted within itself. For example, if the reference tracking of the first output is important than the second, bigger weight should be selected for the first output.

3.3. Prediction Formulation and Solution of MPC Problems

Linearized, discrete time state space model of a dynamical system can be given in the form

$$\begin{aligned} x(k+1) &= Ax(k) + Bu(k) \\ y(k) &= \mathrm{C}_y x(k) \\ z(k) &= \mathrm{C}_z x(k) \end{aligned} \tag{3-1}$$

where x is the state vector, y is the measured outputs, z is the outputs which are to be controlled and u is the input vector. Generally, y and z are the same that is all controlled outputs frequently are measured.

The general formulation of the controlled output z is given in Eqn. (3-2)

$$z(k) = C_z x(k) + D_z u(k) \tag{3-2}$$

However, D_z is assumed to be zero in this study for the ease of computation of optimal $u(k)$. If in real system, D_z is not equal to zero, this complication can be avoided by defining a new variable as follows,

$$\tilde{z}(k) = z(k) - D_z u(k) \tag{3-3}$$

3.3.1. Prediction Formulation

The predicted values of the controlled variables $\hat{z}(k+i|k)$ should be calculated using the estimate of the current state $\hat{x}(k|k)$, the latest input $u(k-1)$ and the assumed future input changes $\Delta\hat{u}(k+i|k)$.

In case of no disturbances and full state measurements that is $\hat{x}(k|k) = x(k) = y(k)$, the future prediction of states can be calculated simply by iterating the state space model as derived in Eqn. (3-4),

$$
\begin{aligned}
\hat{x}(k+1|k) &= Ax(k) + B\hat{u}(k|k) \\
\hat{x}(k+2|k) &= A\hat{x}(k+1|k) + B\hat{u}(k+1|k) \\
&= A^2x(k) + AB\hat{u}(k|k) + B\hat{u}(k+1|k) \\
&\vdots \\
\hat{x}\big(k+H_p|k\big) &= A\hat{x}\big(k+H_p-1|k\big) + B\hat{u}\big(k+H_p-1|k\big) \\
&= A^{H_p}x(k) + A^{H_p-1}B\hat{u}(k|k) + \ldots + B\hat{u}(k+H_p-1|k)
\end{aligned}
\tag{3-4}
$$

For the sake of optimization, it is better to express predictions in terms of $\Delta\hat{u}(k+i|k)$ rather than $\hat{u}(k+i|k)$. Note that $\Delta\hat{u}(k+i|k) = \hat{u}(k+i|k) - \hat{u}(k+i-1|k)$, then,

$$
\begin{aligned}
\hat{u}(k|k) &= \Delta\hat{u}(k|k) + u(k-1) \\
\hat{u}(k+1|k) &= \Delta\hat{u}(k+1|k) + \Delta\hat{u}(k|k) + u(k-1) \\
&\vdots \\
\hat{u}(k+H_m-1|k) &= \Delta\hat{u}(k+H_m-1|k) + \ldots + \Delta\hat{u}(k|k) + u(k-1)
\end{aligned}
\tag{3-5}
$$

If Eqn. (3-4) and (3-5) are combined, state prediction equation can obtained in matrix-vector form and given in Eqn. (3-6).

$$
X(k) = \Psi_x x(k) + \Upsilon_x u(k-1) + \Theta_x \Delta U(k) \tag{3-6}
$$

Definitions of $X(k), \Psi_x$, Υ_x , Θ_x and $\Delta U(k)$[30] are given as follows:

$$
X(k) = \begin{bmatrix} \hat{x}(k+1|k) \\ \vdots \\ \hat{x}(k+H_m|k) \\ \hat{x}(k+H_m+1|k) \\ \vdots \\ \hat{x}\big(k+H_p|k\big) \end{bmatrix}
$$

$$\Psi_x = \begin{bmatrix} A \\ \vdots \\ A^{H_m} \\ A^{H_m+1} \\ \vdots \\ A^{H_p} \end{bmatrix} \quad , \quad \Upsilon_x = \begin{bmatrix} B \\ \vdots \\ \sum_{i=0}^{H_m-1} A^i B \\ \sum_{i=0}^{H_m} A^i B \\ \vdots \\ \sum_{i=0}^{H_p-1} A^i B \end{bmatrix}$$

$$\Theta_x = \begin{bmatrix} B & \cdots & 0 \\ AB+B & \cdots & 0 \\ \vdots & \ddots & \vdots \\ \sum_{i=0}^{H_m-1} A^i B & \cdots & B \\ \sum_{i=0}^{H_m} A^i B & \cdots & AB+B \\ \vdots & \vdots & \vdots \\ \sum_{i=0}^{H_p-1} A^i B & \cdots & \sum_{i=0}^{H_p-H_m} A^i B \end{bmatrix} \quad and \quad \Delta U(k) = \begin{bmatrix} \Delta\hat{u}(k|k) \\ \vdots \\ \Delta\hat{u}(k+H_m-1|k) \end{bmatrix}$$

Finally, the output prediction can be calculated simply as,

$$\begin{aligned} \hat{z}(k+1|k) &= \mathrm{C}_z \hat{x}(k+1|k) \\ \hat{z}(k+2|k) &= \mathrm{C}_z \hat{x}(k+2|k) \\ &\cdot \\ &\cdot \\ \hat{z}(k+H_p|k) &= \mathrm{C}_z \hat{x}(k+H_p|k) \end{aligned} \tag{3-7}$$

or in matrix-vector form,

$$\begin{bmatrix} \hat{z}(k+1|k) \\ \vdots \\ \hat{z}(k+H_p|k) \end{bmatrix} = \begin{bmatrix} \mathrm{C}_z & 0 & \cdots & 0 \\ 0 & \mathrm{C}_z & \cdots & 0 \\ \vdots & \vdots & \ddots & \vdots \\ 0 & 0 & \cdots & \mathrm{C}_z \end{bmatrix} \begin{bmatrix} \hat{x}(k+1|k) \\ \vdots \\ \hat{x}(k+H_p|k) \end{bmatrix} \tag{3-8}$$

3.3.2. Solution of MPC Problem

$$Z(k) = \begin{bmatrix} \hat{z}(k+H_w|k) \\ \vdots \\ \hat{z}\big(k+H_p|k\big) \end{bmatrix}, \;\; T(k) = \begin{bmatrix} \hat{r}(k+H_w|k) \\ \vdots \\ \hat{r}\big(k+H_p|k\big) \end{bmatrix}, \;\; \Delta U(k) = \begin{bmatrix} \Delta\hat{u}(k|k) \\ \vdots \\ \Delta\hat{u}(k+H_m-1|k) \end{bmatrix}$$

$Z(k), T(k), \Delta U(k)$ are the outputs, reference (Target trajectory) and change in the control inputs respectively. Note that if the start index (H_w) is selected greater than unity, it means that the deviations of z from r are not penalized immediately. If Eqn. (3-6) and (3-8) are combined with the $Z(k), T(k), \Delta U(k)$ definitions, the following output prediction equation is obtained,

$$Z(k) = \Psi x(k) + \Upsilon u(k-1) + \Theta \Delta U(k) \tag{3-9}$$

where

$$\Psi = \begin{bmatrix} \mathrm{C}_z & 0 & \cdots & 0 \\ 0 & \mathrm{C}_z & \cdots & 0 \\ \vdots & \vdots & \ddots & \vdots \\ 0 & 0 & \cdots & \mathrm{C}_z \end{bmatrix} \Psi_x \quad , \quad \Upsilon = \begin{bmatrix} \mathrm{C}_z & 0 & \cdots & 0 \\ 0 & \mathrm{C}_z & \cdots & 0 \\ \vdots & \vdots & \ddots & \vdots \\ 0 & 0 & \cdots & \mathrm{C}_z \end{bmatrix} \Upsilon_x$$

$$\Theta = \begin{bmatrix} \mathrm{C}_z & 0 & \cdots & 0 \\ 0 & \mathrm{C}_z & \cdots & 0 \\ \vdots & \vdots & \ddots & \vdots \\ 0 & 0 & \cdots & \mathrm{C}_z \end{bmatrix} \Theta_x$$

The cost function that should be minimized is given as [30],

$$J(k) = \sum_{i=H_w}^{H_p} \|\hat{z}(k+i|k) - \hat{r}(k+i|k)\|^2_{Q(i)} + \sum_{i=0}^{H_m-1} \|\Delta\hat{u}(k+i|k)\|^2_{R(i)} \tag{3-10}$$

Or in more compact form,

$$J(k) = \|Z(k) - T(k)\|_Q^2 + \|\Delta U(k)\|_R^2 \tag{3-11}$$

The tracking error E, that is the difference between Target trajectory and the "free response" of the system is

$$\mathrm{E}(k) = T(k) - \Psi x(k) - \Upsilon u(k-1) \tag{3-12}$$

Free response of the system is the output of the system that changes in the input is zero ($\Delta U(k) = 0$).

Using Eqns. (3-11) and (3-12),

$$\begin{aligned} J(k) &= \|\Theta\Delta U(k) - \mathrm{E}(k)\|_Q^2 + \|\Delta U(k)\|_R^2 \\ &= [\Delta U(k)^T\Theta^T - \mathrm{E}(k)^T]Q[\Theta\Delta U(k) - \mathrm{E}(k)] + \Delta U(k)^T R\Delta U(k) \\ &= \mathrm{E}(k)^T Q\mathrm{E}(k) - 2\Delta U(k)^T\Theta^T Q\mathrm{E}(k) + \Delta U(k)^T[\Theta^T Q\Theta + \\ &\quad R]\,\Delta U(k) \end{aligned} \tag{3-13}$$

Let's define $G = 2\Theta^T Q\mathrm{E}(k)$ and $H = \Theta^T Q\Theta + R)$, then cost equation becomes,

$$J(k) = const - \Delta U(k)^T G + \Delta U(k)^T H\Delta U(k) \tag{3-14}$$

As seen G and H does not depends on $\Delta U(k)$. To find the optimal value of $\Delta U(k)$, the gradient of $J(k)$ with respect to $\Delta U(k)$ should be calculated and set to zero.

$$\nabla_{\Delta U(k)} J = -G + 2H\Delta U(k) \rightarrow 0$$

$$\Delta U(k)_{opt} = \frac{1}{2} H^{-\mathbf{1}} G \tag{3-15}$$

As stated, in MPC only the first part of the solution (Eqn. (3-15)) should be used because of the receding horizon concept. Note that this ensures the closed loop behavior of MPC.

3.4. MPC Framework with SINDY-SAIC Algorithm and Integral Action

The proposed SINDY-SAIC and MPC framework is given in Figure 3.2. After approximate model of the unknown dynamical system is discovered by SINDY-SAIC, this model is used as prediction model in MPC framework to control the system.

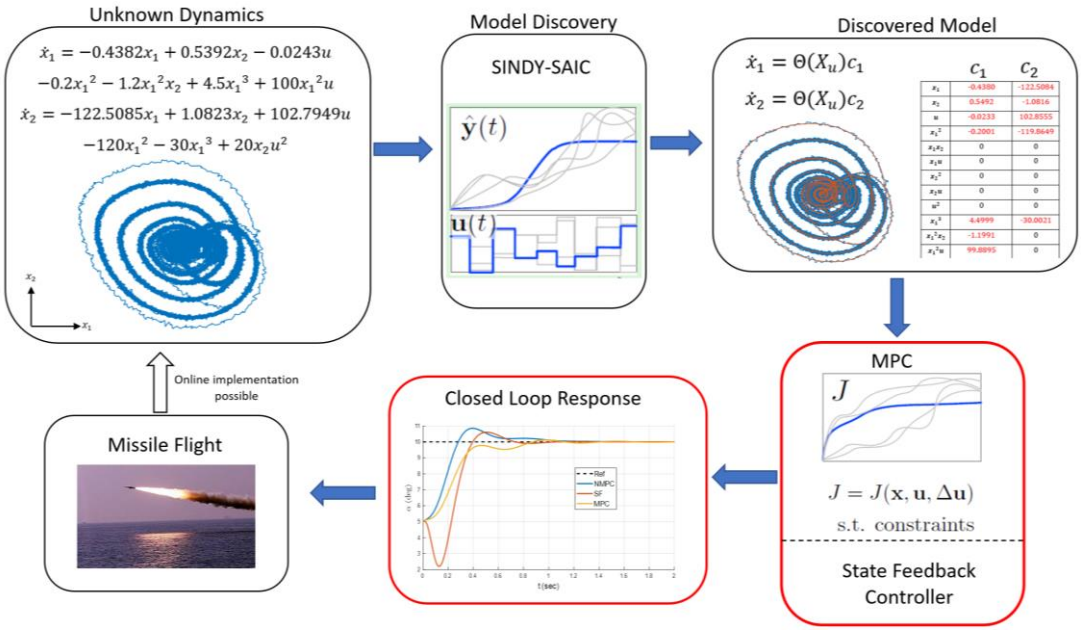

Figure 3.2. Schematic of SINDY-SAIC and MPC framework

In MPC when the prediction model and the true model differs, a steady state error in set point tracking can be observed. This issue is studied a lot in MPC literature, and several solutions are proposed.

One of the approaches to remove the offset is as follows: The disturbance (d) that is the difference between the measured output of the real plant and the predicted output of the model in MPC is calculated (3-16).

$$\hat{d}(k) = y_m(k) - y(k) \tag{3-16}$$

The steady state error is removed from the system by shifting the prediction output as given in Eqn. (3-17). The corrected prediction output (y^*) is fed to the PID controller to remove the offset from tracking. The assumption that disturbance stays constant is not valid for some cases, therefore, in this method the offset free tracking cannot be obtained at all conditions. The details of the implementation can be found in [32].

$$y^*(k+i) = y(k+i) + \hat{d}(k) \tag{3-17}$$

Another approach is to include the tracking error into the states of the system by augmentation [33]. However, this is valid only for linear prediction models and increases the system order that affects the MPC computation time.

In this study, a non-linear integration scheme [34] is used to remove the offset from MPC. The steady state error that is the difference between the set point and the measured output is calculated and fed to a nonlinear function. The output of the nonlinear function is integrated and multiplied by a proper gain and added to the control input of the system Figure 3.3.

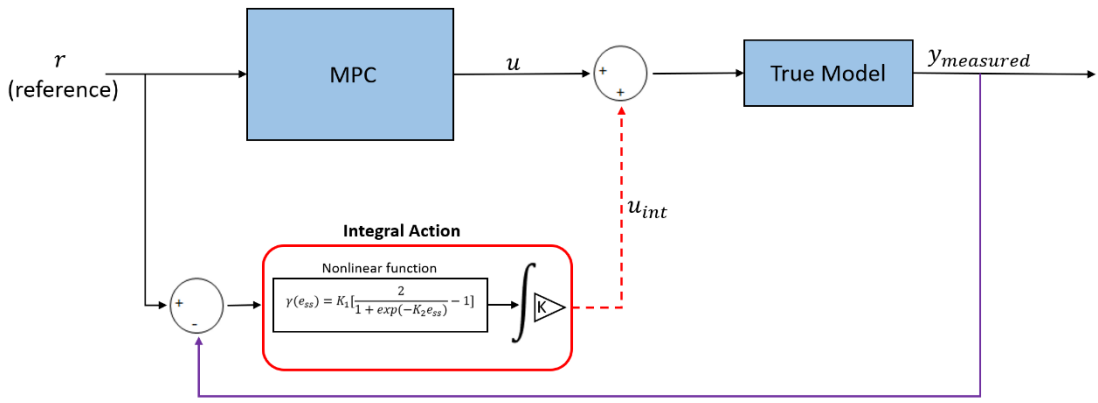

Figure 3.3. Schematic of integral action in MPC

The nonlinear integration differ from the standard integration by means of smoothing the steady state error that does not cause excessive overshoot in the response. The sigmoidal type of tanh nonlinear function is used and given in Eqn. (3-18).

$$\gamma(e_{ss}) = K_1[\frac{2}{1 + exp(-K_2 e_{ss})} - 1] \tag{3-18}$$

K_1 and K_2 are both selected as 0.5 and the output of nonlinear function for different gain values is given in Figure 3.4.

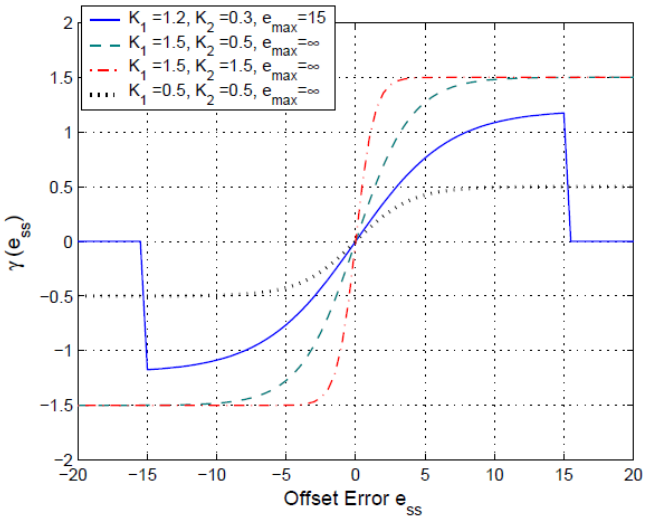

Figure 3.4. Output of non-linear function for different gain values [34]

A properly working integral action method reduces the need for accurate prediction models in MPC. Hence, using integral action, non-linear systems can be controlled by MPC using approximate linear prediction models and provides effective solutions. These results will be presented in the relevant sections.

In this chapter, basic idea behind MPC and general solution to MPC formulation with no constraints case were presented for completeness. The important design parameters in MPC such as prediction and control horizons were explained. The integral action was presented to remove steady state offset. In the next chapter, the derivations of dynamical system equations that are used for model discovery will presented.

CHAPTER 4

MISSILE DYNAMIC MODEL AND STATE FEEDBACK CONTROL

In this chapter missile dynamic model that will be discovered using SINDY-SAIC will be derived using 6 DOF motion equations. Then, the general architecture of state feedback control used for comparison with MPC will be given.

4.1. Longitudinal Missile Dynamics

6 DOF motion equations [35] are given in Eqn. (4-1) through Eqn. (4-6).

$$F_X = m\left(\dot{u} + qw - rv + gsin(\theta)\right) \tag{4-1}$$

$$F_Y = m(\dot{v} + ru - pw - gcos(\theta)\sin(\phi)) \tag{4-2}$$

$$F_z = m(\dot{w} + pv - qu - gcos(\theta)\cos(\phi)) \tag{4-3}$$

$$M_L = I_{xx}\dot{p} - I_{yz}(q^2 - r^2) - I_{zx}(\dot{r} + pq) - I_{xy}(\dot{q} - rp) - \left(I_{yy} - I_{zz}\right)qr \tag{4-4}$$

$$M_M = I_{yy}\dot{q} - I_{zx}(r^2 - p^2) - I_{xy}(\dot{p} + qr) - I_{yz}(\dot{r} - pq) - (I_{zz} - I_{xx})rp \tag{4-5}$$

$$M_N = I_{zz}\dot{r} - I_{xy}(p^2 - q^2) - I_{yz}(\dot{q} + rp) - I_{zx}(\dot{p} - qr) - \left(I_{xx} - I_{yy}\right)pq \tag{4-6}$$

In this study, only the longitudinal dynamics will be discovered using SINDY-SAIC. Hence, Eqns. (4-3) and (4-5) are the ones defining the longitudinal motion of the missile.

For rotationally symmetric missiles, cross product of inertia terms is generally neglected for simplicity that is $I_{zx} = I_{xy} = I_{yz} = 0$. In addition, roll rate of the missile is usually controlled by roll autopilot and can be assumed to zero ($p = 0$). Hence, Eqns. (4-3) and (4-5) becomes,

$$F_z = m(\dot{w} - qu - gcos(\theta)\cos(\phi)) \tag{4-7}$$

$$M_M = I_{yy}\dot{q} \tag{4-8}$$

where m is the mass of the missile, u and w are the body frame velocities in x and z directions respectively, ϕ and θ are the roll and pitch angles, q is the pitch rate, g is the gravitational acceleration, I_{yy} is the moment of inertia in longitudinal plane, F_z and M_M are the aerodynamic force and moment in longitudinal plane.

During the longitudinal autopilot design, the gravitational acceleration acting on the missile generally considered as a disturbance, therefore g is assumed to be zero. Hence, simplified longitudinal equations of missile becomes,

$$F_z = m(\dot{w} - qu) \tag{4-9}$$

$$M_M = I_{yy}\dot{q} \tag{4-10}$$

Note that only the terms belonging to longitudinal dynamics exist in Eqns. (4-9) and (4-10). All the dependence on roll and yaw dynamics are eliminated.

The states that are measured in this study is determined as α and q. Hence, conversion from w to α is required. This accomplished by using small angle assumption. Angle of attack (α) smaller than 15 degrees can be approximated using Eqn. (4-11).

$$\alpha = \tan^{-1}\left(\frac{w}{u}\right) \cong \frac{w}{u} \tag{4-11}$$

The derivative of Eqn. (4-11) under the assumption of constant u velocity gives,

$$\dot{\alpha} = \frac{\dot{w}}{u} \tag{4-12}$$

Therefore, the equations of motion in longitudinal plane become,

$$\dot{\alpha} = \frac{F_z}{mu} + q \tag{4-13}$$

$$\dot{q} = \frac{M_M}{I_{yy}} \tag{4-14}$$

Strong nonlinearity comes from the force and moment terms in Eqns. (4-13) and (4-14). In this study, F_z and M_M are expressed as follows,

$$\begin{aligned} F_z = QA\Big(&Cz_\alpha \cdot \alpha + Cz_{\delta_e} \cdot \delta_e + Cz_q \cdot q\frac{d}{2V} + Cz_{\alpha_2} \cdot \alpha^2 \\ &+ Cz_{q\alpha_2} \cdot q\alpha^2 + Cz_{\alpha_3} \cdot \alpha^3 + Cz_{\alpha_2\delta_e} \cdot \alpha^2\delta_e\Big) \end{aligned} \tag{4-15}$$

$$\begin{aligned} M_M = QAl_{ref}\Big(&Cm_\alpha \cdot \alpha + Cm_{\delta_e} \cdot \delta_e + Cm_q \cdot q\frac{d}{2V} \\ &+ Cm_{\alpha_2} \cdot \alpha^2 + Cm_{\alpha_3} \cdot \alpha^3 + Cm_{q\delta_{e_2}} \cdot q{\delta_e}^2\Big) \end{aligned} \tag{4-16}$$

Note that the type of nonlinearities in F_z and M_M can change depending on the aerodynamic characteristics of the missile.

It is better to use some definition for the clarity of the results. The definitions are given in Table 4.1.

Table 4.1. Definitions for missile equations of motion

$Z_\alpha \triangleq \frac{QA}{mV} Cz_\alpha$	$M_\alpha \triangleq \frac{QA}{I_{yy}} l_{ref} Cm_\alpha$
$Z_{\delta_e} \triangleq \frac{QA}{mV} Cz_{\delta_e}$	$M_{\delta_e} \triangleq \frac{QA}{I_{yy}} l_{ref} Cm_{\delta_e}$
$Z_q \triangleq \frac{QA}{mV} \frac{d}{2V} Cz_q$	$M_q \triangleq \frac{QA}{I_{yy}} l_{ref} \frac{d}{2V} Cm_q$
$Z_{\alpha_2} \triangleq \frac{QA}{mV} Cz_{\alpha_2}$	$M_{\alpha_2} \triangleq \frac{QA}{I_{yy}} l_{ref} Cm_{\alpha_2}$
$Z_{\alpha_3} \triangleq \frac{QA}{mV} Cz_{\alpha_3}$	$M_{\alpha_3} \triangleq \frac{QA}{I_{yy}} l_{ref} Cm_{\alpha_3}$
$Z_{\alpha_2\delta_e} \triangleq \frac{QA}{mV} Cz_{\alpha_2\delta_e}$	$M_{q\delta_{e_2}} \triangleq \frac{QA}{I_{yy}} l_{ref} Cm_{q\delta_{e_2}}$
$Z_{q\alpha_2} \triangleq \frac{QA}{mV} Cz_{q\alpha_2}$	

Finally, using definitions above, the equations (4-13) and (4-14) take the form given in Eqn. (4-17) and (4-18) for nonlinear missile model.

$$\begin{aligned}\dot{\alpha} = Z_\alpha \cdot \alpha + Z_{\delta_e} \cdot \delta_e + \left(Z_q + 1\right) \cdot q + Z_{\alpha_2} \cdot \alpha^2 + Z_{\alpha_3} \cdot \alpha^3 \\ + \ Z_{\alpha_2\delta_e} \cdot \alpha^2 \delta_e + Z_{q\alpha_2} \cdot q\alpha^2\end{aligned} \tag{4-17}$$

$$\dot{q} = M_\alpha \alpha + M_{\delta_e} \delta_e + M_q q + M_{\alpha_2} \cdot \alpha^2 + M_{\alpha_3} \cdot \alpha^3 + M_{q\delta_{e_2}} \cdot q{\delta_e}^2 \tag{4-18}$$

These are the dynamical equations in general form that will be discovered by SINDY-SAIC in the following sections. For the studied highly nonlinear missile model, all the coefficient in Eqns. (4-17) and (4-18) are non-zero. For linear missile model, the coefficients of the nonlinear terms are set to zero. Linear missile model is given in Eqns. (4-19) and (4-20).

$$\dot{\alpha} = Z_\alpha \cdot \alpha + Z_{\delta_e} \cdot \delta_e + \left(Z_q + 1\right) \cdot q \tag{4-19}$$

$$\dot{q} = M_\alpha \alpha + M_{\delta_e} \delta_e + M_q q \tag{4-20}$$

4.2. State Feedback Control

The state space formulation of linear or linearized system (for non-linear missile model) is given by Eqns. (4-21) and (4-22). Here the states are $x = [\alpha, q]^T$ and the output to be controlled is angle of attack, α.

$$\boldsymbol{A} = \begin{bmatrix} Z_\alpha & \left(Z_q + 1\right) \\ M_\alpha & M_q \end{bmatrix}, \qquad \boldsymbol{B} = \begin{bmatrix} Z_{\delta_e} \\ M_{\delta_e} \end{bmatrix} \tag{4-21}$$

$$\boldsymbol{C} = [1 \quad 0], \qquad D = [\,0] \tag{4-22}$$

The plant A has no integrator and therefore an integrator will be added in the feedforward path. The schematic of the state feedback controller is given in Figure 4.1.

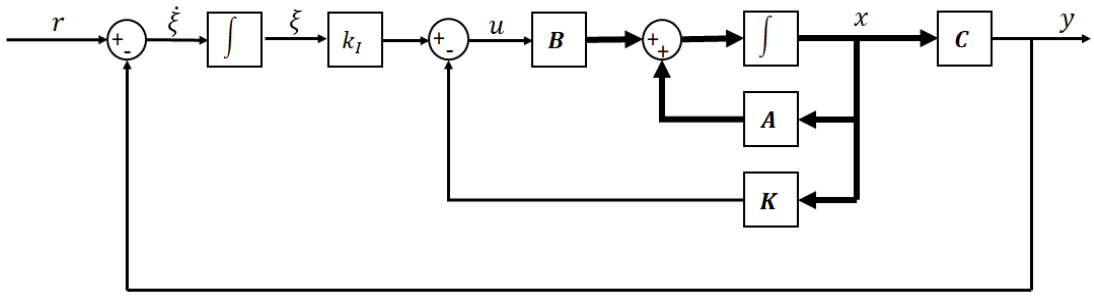

Figure 4.1. State Feedback Controller Structure [36]

From Figure 4.1, the following set of equations can be obtained [36] ,

$$\begin{gathered}\dot{\boldsymbol{x}} = \boldsymbol{A}\boldsymbol{x} + \boldsymbol{B}u \\ y = \boldsymbol{C}\boldsymbol{x} \\ u = -\boldsymbol{K}\boldsymbol{x} + k_I\xi \\ \dot{\xi} = r - y = r - \boldsymbol{C}x\end{gathered} \tag{4-23}$$

where u is the control input, y =output of the system, ξ is the output of the integrator (augmented state variable) and r is the reference signal. If the n dimensional state x and the integrator output ξ are augmented to form a new state space model, Eqns.(4-23) can be expressed in the form,

$$\begin{bmatrix} \dot{\boldsymbol{x}} \\ \dot{\xi} \end{bmatrix} = \begin{bmatrix} \boldsymbol{A} & \boldsymbol{0} \\ -\boldsymbol{C} & 0 \end{bmatrix} \begin{bmatrix} \boldsymbol{x} \\ \xi \end{bmatrix} + \begin{bmatrix} \boldsymbol{B} \\ 0 \end{bmatrix} u(t) \ + \begin{bmatrix} \boldsymbol{0} \\ 1 \end{bmatrix} r(t) \tag{4-24}$$

Note that at steady state $\dot{\xi}(\mathrm{t}) = 0$ and $\mathrm{y}(\infty) = r$.

$$\begin{bmatrix} \dot{\boldsymbol{x}}(\infty) \\ \dot{\xi}(\infty) \end{bmatrix} = \begin{bmatrix} \boldsymbol{A} & \boldsymbol{0} \\ -\boldsymbol{C} & 0 \end{bmatrix} \begin{bmatrix} \boldsymbol{x}(\infty) \\ \xi(\infty) \end{bmatrix} + \begin{bmatrix} \boldsymbol{B} \\ 0 \end{bmatrix} u(\infty) \ + \begin{bmatrix} \boldsymbol{0} \\ 1 \end{bmatrix} r(\infty) \tag{4-25}$$

Notice that $r(t)$ is a step input and hence, $r(\infty) \ = r(t) \ = r$.

Subtracting Eqn. (4-25) from (4-24) yields,

$$\begin{bmatrix} \dot{\boldsymbol{x}}_{\boldsymbol{e}}(t) \\ \dot{\xi}_e(t) \end{bmatrix} = \begin{bmatrix} \boldsymbol{A} & \boldsymbol{0} \\ -\boldsymbol{C} & 0 \end{bmatrix} \begin{bmatrix} \boldsymbol{x}_{\boldsymbol{e}}(t) \\ \xi_e(t) \end{bmatrix} + \begin{bmatrix} \boldsymbol{B} \\ 0 \end{bmatrix} u_e(t) \tag{4-26}$$

where $\boldsymbol{x}_{\boldsymbol{e}}(\boldsymbol{t}) = \boldsymbol{x}(\boldsymbol{t}) - \boldsymbol{x}(\infty)$ and same definitions are valid for $\xi_{\mathrm{e}}(\mathrm{t})$ and $u_{\mathrm{e}}(t)$.

$$u_{\mathrm{e}}(t) = -\boldsymbol{K}\boldsymbol{x}_{\mathbf{e}}(t) + k_I\xi_{\mathrm{e}}(\mathrm{t}).$$

In more compact form, Eqn. (4-26) can be given as [36],

$$\dot{\boldsymbol{e}} = \widehat{\boldsymbol{A}}\boldsymbol{e} + \widehat{\boldsymbol{B}}u_{\mathrm{e}} \tag{4-27}$$

where

$$\widehat{\boldsymbol{A}} = \begin{bmatrix} \boldsymbol{A} & \boldsymbol{0} \\ -\boldsymbol{C} & 0 \end{bmatrix}, \qquad \widehat{\boldsymbol{B}} = \begin{bmatrix} \boldsymbol{B} \\ 0 \end{bmatrix}, \qquad \boldsymbol{e} = \begin{bmatrix} \boldsymbol{x_e} \\ \xi_e \end{bmatrix}, \quad u_{\mathrm{e}} = -\widehat{\boldsymbol{K}} e \tag{4-28}$$

$$\widehat{\boldsymbol{K}} = [\boldsymbol{K}, -k_I]$$

The error equation of states can be obtained by substituting $u_{\mathrm{e}} = -\widehat{\boldsymbol{K}} e$ into Eqn. (4-27).

$$\dot{\boldsymbol{e}} = (\widehat{\boldsymbol{A}} - \widehat{\boldsymbol{B}}\widehat{\boldsymbol{K}})\boldsymbol{e} \tag{4-29}$$

The desired closed loop poles of the $\widehat{\boldsymbol{A}} - \widehat{\boldsymbol{B}}\widehat{\boldsymbol{K}}$ matrix is specified during the design of the State Feedback (SF) controller in this study. $\boldsymbol{K}$ and k_I are determined by means of pole placement technique.

Note that if the matrix $\begin{bmatrix} \boldsymbol{A} & \boldsymbol{B} \\ -\boldsymbol{C} & 0 \end{bmatrix}$ has rank (n+1), then the system defined by Eqn. (4-29) is completely controllable [36].

In this section, nonlinear and linear equations of longitudinal missile dynamics were derived using 6 DOF motion equations. The brief information about state feedback control were given for completeness.

In the next section, numerical results about SINDY-SAIC algorithm will be presented as prediction comparison. Then, the comparison of the control methods (MPC, NMPC and SF) will be given.

CHAPTER 5

NUMERICAL RESULTS

In this chapter, the results obtained from SINDY-SAIC algorithm will be presented in Prediction Comparison section. Then, the control performance results of the MPC, NMPC and SF controllers will be presented using discovered linear and nonlinear models.

5.1. Prediction Comparison

The prediction performance of SINDY algorithm for the interested dynamical system is presented in this section.

The dynamical systems whose prediction performances are presented is as follows,

1. Longitudinal Linear Missile Dynamics
2. Longitudinal Highly non-linear Missile Dynamics

5.1.1. Linear Missile Dynamics - Longitudinal

The continuous formulation of linear longitudinal missile dynamic derived earlier is given in Eqn. (5-1)

$$\begin{aligned} \dot{\alpha} &= Z_\alpha \alpha + Z_{\delta_e}\delta_e + \left(Z_q + 1\right)q \\ \dot{q} &= M_\alpha \alpha + M_{\delta_e}\delta_e + M_q q \end{aligned} \tag{5-1}$$

where

$$Z_\alpha = -0.4382 \quad Z_{\delta_e} = -0.0243 \quad Z_q = -0.4608$$
$$M_\alpha = -122.5085 \quad M_{\delta_e} = 102.7949 \quad M_q = -1.0823$$

After substituting $[x_1, x_2\,] = [\alpha, q]$ and coefficients, the dynamical equation becomes

$$\begin{aligned} \dot{x}_1 &= -0.4382x_1 + 0.5392x_2 - 0.0243u \\ \dot{x}_2 &= -122.5085x_1 - 1.0823x_2 + 102.7949u \end{aligned} \tag{5-2}$$

The data generation procedure is performed as follows:

1. Dynamics are discretized using the Runge Kutta 4th Order method with time step $T_s = 0.0025$s.
2. Using discretized dynamics, a trajectory data lasting 400 seconds is generated.
3. The initial condition is selected as [5 deg, -30 deg/s],
4. The control input u is generated using

$$u = [0.5sin(5t)sin(0.5t) + 0.1]^{\,3}\,, rad$$

The control input u and the generated measurements angle of attack and pitch rate are given in Figure 5.1, Figure 5.2 and Figure 5.3 respectively for first 50 seconds.

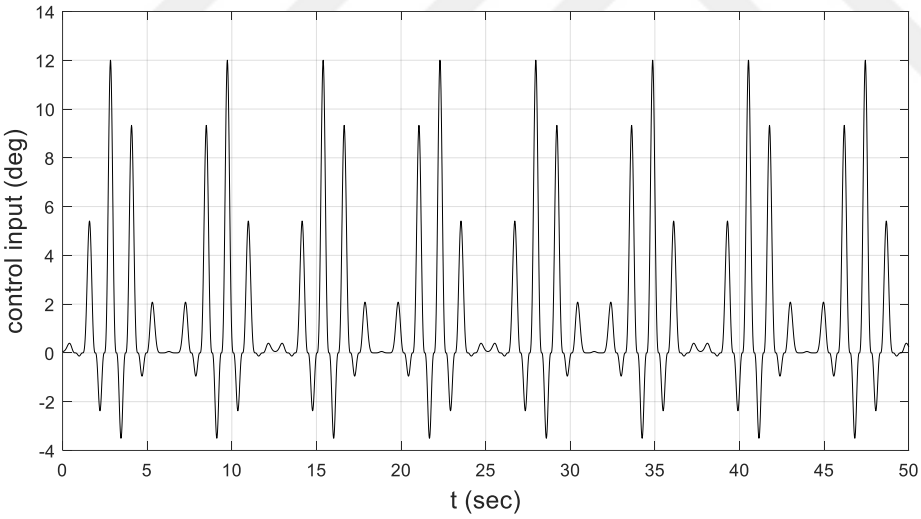

Figure 5.1. Control Input (u)

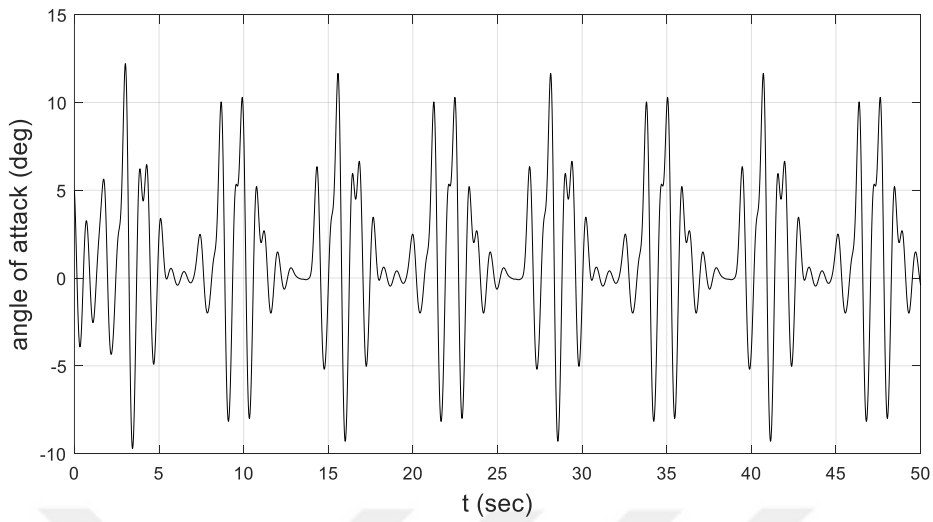

Figure 5.2. Angle of Attack (x_1)

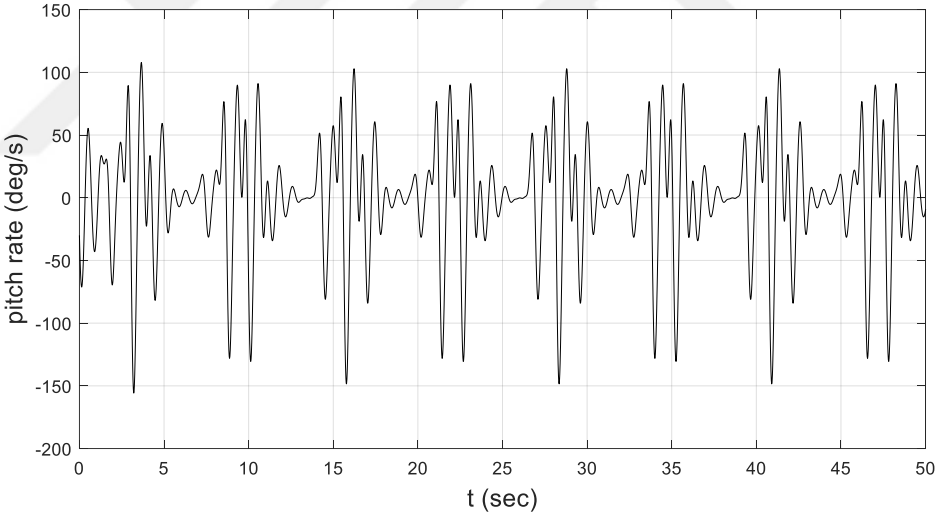

Figure 5.3. Pitch Rate (x_2)

For the linear missile model discovery, 2 cases are studied.

1. Clean State (x) - Clean Derivate ($\dot{x}$) Case
2. Noisy State (x) - Derivative ($\dot{x}$) Calculated from Noisy States Measurements

5.1.1.1. Clean State (x) - Clean Derivative (dx) Case

In this case, it is assumed that states are measured without noise and derivatives are measured directly or calculated from clean state measurements perfectly.

Polynomial orders up to 2 is used to construct the library functions. Number of terms in the discovered model is restricted between 1 to 7. All the models that SINDY generated are given in Table 5.1. According to the AIC scores of these models, the model with the minimum AIC score is selected. As can be seen in Figure 5.4, the minimum AIC scores is obtained for the models with 3 number of terms both for $\dot{x}_1$ and $\dot{x}_2$ equations.

Table 5.1. Candidate models that SINDY generates.

	True model	Number of Terms in the Discovered Model						
		1	2	3	4	5	6	7
	$\dot{x}_1$							
x_1	-0.4382	0	-0.45104	-0.4382	-0.4382	-0.4382	-0.4382	-0.4382
x_2	0.5392	0.535881	0.538839	0.5392	0.5392	0.5392	0.5392	0.5392
u	-0.0243	0	0	-0.0243	-0.0243	-0.0243	-0.0243	-0.0243
${x_1}^2$	0	0	0	0	0	0	-7E-07	-1.6E-06
x_1x_2	0	0	0	0	0	0	0	-1.5E-07
x_1u	0	0	0	0	0	-3.5E-07	1.45E-06	4.83E-06
${x_2}^2$	0	0	0	0	0	0	0	0
x_2u	0	0	0	0	0	0	0	0
u^2	0	0	0	0	-7.2E-07	-4.3E-07	-9.1E-07	-2.4E-06
	$\dot{x}_2$							
x_1	-122.5085	-67.802	-119.873	-122.5085	-122.508	-122.508	-122.508	-122.508
x_2	-1.0823	0	0	-1.0823	-1.0823	-1.0823	-1.0823	-1.0823
u	102.7949	0	96.26163	102.7949	102.7949	102.7949	102.7949	102.7949
${x_1}^2$	0	0	0	0	6.9E-06	1.57E-05	1.79E-05	1.79E-05
x_1x_2	0	0	0	0	0	0	0	0
x_1u	0	0	0	0	0	-2.4E-05	-2.4E-05	-2.4E-05
${x_2}^2$	0	0	0	0	0	0	-5.2E-08	-5.2E-08
x_2u	0	0	0	0	0	0	0	0
u^2	0	0	0	0	0	0	0	1.46E-07

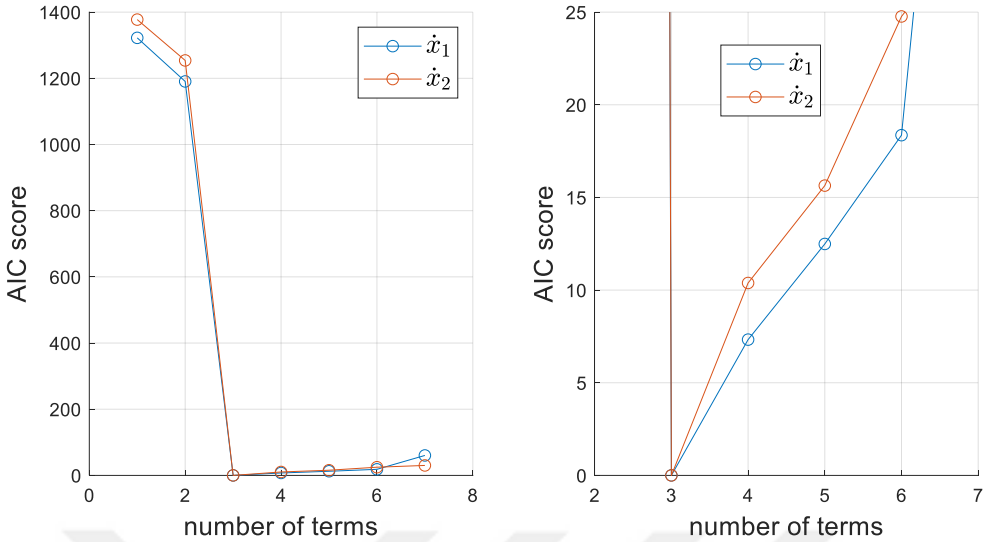

Figure 5.4. AIC scores of the candidate models (the figure on the right is zoomed for better readability)

True model and the selected model parameters are highlighted in Table 5.1. As can be seen all model parameters are discovered with minor error using SINDY. The results of the true and the discovered models are shown in Figure 5.5 for training data. The lines in Figure 5.5 almost completely overlap, as the discovered model parameters match the true model parameters with great precision.

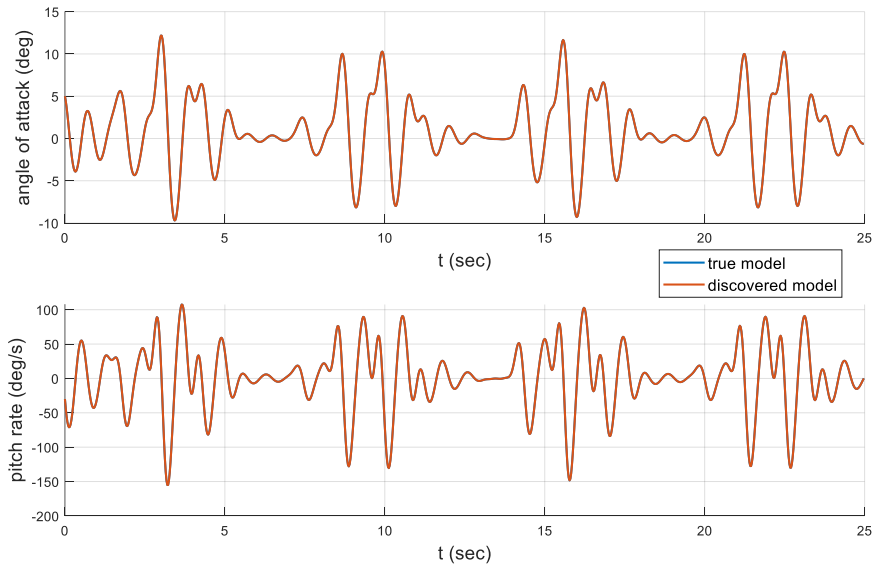

Figure 5.5. Prediction over **training data** of SINDY vs true model for clean measurements

The discovered model should be tested as well for data that the model never seen before. Therefore, the prediction performance of SINDY is given in Figure 5.6 for test data. To generate test data, new set of inputs is used and given in Figure 5.7. It is seen that the model is highly accurate for the test data as well.

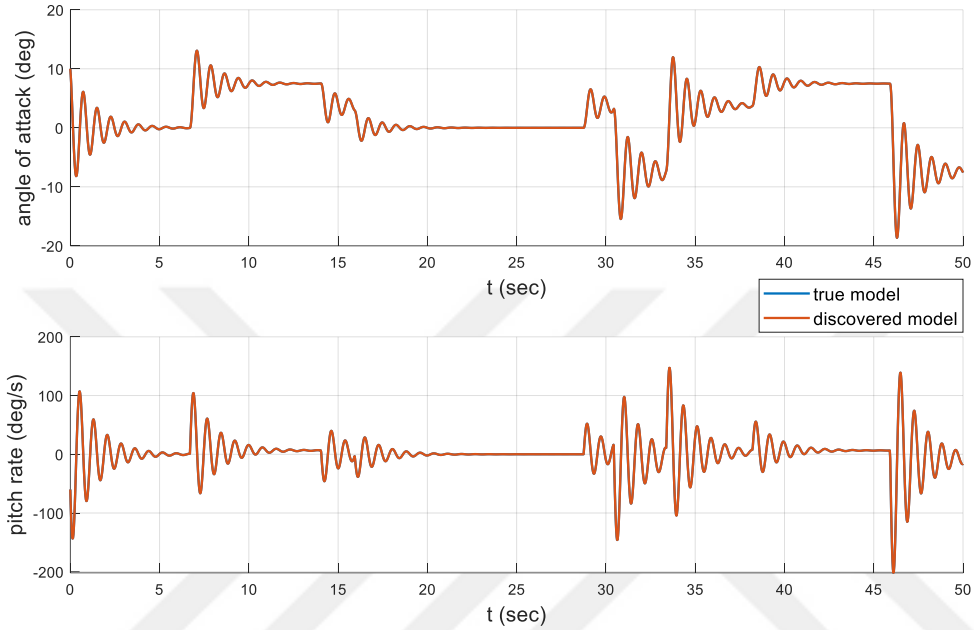

Figure 5.6. Prediction over **test data** of SINDY for clean measurements of states

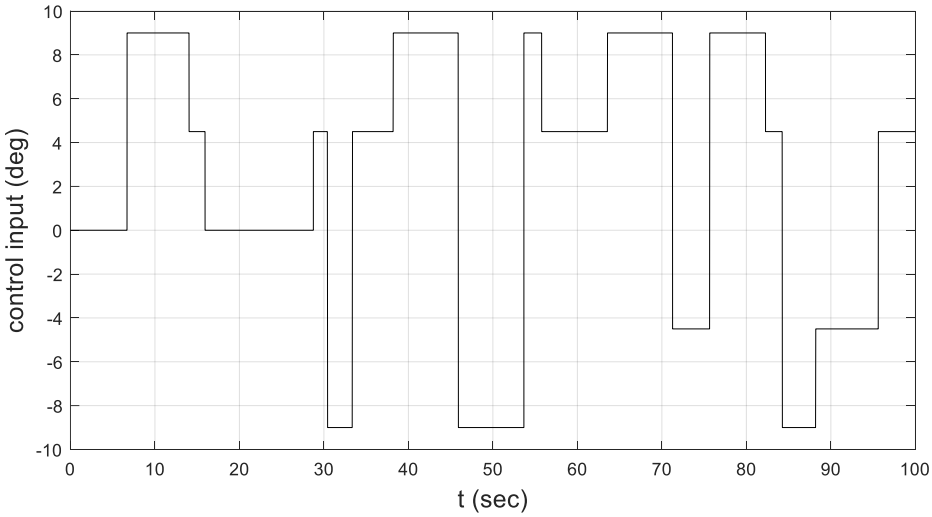

Figure 5.7. Control Input u for the Test Data

Table 5.2. RMSE values for training and test data (clean measurements)

	Root Mean Squared Error (RMSE)	
	x_1	x_2
Training Data	0.00053	0.0076
Test Data	0.00048	0.0072

5.1.1.2. Noisy State (x) - Derivative (dx) Calculated from Noisy Data

In this case, Gaussian noise is added to state measurements and derivatives are calculated with noisy measurements using special technique called sliding window approach. Noisy and clean measurements are given in Figure 5.8.

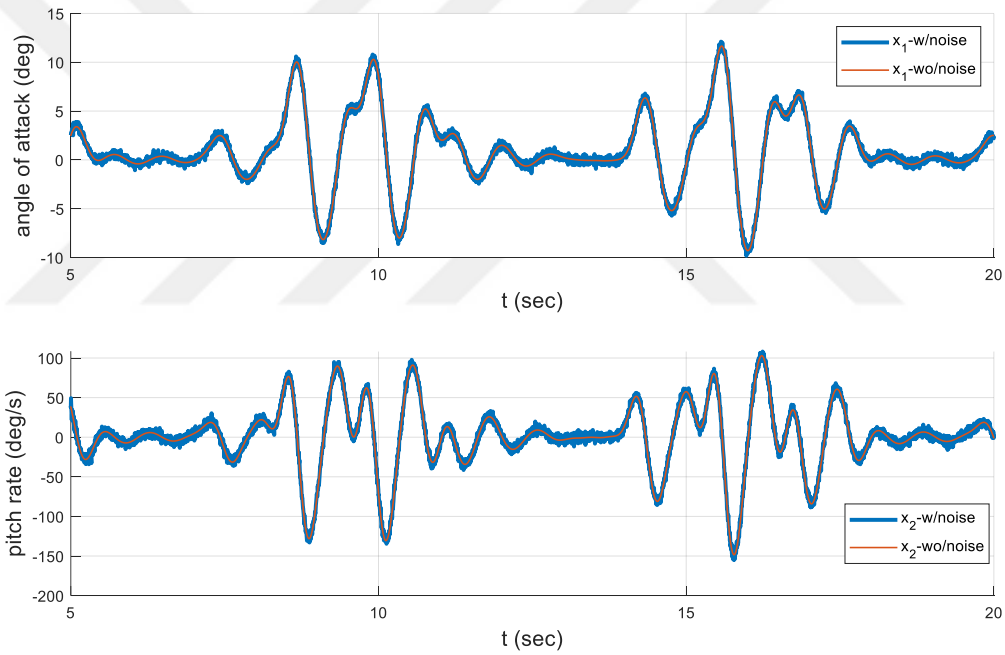

Figure 5.8. State measurements with and without noise

Noise level is calculated as the ratio of L^2 norm of the noise to that of the clean data and given in Eqn. (5-3).

$$noiselevel(\%) = \frac{\left\|x_{noisy} - x_{clean}\right\|_2}{\|x_{clean}\|_2} x100 \tag{5-3}$$

Two noise levels (moderate and high) are used and given in Table 5.3.

Table 5.3. Noise levels for Linear Missile Dynamics

	Noise Level (%) of $\boldsymbol{x_1}$	Noise Level (%) of $\boldsymbol{x_2}$
Clean	0	0
Moderate	6.0	7.7
High	18.1	23.0

.

Polynomial orders up to 3 is used to construct the library functions. Number of terms in the discovered model is restricted between 1 to 7. All the models that SINDY generated are given in Table 5.4.

Table 5.4. Candidate models that SINDY generates (moderate noise level)

		Number of Terms in the Discovered Model						
	True Model	1	2	3	4	5	6	7
		$\dot{x}_1$						
x_1	-0.4382	0	-0.4413	-0.43828	-0.43999	-0.45161	-0.45144	-0.45621
x_2	0.5392	0.532667	0.5356	0.535711	0.535669	0.536512	0.536491	0.53633
u	-0.0243	0	0	0	0	0	0	0
${x_1}^2$	0	0	0	0	0	0	0	0
x_1x_2	0	0	0	0	0	0	0	0
x_1u	0	0	0	0	0	0	0	0
${x_2}^2$	0	0	0	0	0	0	0	0
x_2u	0	0	0	0	0	0	0	-0.13134
u^2	0	0	0	0	0	0	0	0
${x_1}^3$	0	0	0	0	0	0	0	0
${x_1}^2x_2$	0	0	0	0	0	0	0	0
${x_1}^2u$	0	0	0	0	0	0	0	0
$x_1{x_2}^2$	0	0	0	0	0	0	0	0
x_1x_2u	0	0	0	0	0	-0.85899	-0.81243	-1.40003
x_1u^2	0	0	0	0	0.767156	9.595147	9.359713	15.15915
${x_2}^3$	0	0	0	0	0	0	0	0
${x_2}^2u$	0	0	0	0	0	0	0	0
x_2u^2	0	0	0	0	0	0	-0.03851	1.064786
u^3	0	0	0	-0.35735	-0.77426	-3.36561	-3.1842	-6.5649
		$\dot{x}_2$						
x_1	-122.5085	-67.5105	-119.062	-121.647	-121.172	-121.085	-120.065	-120.062
x_2	-1.0823	0	0	-1.06267	-1.06291	-1.06275	-1.06738	-1.07369
u	102.7949	0	95.55336	101.9802	99.95954	99.60682	96.70618	96.73651
${x_1}^2$	0	0	0	0	0	0	-8.1123	-11.6288
x_1x_2	0	0	0	0	0	0	0	0
x_1u	0	0	0	0	0	0	0	13.93773
${x_2}^2$	0	0	0	0	0	0	0	0
x_2u	0	0	0	0	0	0	0	0
u^2	0	0	0	0	11.65835	20.97148	65.26909	54.83435
${x_1}^3$	0	0	0	0	0	0	0	0
${x_1}^2x_2$	0	0	0	0	0	0	0	0
${x_1}^2u$	0	0	0	0	0	0	0	0
$x_1{x_2}^2$	0	0	0	0	0	0	0	0
x_1x_2u	0	0	0	0	0	0	0	0
x_1u^2	0	0	0	0	0	0	0	0
${x_2}^3$	0	0	0	0	0	0	0	0
${x_2}^2u$	0	0	0	0	0	0	0	0
x_2u^2	0	0	0	0	0	0	0	0
u^3	0	0	0	0	0	-43.6794	-197.461	-178.765

According to the AIC scores of these models, the model with the minimum AIC score is selected. As can be seen in Figure 5.9, the minimum AIC scores is obtained for the models with 2 number of terms both for $\dot{x}_1$ and 3 number of terms for $\dot{x}_2$ equations.

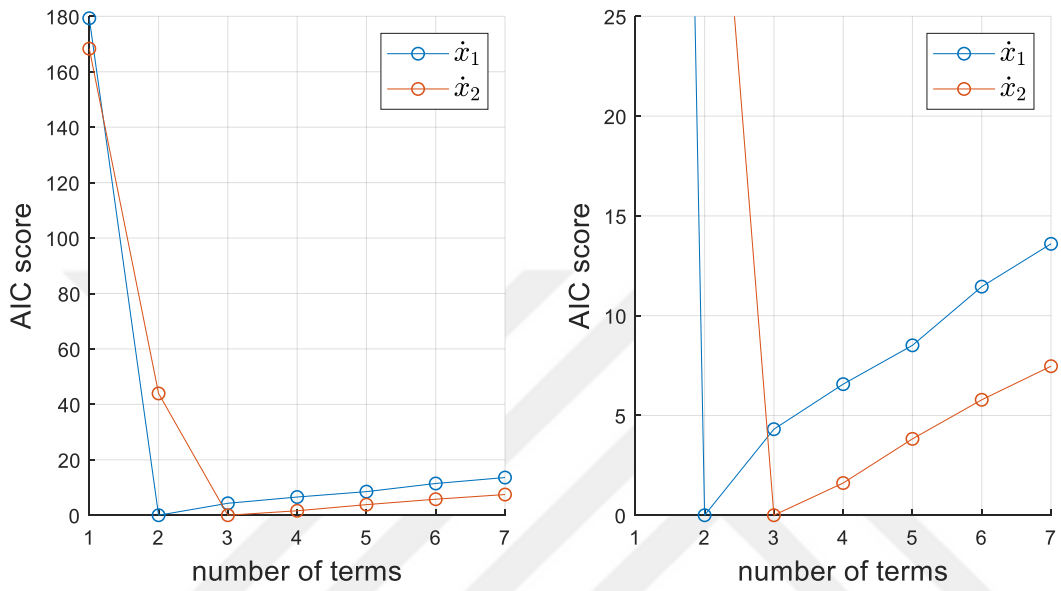

Figure 5.9. AIC scores of the candidate models (the figure on the right is zoomed for better readability)

The selected model and the true model parameters are highlighted in Table 5.4. There is only one major difference between discovered and the true model. It is seen that SINDY could not find the coefficient of the term “u” which exists in the true model in $\dot{x}_1$ equation.

If the discovered model for $\dot{x}_1$ equation having same number of terms with true model is analyzed, it is seen that additional discovered term (u^3) does not exist in the true model. Note that true model has "u" term as a third active parameter. Therefore, the algorithm selected the sparse solution that is having two terms even though it was missing one parameter. When the output of the discovered model is compared with

the true model (see Figure 5.10), it is understood that the effect of missing term is not very significant. The prediction performance for training set is given in Figure 5.10.

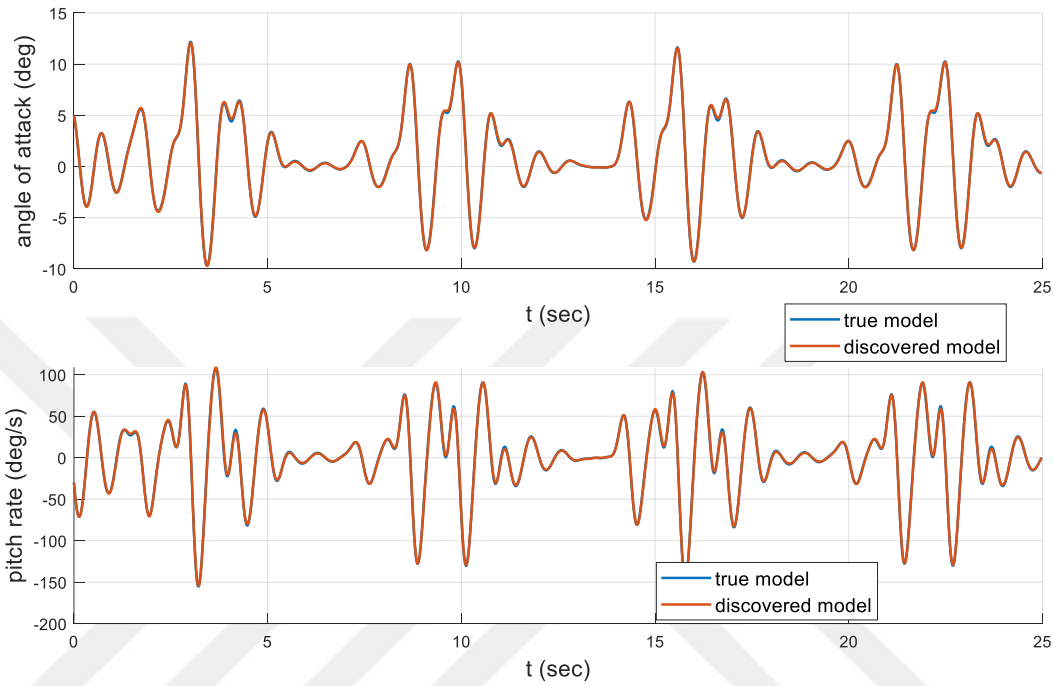

Figure 5.10. Prediction over **training data** of SINDY vs true model for noisy measurements of states and calculated derivatives

On the other hand, the best way to see if there is really a significant difference between the true model and the prediction model is to compare the results of the test data. The prediction performance of SINDY is given in Figure 5.11. It is seen that the model is highly accurate for the test data as well. The input used for test data is given in Figure 5.7

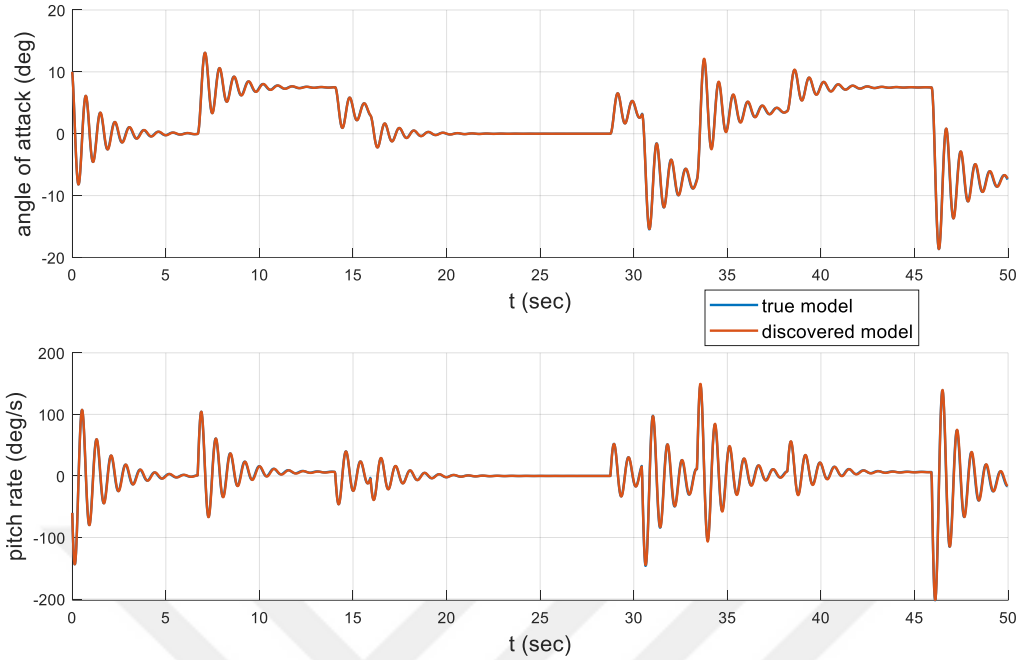

Figure 5.11. Prediction over **test data** of SINDY vs true model for noisy measurements of states

Note that SINDY captures the dynamics accurately in both clean and noisy measurements for linear missile dynamics. It is observed that differentiation using sliding window approach significantly increases the robustness of SINDY to noisy data. The RMSE values is given in Table 5.5. Compared to clean data case, the RSME values increased approximately 3 times for training data and 4 times for test data, however still the performance of the identified model is very satisfactory for prediction.

Table 5.5. RMSE values for training and test data (moderate noise)

	Root Mean Squared Error (RMSE)	
	x_1	x_2
Training Data	0.0016	0.0251
Test Data	0.0021	0.0324

Next, noise level has increased to high noise level to examine the system's performance more clearly under different noise levels. The measurements which is clean and having moderate and high level of noise is given in Figure 5.12.

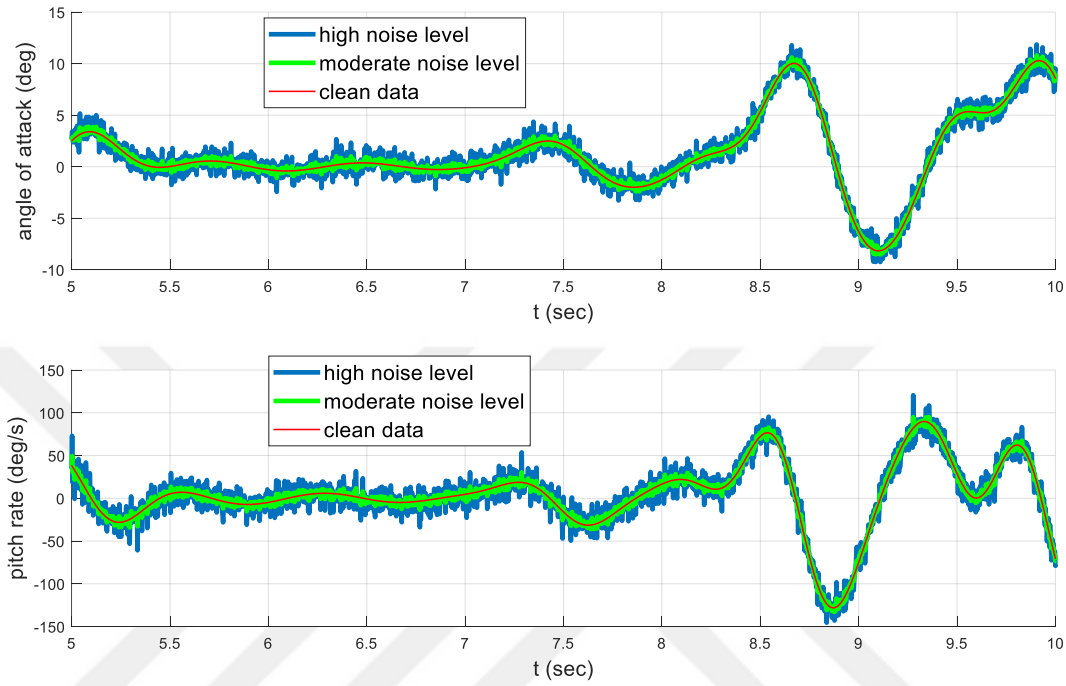

Figure 5.12. State measurements with different noise levels

Table 5.6. True and discovered model for high level of noise

	True Model	Discovered Model
	$\dot{x}_1$	
x_1	-0.4382	-0.4719
x_2	0.5392	0.5085
u	-0.0243	0
${x_1}^2 u$	0	7.9094
	$\dot{x}_2$	
x_1	-122.5085	-114.4319
x_2	-1.0823	-0.9413
u	102.7949	94.8600

The discovered model using SINDY under high level of noise is given in Table 5.6. The parameters having zero coefficient are not displayed. The prediction result on test data is shown in Figure 5.14. It is seen that SINDY is able to capture important dynamics of the system even under high level of noise. In addition, prediction performance on training and test set is acceptable especially for short term predictions (Figure 5.13 and Figure 5.14). Therefore, the discovered model is tried to be used for MPC that requires short term predictions.

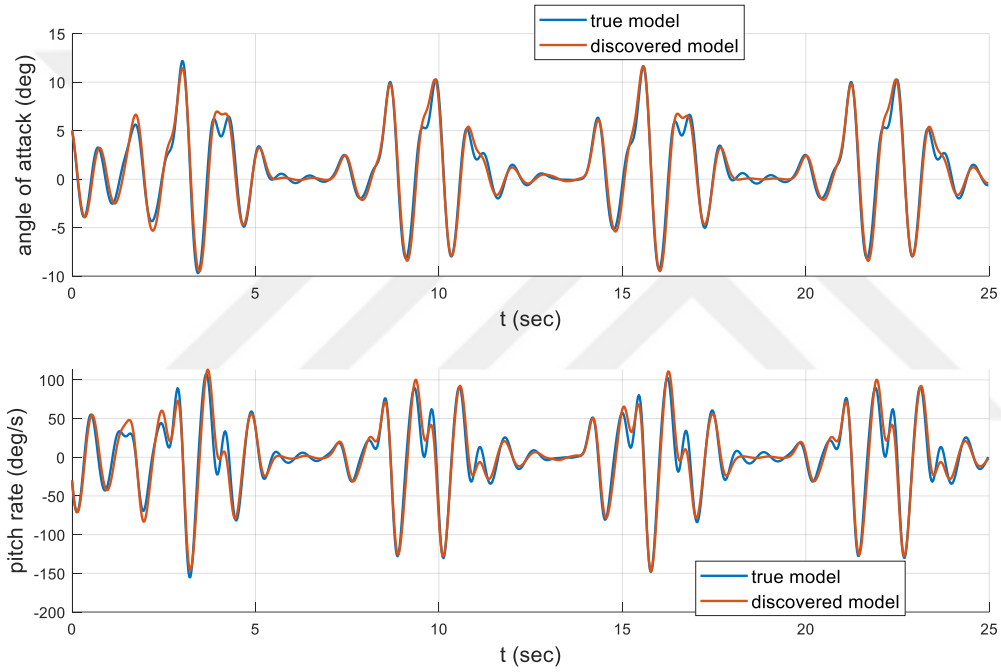

Figure 5.13. Prediction over **training data** of SINDY vs true model for high level of noise

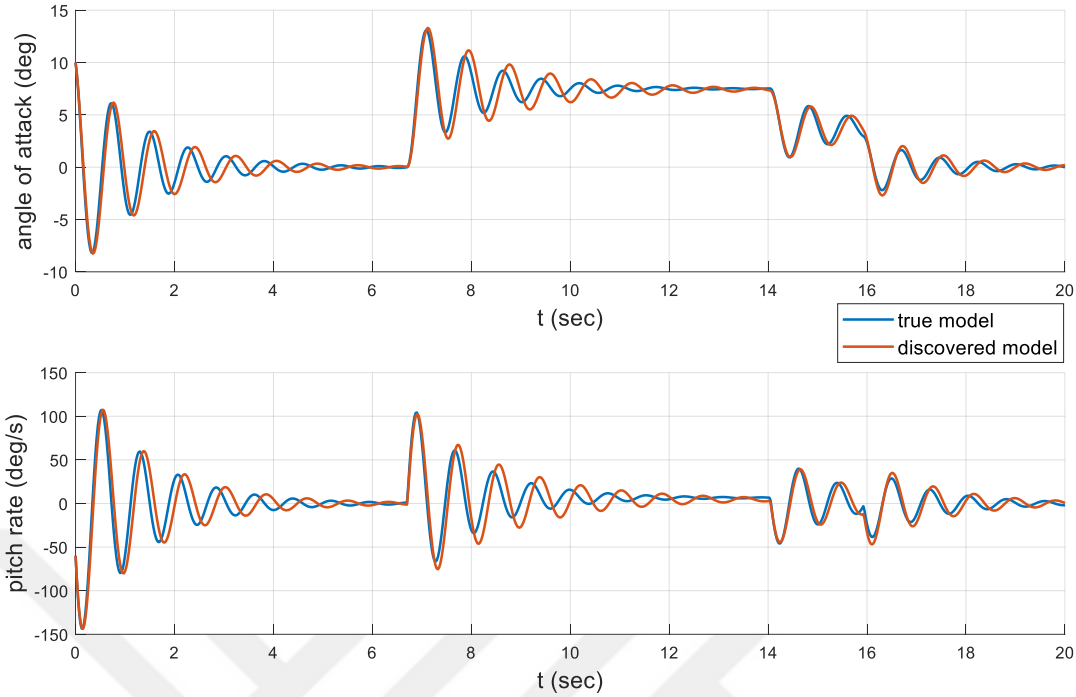

Figure 5.14. Prediction over **test data** of SINDY vs true model for high level of noise

The RSME values are given in Table 5.7. Note that the RMSE increased 6-7 times that of moderate level of noise.

Table 5.7. RSME values for high level of noise

	Root Mean Squared Error (RMSE)	
	x_1	x_2
Training Data	0.0113	0.1785
Test Data	0.0208	0.3110

5.1.2. Highly Nonlinear Missile Dynamics – Longitudinal

The continuous formulation of nonlinear longitudinal missile dynamic derived earlier is given in Eqns. (5-4) and (5-5).

$$\dot{\alpha} = Z_\alpha \alpha + Z_{\delta_e}\delta_e + (Z_q + 1)q + Z_{\alpha_2}\alpha^2 + Z_{\alpha_3}\alpha^3 + Z_{\alpha_2\delta_e}\alpha^2\delta_e + Z_{q\alpha_2}q\alpha^2 \tag{5-4}$$

$$\dot{q} = M_\alpha \alpha + M_{\delta_e}\delta_e + M_q q + M_{\alpha_2}\alpha^2 + M_{\alpha_3}\alpha^3 + M_{q\delta_{e_2}} q {\delta_e}^2 \tag{5-5}$$

where

$$Z_\alpha = -0.4382 \qquad Z_{\delta_e} = -0.0243 \qquad Z_q = -0.4608$$
$$Z_{\alpha_2} = -0.2 \qquad Z_{\alpha_3} = 4.5 \qquad Z_{\alpha_2\delta_e} = 25.0$$
$$Z_{q\alpha_2} = -1.2 \qquad M_\alpha = -122.5085 \qquad M_{\delta_e} = 102.7949$$
$$M_q = -1.0823 \qquad M_{\alpha_2} = -120 \qquad M_{\alpha_3} = -30$$
$$M_{q\delta_{e_2}} = 20.0$$

After substituting $[x_1, x_2] = [\alpha, q]$ and coefficients, the dynamical equation becomes

$$\begin{aligned} \dot{x}_1 &= -0.4382x_1 + 0.5392x_2 - 0.0243u - 0.2{x_1}^2 - 1.2{x_1}^2x_2 + 4.5{x_1}^3 + 100{x_1}^2u \\ \dot{x}_2 &= -122.5085x_1 + 1.0823x_2 + 102.7949u - 120{x_1}^2 - 30{x_1}^3 + 20x_2u^2 \end{aligned} \tag{5-6}$$

The data generation procedure is performed as follows:

1. Dynamics are discretized using the Runge Kutta 4th Order method with time step Ts=0.0025s.
2. Using discretized dynamics, a trajectory data lasting 400 seconds is generated.
3. The initial condition is selected as [5 deg, -30 deg/s],
4. The control input u is generated using

$$u = [0.5sin(5t)sin(0.5t) + 0.1]^3, rad$$

The control input u and the generated measurements angle of attack and pitch rate are given in Figure 5.15, Figure 5.16 and Figure 5.17 respectively for first 50 seconds.

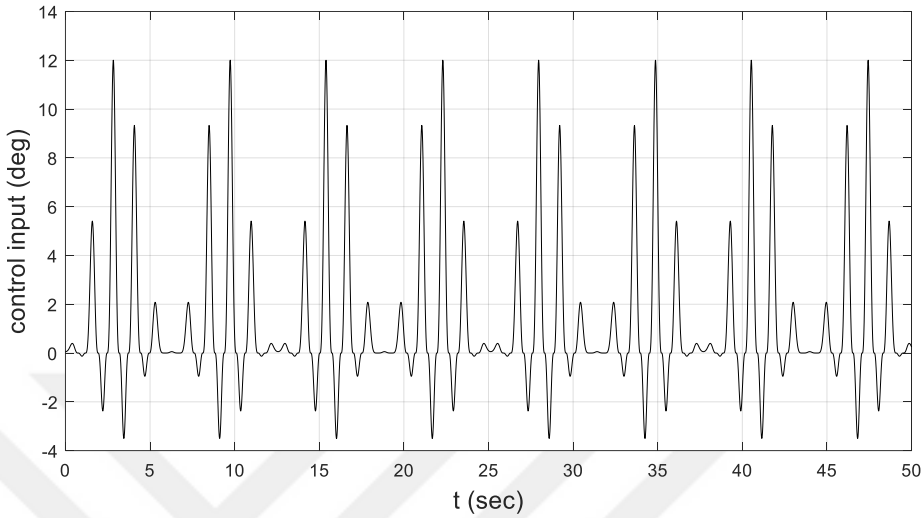

Figure 5.15. Control Input (u)

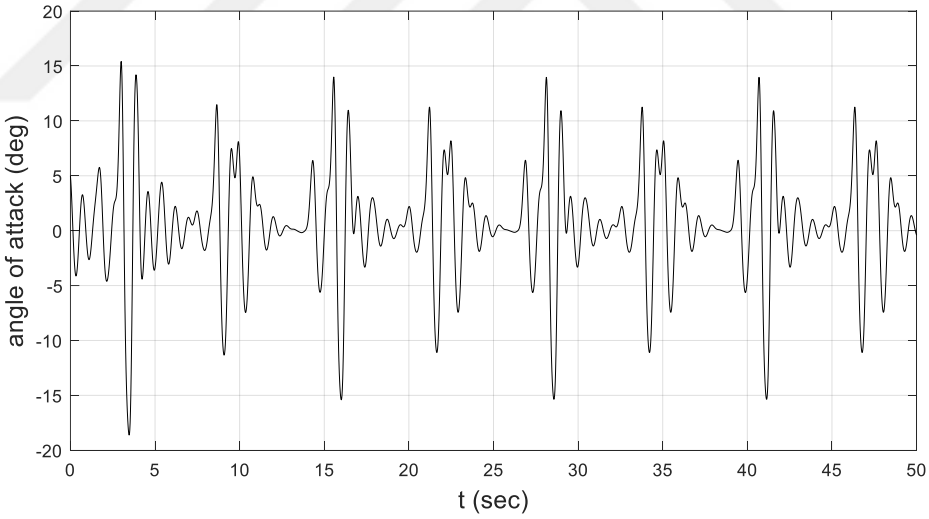

Figure 5.16. Angle of Attack (x_1)

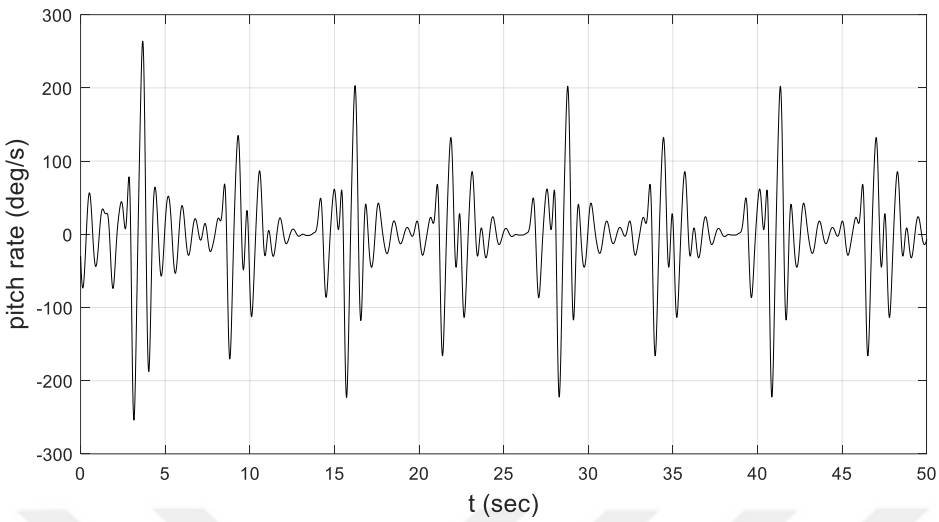

Figure 5.17. Pitch Rate (x_2)

For the non-linear missile model, 2 cases are studied which are:

1. Clean State (x) - Clean Derivate ($\dot{x}$) Case
2. Noisy State (x) - Derivative ($\dot{x}$) Calculated from Noisy States Measurements

5.1.2.1. Clean State (x) - Clean Derivative (dx) Case

In this case, it is assumed that states are measured without noise and derivatives are measured directly or calculated from clean state measurements perfectly.

Polynomial orders up to 3 is used to construct the library functions. Number of terms in the discovered model is restricted between 1 to 10. All the models that SINDY generated are given in Table 5.8 and Table 5.9. According to the AIC scores of these models, the model with the minimum AIC score is selected. As can be seen in Figure 5.18, the minimum AIC scores is obtained for the models containing 6 number of terms for both $\dot{x}_1$ and $\dot{x}_2$ equations.

Table 5.8. Candidate models that SINDY generates for $\dot{x}_1$ (clean data)

		Number of Terms in the Discovered Model									
	True Model	1	2	3	4	5	6	7	8	9	10
		$\dot{x}_1$									
x_1	-0.4382	0	0	-0.3134	-0.3520	-0.4583	-0.4495	-0.4382	-0.4382	-0.4382	-0.4382
x_2	0.5392	0.5177	0.5253	0.5240	0.5407	0.5392	0.5392	0.5392	0.5392	0.5392	0.5392
u	-0.0243	0	0	0	0	0	0	-0.0243	-0.0243	-0.0243	-0.0243
${x_1}^2$	-0.2	0	0	0	0	0	-0.190	-0.200	-0.200	-0.200	-0.200
x_1x_2	0	0	0	0	0	0	0	0	0	0	0
x_1u	0	0	0	0	0	0	0	0	0	0	1.7E-06
${x_2}^2$	0	0	0	0	0	0	0	0	0	0	0
x_2u	0	0	0	0	0	0	0	0	0	0	0
u^2	0	0	0	0	0	0	0	0	0	-1.5E-06	-1.8E-06
${x_1}^3$	4.5	0	0	0	0	5.888	4.927	4.500	4.5000	4.5000	4.5000
${x_1}^2x_2$	-1.2	0	0	0	-1.384	-1.183	-1.197	-1.200	-1.2000	-1.2000	-1.2000
${x_1}^2u$	100	0	88.15	107.0	103.7	96.79	98.77	100.0	100.0	99.99	99.99
$x_1{x_2}^2$	0	0	0	0	0	0	0	0	0	0	0
x_1x_2u	0	0	0	0	0	0	0	0	0	0	0
x_1u^2	0	0	0	0	0	0	0	0	2.7E-05	3.9E-05	3.6E-05
${x_2}^3$	0	0	0	0	0	0	0	0	0	0	0
${x_2}^2u$	0	0	0	0	0	0	0	0	0	0	0
x_2u^2	0	0	0	0	0	0	0	0	0	0	0
u^3	0	0	0	0	0	0	0	0	0	0	0

Table 5.9. Candidate models that SINDY generates for $\dot{x}_2$ (clean data)

		Number of Terms in the Discovered Model									
	True Model	1	2	3	4	5	6	7	8	9	10
		$\dot{x}_2$									
x_1	-122.5085	-78.3	-116.1	-121.5	-123.6	-123.5	-122.5	-122.5	-122.5	-122.5	-122.5
x_2	-1.0823	0	0	0	-1.032	-1.078	-1.082	-1.082	-1.082	-1.082	-1.082
u	102.7949	0	90.92	101.71	103.41	103.05	102.79	102.79	102.79	102.79	102.79
${x_1}^2$	-120	0	0	-115.9	-118.05	-118.87	-120.00	-120.00	-120.00	-120.00	-120.00
x_1x_2	0	0	0	0	0	0	0	0	0	0	0
x_1u	0	0	0	0	0	0	0	0	0	0	0
${x_2}^2$	0	0	0	0	0	0	0	0	-4.5E-08	-4.3E-08	-4.3E-08
x_2u	0	0	0	0	0	0	0	0	0	0	0
u^2	0	0	0	0	0	0	0	0	0	0	0
${x_1}^3$	-30	0	0	0	0	0	-30.00	-30.00	-30.000	-30.00	-30.000
${x_1}^2x_2$	0	0	0	0	0	0	0	0	0	0	0
${x_1}^2u$	0	0	0	0	0	0	0	0	0	0	0
$x_1{x_2}^2$	0	0	0	0	0	0	0	0	0	0	0
x_1x_2u	0	0	0	0	0	0	0	0	0	-1.4E-05	-1.4E-05
x_1u^2	0	0	0	0	0	0	0	-0.0002	-0.0002	-0.0002	-0.0002
${x_2}^3$	0	0	0	0	0	0	0	0	0	0	0
${x_2}^2u$	0	0	0	0	0	0	0	0	0	0	0
x_2u^2	20	0	0	0	0	19.92	20.00	20.00	20.000	20.000	20.000
u^3	0	0	0	0	0	0	0	0	0	0	4.1E-05

It is obvious that for $\dot{x}_1$ equation, model having 7 number of terms instead of 6 would be a better choice (see Table 5.8). However, missing term has little effect on system

performance as can be seen in the top of the Figure 5.19. The algorithm selected most sparse solution among the models having nearly same error magnitudes as expected.

For $\dot{x}_2$ equation, model having 6 number of terms which is same as the true model is selected. The discovered and the true model parameters are almost identical with the minor differences.

Finally, true model and the selected model parameters is highlighted in Table 5.8 and Table 5.9. As can be seen all model parameters are discovered with minor error using SINDY.

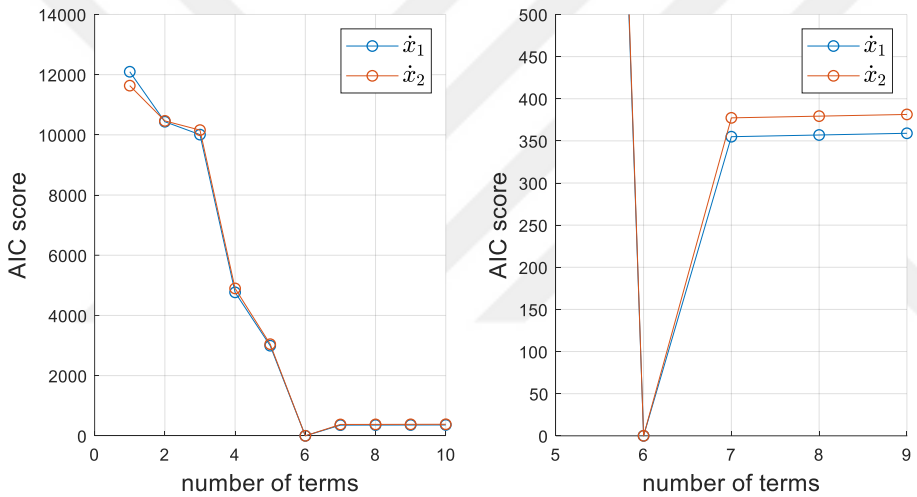

Figure 5.18. AIC scores of the candidate models (the figure on the right is zoomed for better readability)

The results of the true and the discovered models are shown in Figure 5.19 for training data. The lines almost completely overlap, as the discovered model parameters match the true model parameters with great precision.

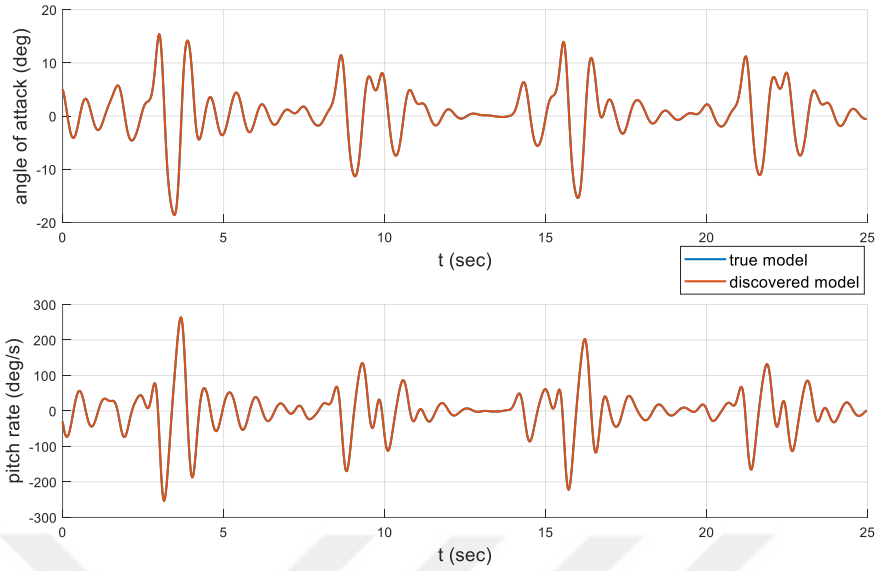

Figure 5.19. Prediction over **training data** of SINDY vs true model for clean measurements of states and derivatives

The discovered model should be tested as well for data that the model never seen before. Therefore, the prediction performance of SINDY is given in Figure 5.20 for test data. To generate test data, new set of inputs is used and given in Figure 5.7. It is seen that the model is highly accurate for the test data as expected.

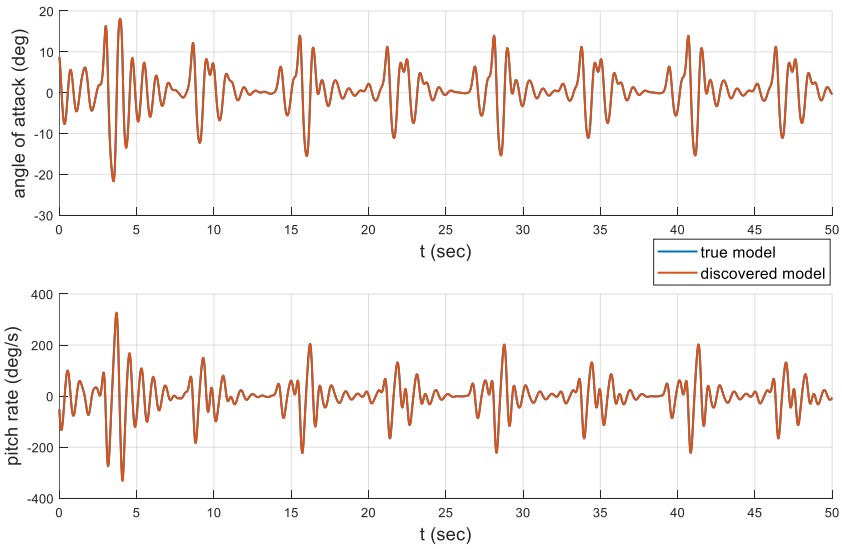

Figure 5.20. Prediction over **test data** of SINDY for clean measurements of states

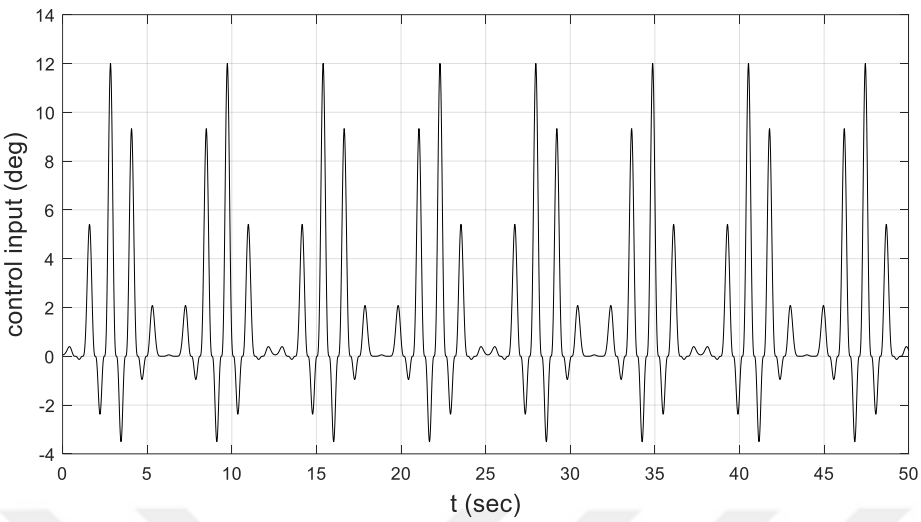

Figure 5.21. Control Input u for the Test Data

Table 5.10. RMSE values for training and test data

	Root Mean Squared Error (RMSE)	
	$\boldsymbol{x_1}$	$\boldsymbol{x_2}$
Training Data	0.00058	0.00852
Test Data	0.00123	0.01880

5.1.2.2. Noisy State (x) - Derivative (dx) Calculated from Noisy Data

In this case, gaussian noise is added to state measurements and derivatives are calculated with noisy measurements using special technique called sliding window approach. Noisy and clean measurements are given in Figure 5.22.

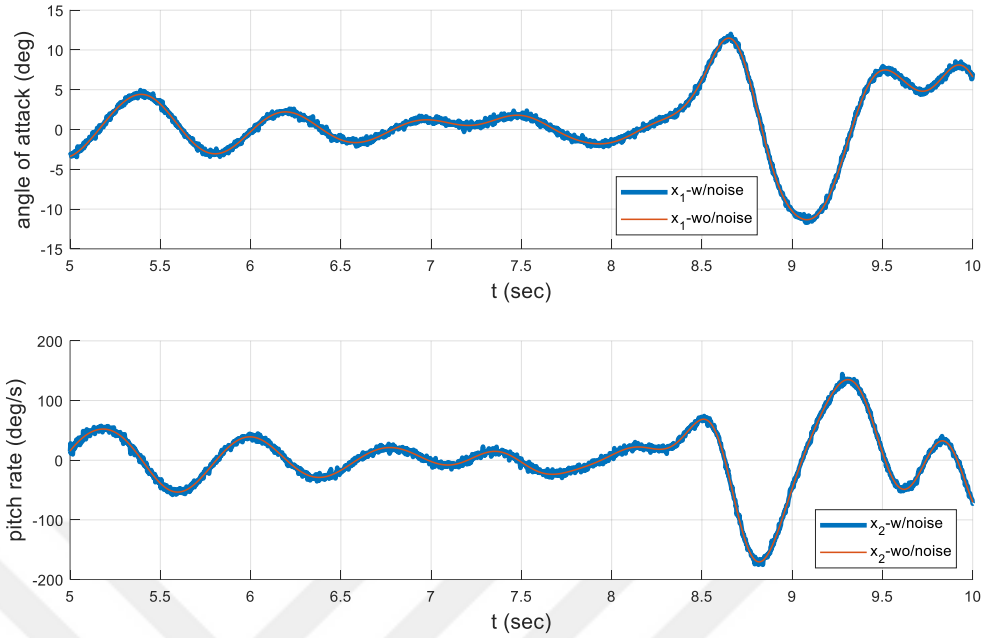

Figure 5.22. State measurements with and without noise

Two noise levels (moderate and high) are used and given in Table 5.11.

Table 5.11. Noise levels for Non-Linear Missile Dynamics

	Noise Level (%) of x_1	Noise Level (%) of x_2
Clean	0	0
Moderate	5.2	6.0
High	12.9	15.0

.

Polynomial orders up to 3 is used to construct the library functions. Number of terms in the discovered model is restricted between 1 to 10. All the models that SINDY generated are given in Table 5.12 and Table 5.13.

Table 5.12. Candidate models that SINDY generates for $\dot{x}_1$ (moderate noise level)

		Number of Terms in the Discovered Model									
	True Model	1	2	3	4	5	6	7	8	9	10
		$\dot{x}_1$									
x_1	-0.4382	0	0	-0.3033	-0.3411	-0.4454	-0.4454	-0.4462	-0.4447	-0.4334	-0.4230
x_2	0.5392	0.5157	0.5232	0.5220	0.5382	0.5368	0.5368	0.5367	0.5340	0.5340	0.5341
u	-0.0243	0	0	0	0	0	0	0	0	0	-0.0295
${x_1}^2$	-0.2	0	0	0	0	0	0	0	0	-0.1998	-0.2022
x_1x_2	0	0	0	0	0	0	0	0	0	0	0
x_1u	0	0	0	0	0	0	0	0	0	0	0
${x_2}^2$	0	0	0	0	0	0	0	0	0	0	0
x_2u	0	0	0	0	0	0	0	0	0	0	0
u^2	0	0	0	0	0	0	0	0	0	0	0
${x_1}^3$	4.5	0	0	0	0	5.7781	5.7728	6.0656	6.3389	5.1764	4.8038
${x_1}^2x_2$	-1.2	0	0	0	-1.3472	-1.1508	-1.1508	-1.1564	-1.1459	-1.1600	-1.1615
${x_1}^2u$	100	0	87.7066	105.9054	102.7670	95.9496	95.9749	93.7895	91.6935	94.2458	95.9758
$x_1{x_2}^2$	0	0	0	0	0	0	0	0	0	0	0
x_1x_2u	0	0	0	0	0	0	0	0	0	0	0
x_1u^2	0	0	0	0	0	0	-0.0215	3.5795	6.4831	6.7106	4.6737
${x_2}^3$	0	0	0	0	0	0	0	0	0.0004	0.0004	0.0004
${x_2}^2u$	0	0	0	0	0	0	0	0	0	0	0
x_2u^2	0	0	0	0	0	0	0	0	0	0	0
u^3	0	0	0	0	0	0	0	-1.3513	-2.2116	-2.6989	-1.3475

Table 5.13. Candidate models that SINDY generates for $\dot{x}_2$ (moderate noise level)

		Number of Terms in the Discovered Model									
	True Model	1	2	3	4	5	6	7	8	9	10
		$\dot{x}_2$									
x_1	-122.5085	-78.1146	-115.6962	-120.8325	-122.9857	-122.9884	-121.4774	-121.1278	-120.9452	-120.9481	-120.8499
x_2	-1.0823	0	0	0	-1.0204	-1.0666	-1.0730	-1.0741	-1.0773	-1.0772	-1.0761
u	102.7949	0	90.5177	101.2121	102.9230	102.5359	102.1638	100.4928	99.5841	99.5489	98.9839
${x_1}^2$	-120	0	0	-115.0204	-117.1365	-117.9593	-119.5889	-120.2380	-121.3184	-121.6700	-119.7359
x_1x_2	0	0	0	0	0	0	0	0	0	0	0
x_1u	0	0	0	0	0	0	0	0	0	0	-13.3255
${x_2}^2$	0	0	0	0	0	0	0	0	0	0	0
x_2u	0	0	0	0	0	0	0	0	0	0	0
u^2	0	0	0	0	0	0	0	10.3742	29.2113	28.9525	44.5411
${x_1}^3$	-30	0	0	0	0	0	-43.5719	-44.5802	-44.6968	-47.7719	-50.0045
${x_1}^2x_2$	0	0	0	0	0	0	0	0	0	0	0
${x_1}^2u$	0	0	0	0	0	0	0	0	0	0	0
$x_1{x_2}^2$	0	0	0	0	0	0	0	0	0	0	0
x_1x_2u	0	0	0	0	0	0	0	0	0	0	0
x_1u^2	0	0	0	0	0	0	0	0	0	40.2827	110.2658
${x_2}^3$	0	0	0	0	0	0	0	0	0	0	0
${x_2}^2u$	0	0	0	0	0	0	0	0	0	0	0
x_2u^2	20	0	0	0	0	20.0004	20.1120	19.1744	19.7179	19.0022	18.9180
u^3	0	0	0	0	0	0	0	0	-78.3029	-95.7587	-166.547

Based on the AIC scores of these models, the model having minimum AIC score is selected. As can be seen in Figure 5.23, the minimum AIC scores is obtained for the models with 5 number of terms both for $\dot{x}_1$ and $\dot{x}_2$ equations.

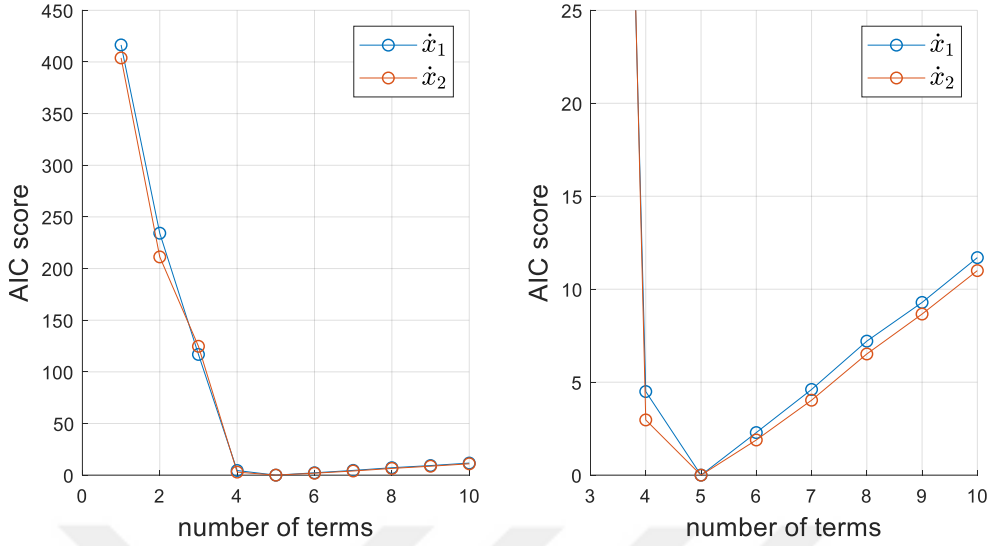

Figure 5.23. AIC scores of the candidate models (the figure on the right is zoomed for better readability)

The selected model and the true model parameters are highlighted in Table 5.12. There are three differences between discovered and the true model. It is seen that SINDY could not find the coefficient of the term u and x_1^2 for the $\dot{x}_1$ equation and could not found a coefficient belonging to the term x_1^3 for $\dot{x}_2$ equation. However, when the output of the discovered model is compared with the true model (see Figure 5.10), it is understood that the effect of these terms is not very significant. The prediction performance for training set is given in Figure 5.24.

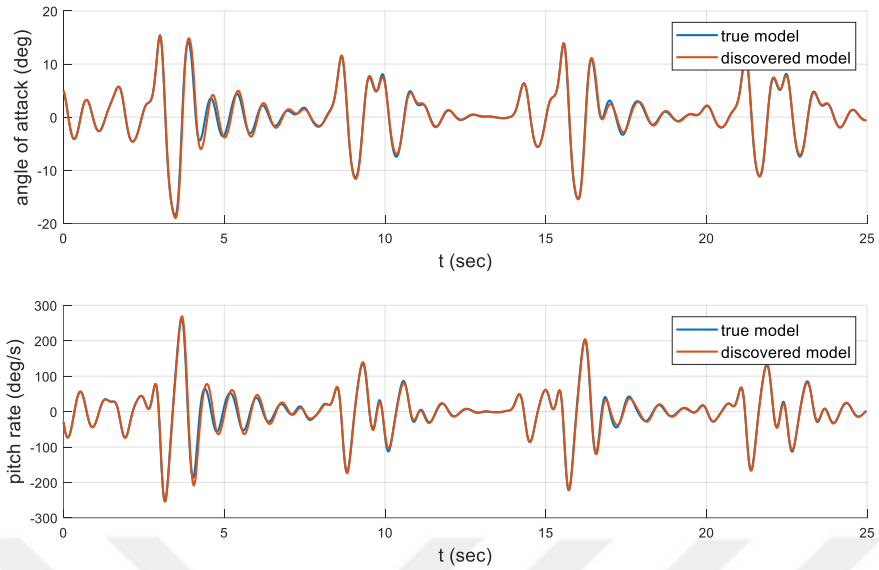

Figure 5.24. Prediction over **training data** of SINDY vs true model for noisy measurements of states and calculated derivatives

On the other hand, the best way to see if there is really a significant difference between the true model and the prediction model is to compare the results of the test data. The prediction performance of SINDY is given in Figure 5.25. It is seen that the model is highly accurate for the test data as well. The input used for test data is given in Figure 5.21.

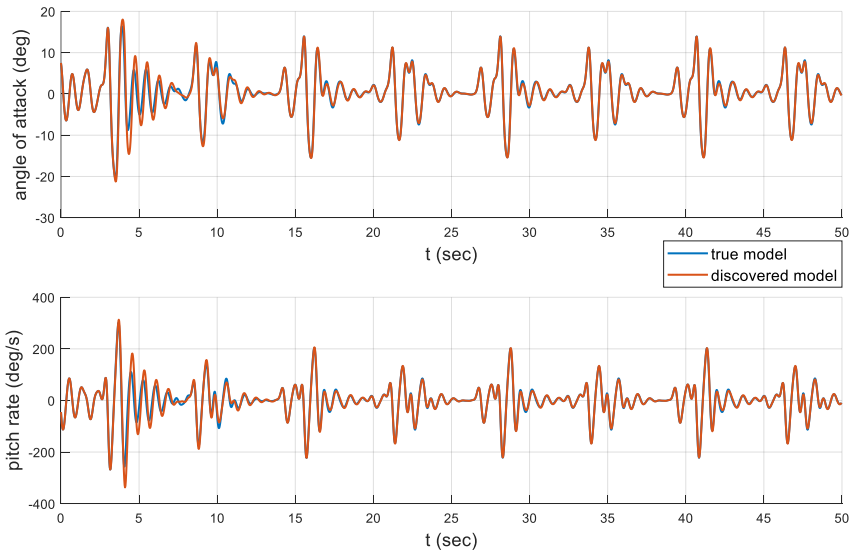

Figure 5.25. Prediction over **test data** of SINDY vs true model for noisy measurements of states

As can be seen SINDY captures the dynamics accurately in both clean and noisy measurements for non-linear missile dynamics. It is observed that differentiation using sliding window approach significantly increases the robustness of SINDY to noisy data. The RMSE values are given in Table 5.14. Compared to clean data case, the RSME values increased approximately 6 times for training and test data, however still the performance of the identified model is very satisfactory for long term predictions.

Table 5.14. RMSE values for training and test data (moderate noise level)

	Root Mean Squared Error (RMSE)	
	x_1	x_2
Training Data	0.0042	0.0650
Test Data	0.0168	0.2562

The level of noise is increased from moderate to high to test SINDY algorithm under different noise levels for non-linear systems.

Table 5.15. True and discovered model for high level of noise

	True Model	**Discovered Model**
	$\dot{x}_1$	
x_1	-0.4382	-0.3981
x_2	0.5392	0.5085
u	-0.0243	0
${x_1}^2$	-0.2	0
${x_1}^3$	4.5	5.4889
${x_1}^2 x_2$	-1.2	-0.9221
${x_1}^2 u$	100	91.9266
	$\dot{x}_2$	
x_1	-122.5085	-119.7355
x_2	-1.0823	-0.9822
u	102.7949	99.3816
${x_1}^2$	-120	110.1007
${x_1}^3$	-30	0
$x_2 u^2$	20	0

The discovered model using SINDY under high level of noise is given in Table 5.15. The parameters having zero coefficient are not displayed. SINDY capture the 9 terms out of 13 successfully with at most 10% error. The prediction result on training and test data are shown in Figure 5.26 and Figure 5.27. It is seen that SINDY can capture important dynamics of the system even under high level of noise. Prediction performance on test set is acceptable especially for short term predictions (Figure 5.27). Therefore, the discovered model is tried to be used for MPC that requires short term predictions.

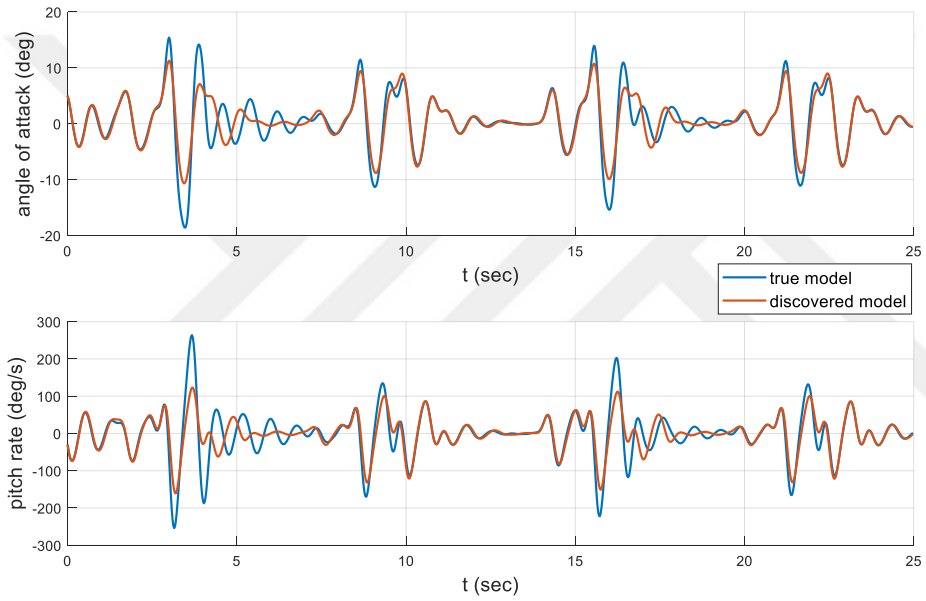

Figure 5.26. Prediction over **training data** of SINDY vs true model for high level of noise

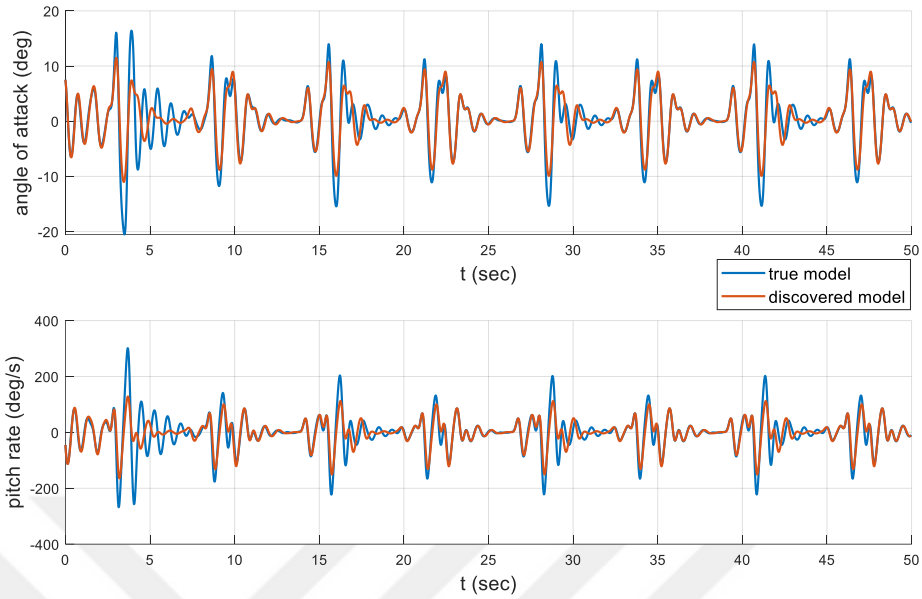

Figure 5.27. Prediction over **test data** of SINDY vs true model for high level of noise

The RSME values are given in Table 5.16. Note that the RMSE increased 4-5 times that of moderate level of noise.

Table 5.16. RSME values for high level of noise

	Root Mean Squared Error (RMSE)	
	x_1	x_2
Training Data	0.0298	0.4816
Test Data	0.0386	0.6220

5.1.3. Comparison of SINDY-SAIC with Sequential Threshold Least Square SINDY (SINDY-T) Algorithm

Finally, prediction performance of the proposed SINDY-SAIC algorithm is compared with the commonly used SINDY-T algorithm in [18] for moderate noise level. The comparison will be in terms of RMSE values and the execution time of the algorithms.

The discovered model parameters of both methods and their percent error in model parameters are given in Table 5.17 and Table 5.18 for $\dot{x}_1$ and $\dot{x}_2$ equations respectively. It is seen that both methods successfully discovered the important dynamics. However, for the examined dynamical system, SINDY- SAIC has slightly lover percent error in some of the coefficients for $\dot{x}_2$ equation. Furthermore, SINDY-SAIC captures the dynamics related to x_2u^2 term successfully whereas SINDY-T does not.

Table 5.17. Comparison of SINDY methods for $\dot{x}_1$

	$\dot{x}_1$			% Error in the Parameters	
	True Model	SINDY-SAIC	SINDY-T	SINDY-SAIC	SINDY-T
x_1	-0.4382	-0.4454	-0.4454	1.64	1.65
x_2	0.5392	0.5368	0.5368	0.45	0.45
u	-0.0243	0	0	100.00	100.00
${x_1}^2$	-0.2000	0	0	100.00	100.00
x_1x_2	0	0	0		
x_1u	0	0	0		
${x_2}^2$	0	0	0		
u^2	0	0	0		
${x_1}^3$	4.5000	5.7781	5.7781	28.40	28.40
${x_1}^2x_2$	-1.2000	-1.1508	-1.1508	4.10	4.10
${x_1}^2u$	100.0000	95.9496	95.9496	4.05	4.05
$x_1{x_2}^2$	0	0	0		
x_1x_2u	0	0	0		
x_1u^2	0	0	0		
${x_2}^3$	0	0	0		
${x_2}^2u$	0	0	0		
x_2u^2	0	0	0		
u^3	0	0	0		

Table 5.18. Comparison of SINDY methods for $\dot{x}_2$

	$\dot{x}_1$			% Error in the Parameters	
	True Model	SINDY-SAIC	SINDY-T	SINDY-SAIC	SINDY-T
x_1	-122.5081	-122.9884	-122.9857	0.39	0.39
x_2	-1.0823	-1.0666	-1.0204	1.45	5.72
u	102.7944	102.5359	102.9230	0.25	0.13
${x_1}^2$	-120.0000	-117.9593	-117.1365	1.70	2.39
x_1x_2	0	0	0		
x_1u	0	0	0		
${x_2}^2$	0	0	0		
x_2u	0	0	0		
u^2	0	0	0		
${x_1}^3$	-30.0000	0	0		
${x_1}^2x_2$	0	0	0		
${x_1}^2u$	0	0	0		
$x_1{x_2}^2$	0	0	0		
x_1x_2u	0	0	0		
x_1u^2	0	0	0		
${x_2}^3$	0	0	0		
${x_2}^2u$	0	0	0		
x_2u^2	20.0000	20.0004	0	0.00	100.00
u^3	0	0	0		

The RMSE values of both algorithms are given in Table 5.19. It is seen that SINDY-SAIC algorithm has lover RSME values than the SINDY-T algorithm. This result is consistent with that the later one captured one less term than the former.

Table 5.19. RSME values of SINDY methods

	Root Mean Squared Error (RMSE)			
	x_1		x_2	
	SINDY-SAIC	**SINDY-T**	**SINDY-SAIC**	**SINDY-T**
Training Data	0.0042	0.0048	0.0650	0.0735
Test Data	0.0168	0.0371	0.2565	0. 4807

The time of execution for methods are measured and observed that SINDY-SAIC converges 5.6 faster than the SINDY-T. SINDY-SAIC algorithm produces a much

smaller number of candidate models and hence execution time is much shorter. In this example, SINDY-SAIC algorithm generated 10 candidate models, while the SINDY-T algorithm generated 56 candidate models. All the time difference come from the number of candidate models generated by methods.

5.2. Control Performance Comparison

In this section control performances of the discovered models and the different kind of controller are to be analyzed. The cases studied are given as follows.

1. Linear Missile Model Control (with clean and noisy measurement)
    1. MPC
    2. State Feedback (SF)
2. Non-Linear Missile Model (with clean and noisy measurement)
    1. Non-linear MPC
    2. State Feedback (SF)
    3. MPC

The performances are to be compared in terms of The Tracking Error (TE), Control Expenditure (CE) and Control Rate Expenditure (CRE) and the definitions are given in Eqn. (5-7).

$$Tracking\ Error := \int_0^{T_{settling}} \left|(\alpha - \alpha_{ref})\right|$$

$$Control\ Expanditure := \int_0^{T_{settling}} |\delta| \tag{5-7}$$

$$Control\ Rate\ Expanditure := \int_0^{T_{settling}} \left|\dot{\delta}\right|$$

5.2.1. Control Performance Comparison for Linear Missile Model

In this section, discovered model is used to control the linear missile model using MPC and state feedback (SF) control methods. In MPC discovered model is used for prediction whereas in state feedback control it is used during the pole placement procedure. Both control methods are compared for clean and noisy measurements. The true model and the previously discovered models for clean and noisy measurements are given in Table 5.20.

Table 5.20. Discovered models using SINDY

	True model	Model-1 (Clean Measurement)	Model-2 (Moderate Noise)	Model-3 (High Noise)
	$\dot{x}_1$			
x_1	-0.4382	-0.4382	-0.4413	-0.4719
x_2	0.5392	0.5392	0.5355	0.5085
u	-0.0243	-0.0243	0	0
	$\dot{x}_2$			
x_1	-122.5085	-122.5085	-121.6470	-114.4319
x_2	-1.0823	-1.0823	-1.0627	-0.9413
u	102.7949	102.7949	101.9802	94.8600

MPC and State Feedback (SF) design parameters are given in Table 5.21 and Table 5.22 respectively.

Table 5.21. MPC design parameters for linear system

MPC Design Parameters	Values
Sample Time (Ts)	0.025
Prediction Horizon (Hp)	35
Control Horizon (Hm)	4
Output Weight (Q)	1
Input Rate Weight (R)	2.5
Input Constraints	[-15, 15] deg
Input Rate Constraints	[-250, 250] deg/s

Table 5.22. SF design parameters

SF Design Parameters	Values
Sample Time (Ts)	0.0025
Desired CL Damping Ratio (ζ)	0.55
Desired CL Natural Frequency (ω_n)	1.3 x ($\omega_n of\ open\ loop$)

It is better to analyze the open loop response of the real system before starting control system design. The open loop response for zero initial condition and step input is given in Figure 5.28(a) whereas free response for $x_0 = [5\ 15]$ is given in Figure 5.28(b). The damping ratio and the natural frequency of the open loop system is 0.09 and 8.2 rad/s respectively. It can be observed that open loop system has very low damping ratio. Also noted that, for $x_0 = [5\ 15]$ the system exhibits rapid movement toward zero which may degrade the performance of the controller for specific cases especially for State Feedback.

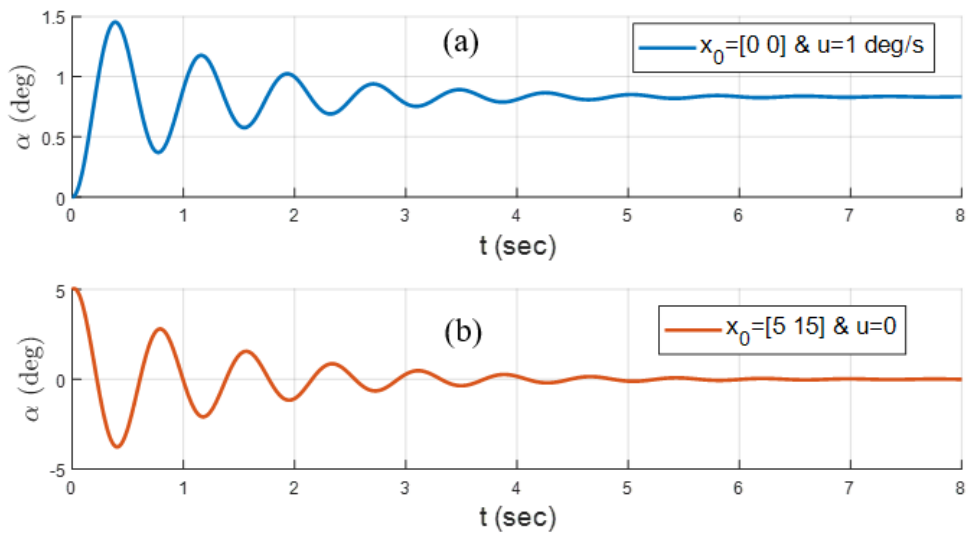

Figure 5.28. Open loop response for $x_0 = [0\ 0]$ and $x_0 = [5\ 15]$

5.2.1.1. Control of Linear Missile Model Discovered from Clean Data

The model discovered from clean measurements (Model-1 in Table 5.20) is used for the design of controllers. The results of MPC and SF for initial condition $x_0 = [0\ 0]$ are given in Figure 5.29 through Figure 5.32. Both controllers are tuned to be close to each other in zero initial condition in terms of tracking performance for better comparison.

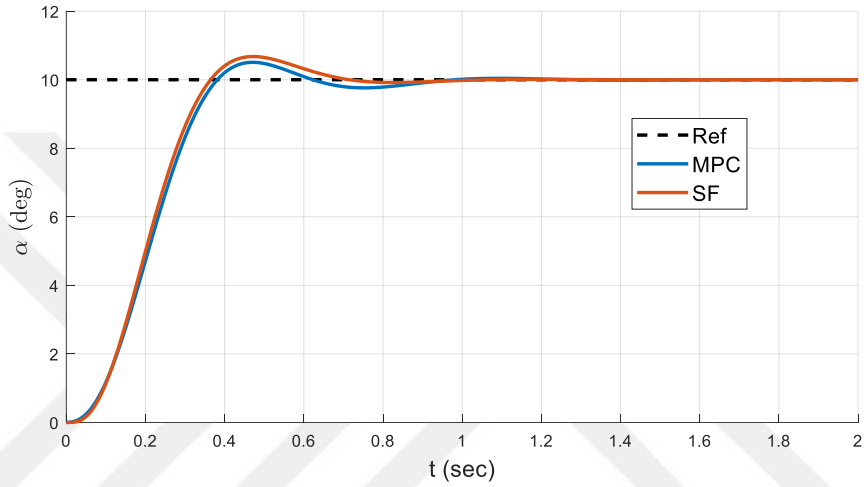

Figure 5.29. Angle of attack results for $x_0 = [0\ 0]$

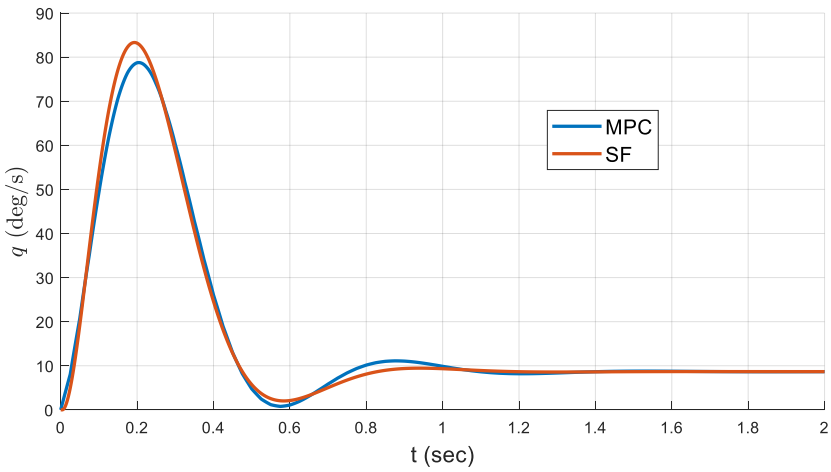

Figure 5.30. Pitch rate results for $x_0 = [0\ 0]$

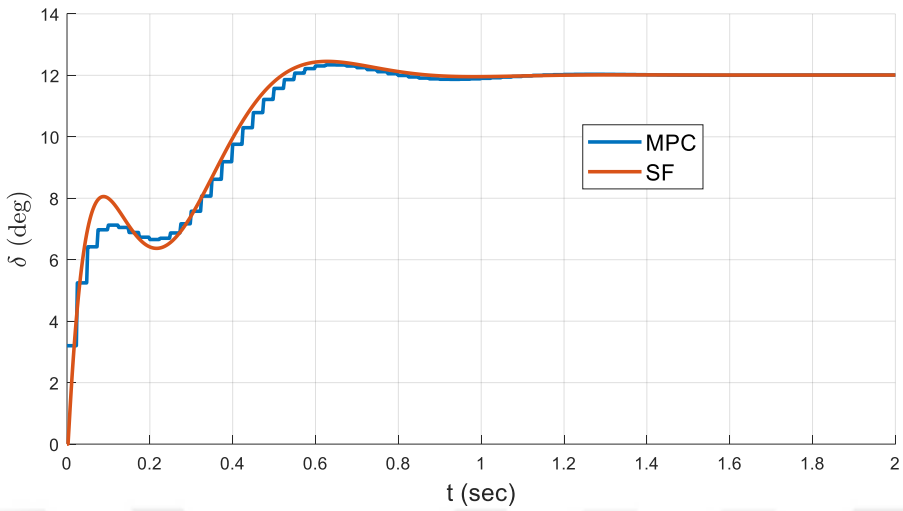

Figure 5.31. Delta results for $x_0 = [0\ 0]$

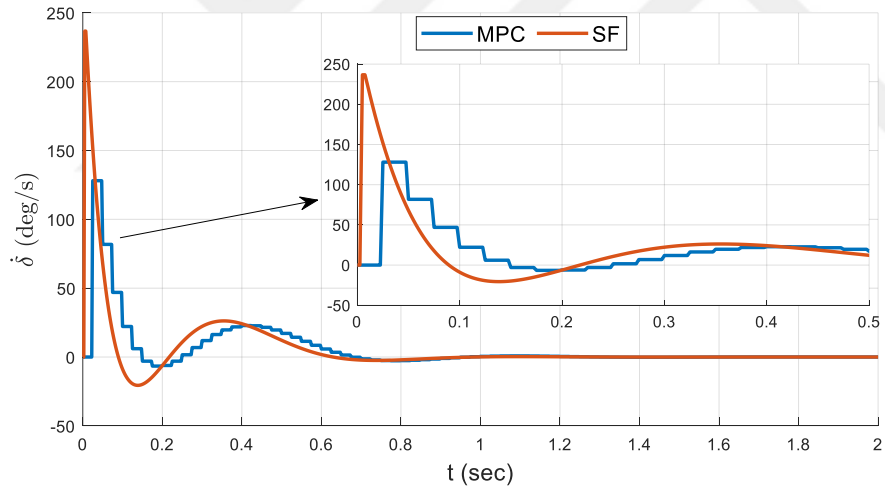

Figure 5.32. Delta dot results for $x_0 = [0\ 0]$

For zero initial condition case, it is seen that MPC and SF controllers exhibits almost the same performance. The only difference is that MPC requires slightly less $\dot{\delta}$ than SF controller especially at the beginning of the simulation.

The results of MPC and SF for initial condition $x_0 = [15\ 5]$ are given in Figure 5.33 through Figure 5.36.

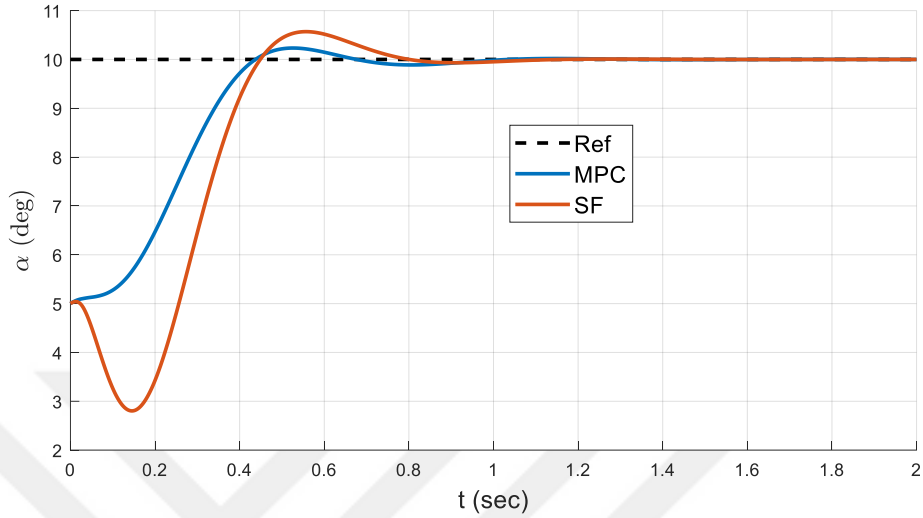

Figure 5.33. Angle of attack results for $x_0 = [5\ 15]$

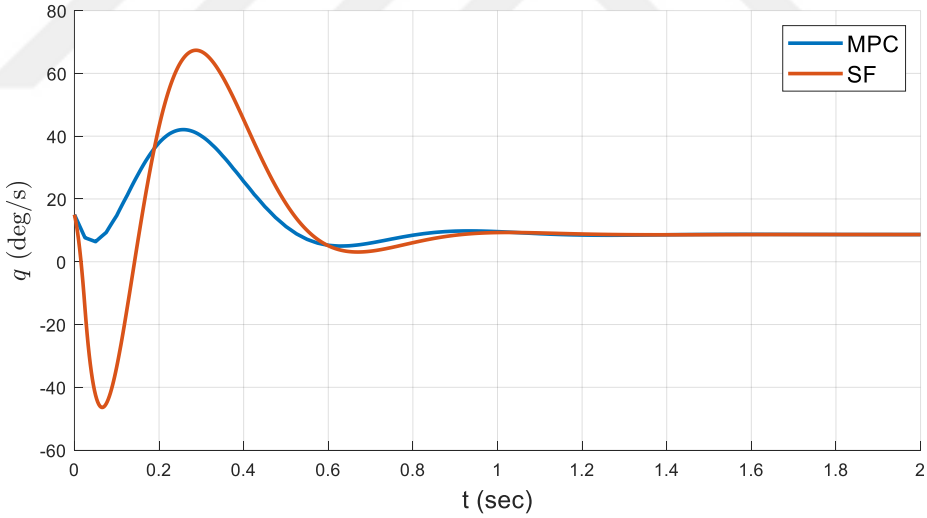

Figure 5.34. Angle of attack results for $x_0 = [5\ 15]$

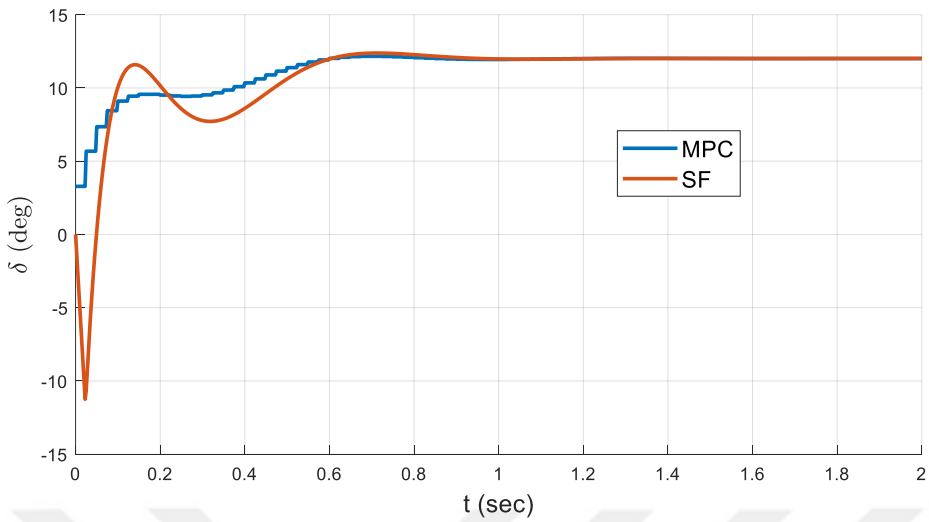

Figure 5.35. Angle of attack results for $x_0 = [5\ 15]$

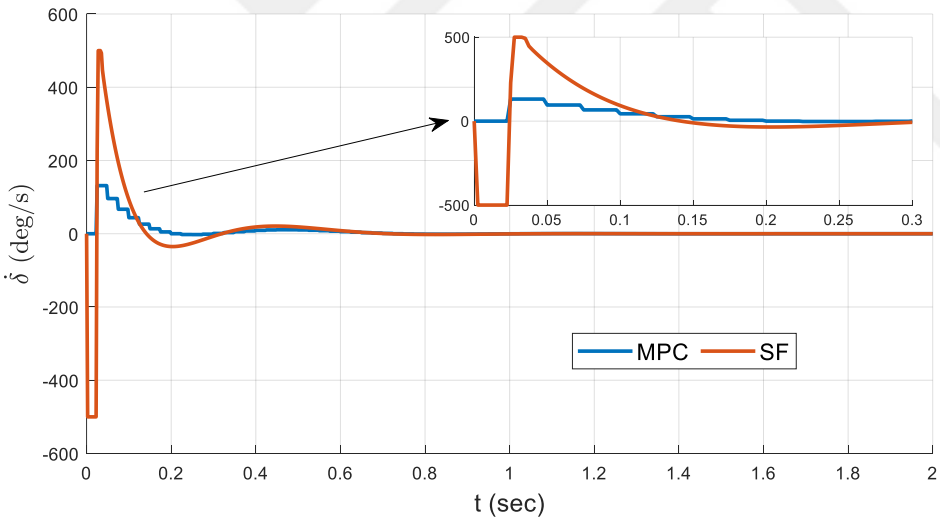

Figure 5.36. Angle of attack results for $x_0 = [5\ 15]$

For $x_0 = [5\ 15]$ case, MPC outperforms SF in terms of tracking. Transient characteristics such as rise time, maximum overshoot of MPC is better than SF. There is also an undershoot behavior in the SF response initially which can be seen in the open loop response given in Figure 5.28 (b).

When the SF controller tries to follow a setpoint value above 5 degrees, an undershoot behavior occurs due to the system's tendency to return to zero. In addition, SF makes sharp movement in control action and control rate is saturated which can be seen in Figure 5.36.

Table 5.23. Performance Metrics of MPC and SF for Different ICs

	$\boldsymbol{x_0 = [0\ 0]}$		$\boldsymbol{x_0 = [5\ 15]}$	
	MPC	**SF**	**MPC**	**SF**
Tracking Error (TE, deg)	126.9	124.5	76.1	122.1
Control Expenditure (CE, deg)	907.9	918.3	948.7	935.8
Control Rate Expenditure (CRE, deg/s)	798.6	938.9	730.6	2469.0

Performance metrics are also calculated to compare the results numerically and given in Table 5.23. MPC and SF performance metrics are nearly same for zero initial condition case except control rate expenditure. SF has 17 % higher CRE than MPC. For the second initial condition ($x_0 = [5\ 15]$), MPC has much better performance in terms of TE and CRE whereas CE values are similar. MPC has 60 % lower tracking error than SF controller.

To summarize the effect of initial conditions on the controller's performance, MPC appears to be more successful than SF, especially at nonzero initial conditions. This is because the SF is designed at zero initial condition and MPC has a prediction model which increases the robustness of MPC for different initial conditions. The fact that MPC is better in terms of CRE in both cases is related to the presence of constraints in MPC design.

5.2.1.2. Control of Linear Missile Model Discovered from Noisy Data

The model discovered from measurements with high level noise (Model-3 in Table 5.20) is used for the design of controllers. The results of MPC and SF responses for initial condition $x_0 = [0\ 0]$ are given in Figure 5.37 through Figure 5.40.

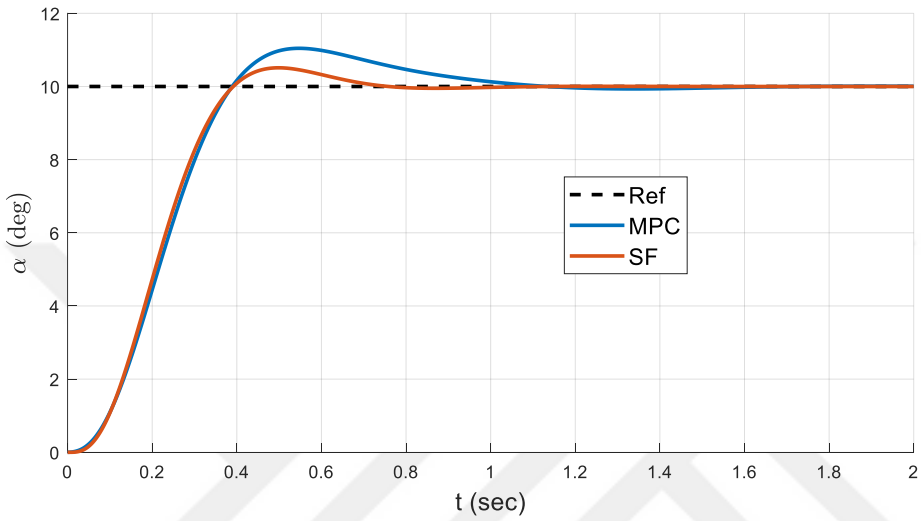

Figure 5.37. Angle of attack results for $x_0 = [0\ 0]$

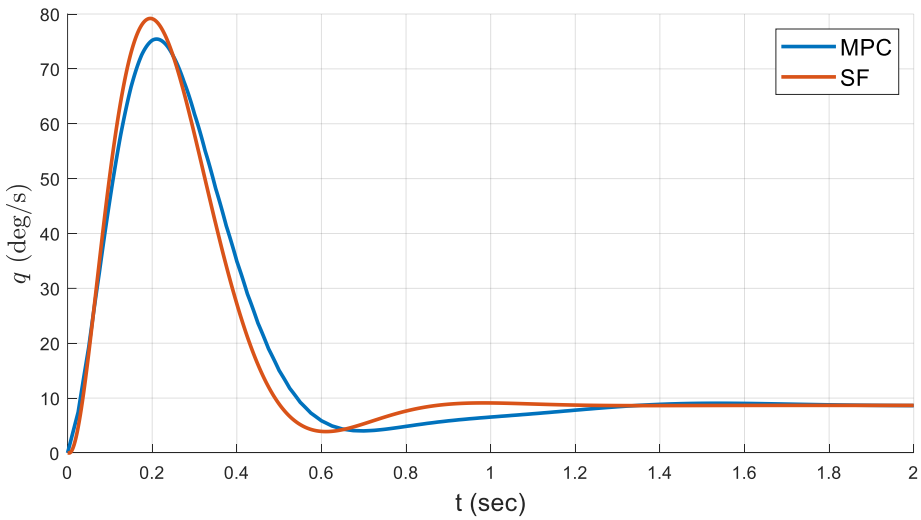

Figure 5.38. Pitch rate results for $x_0 = [0\ 0]$

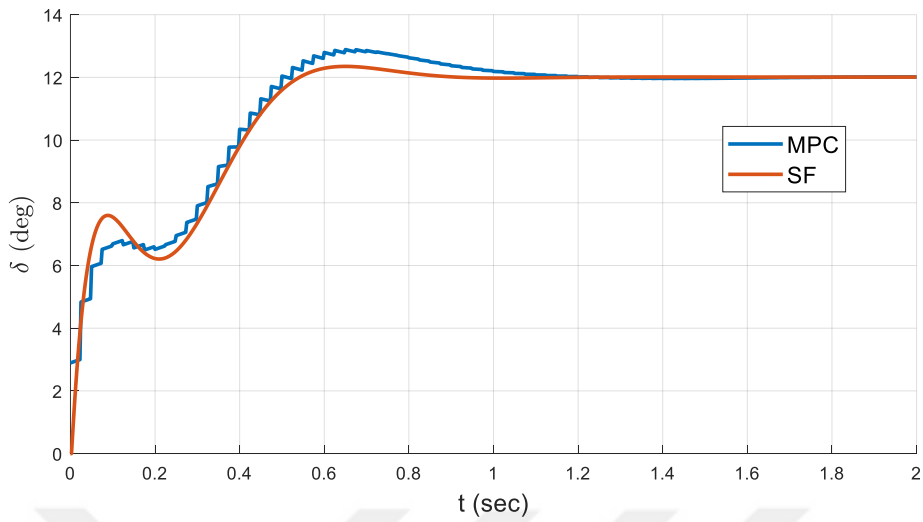

Figure 5.39. Delta results for $x_0 = [0\ 0]$

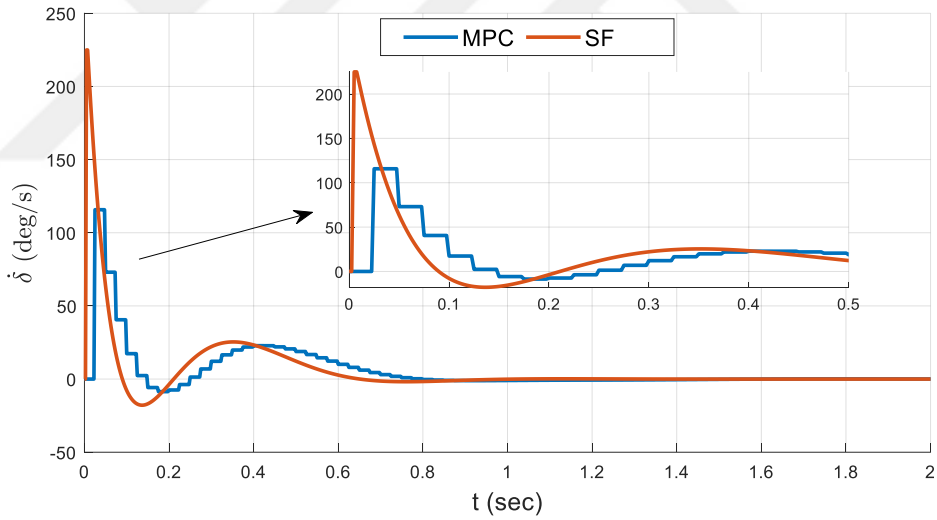

Figure 5.40. Delta dot results for $x_0 = [0\ 0]$

For zero initial condition case, it is seen that SF controllers exhibits better performance in term of settling time and percent overshoot than MPC. It is due to model mismatch between the real system and the model used for prediction in MPC for high level of

noise case. MPC still has enough set point tracking and requires slightly less $\dot{\delta}$ than SF controller especially at the beginning of the simulation.

The results of MPC and SF for initial condition $x_0 = [15\ 5]$ are given in Figure 5.41 through Figure 5.44.

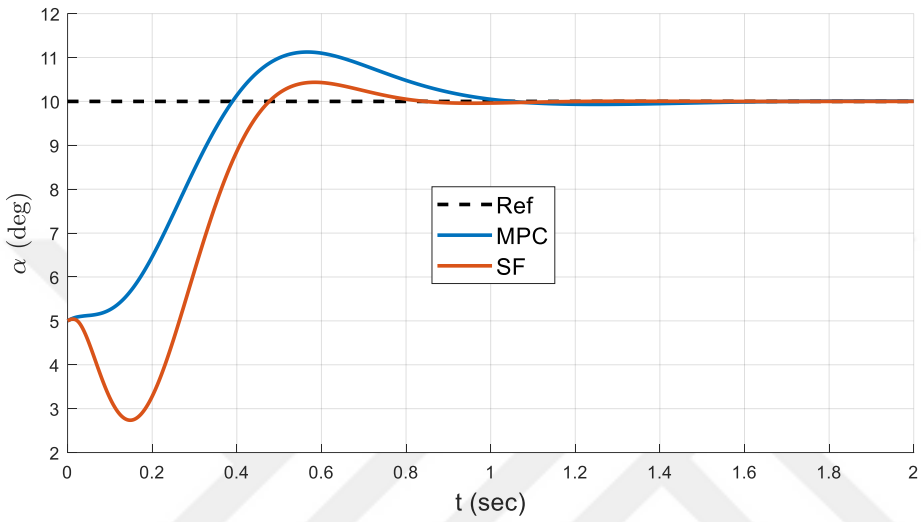

Figure 5.41. Angle of attack results for $x_0 = [5\ 15]$

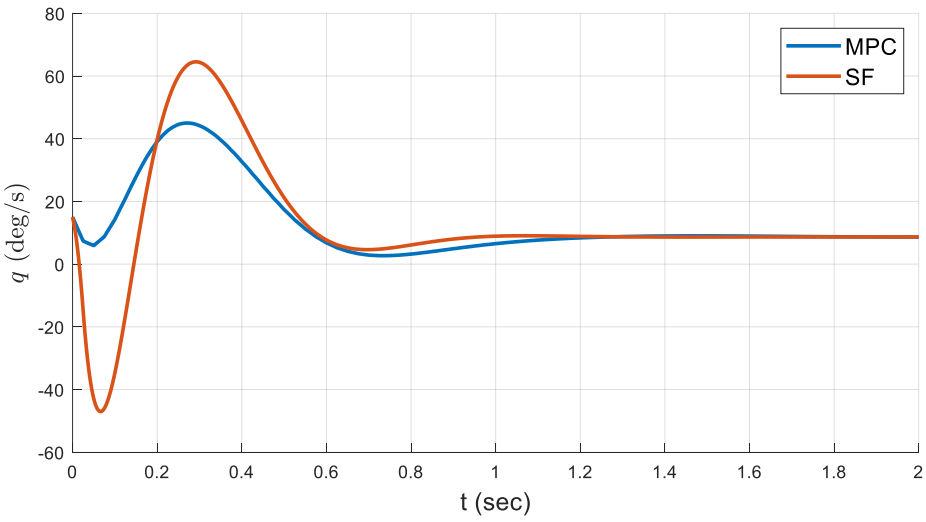

Figure 5.42. Angle of attack results for $x_0 = [5\ 15]$

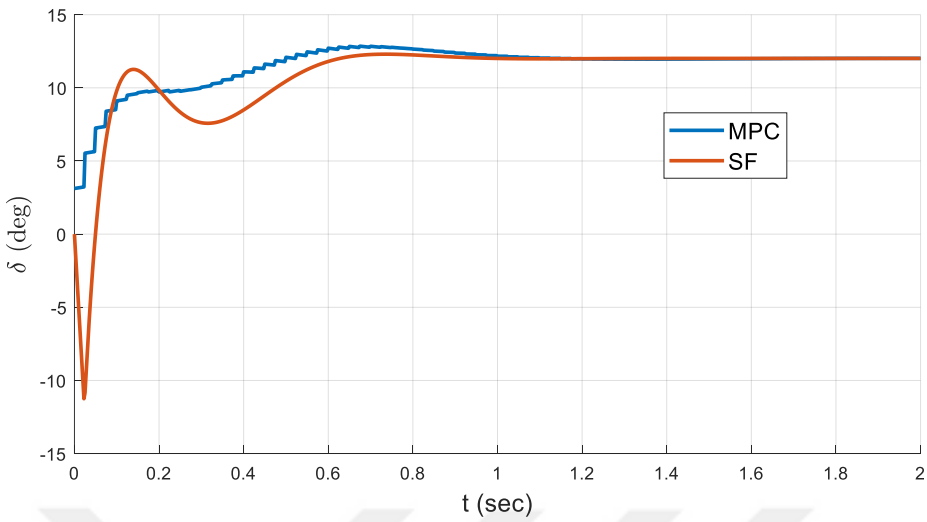

Figure 5.43. Angle of attack results for $x_0 = [5\ 15]$

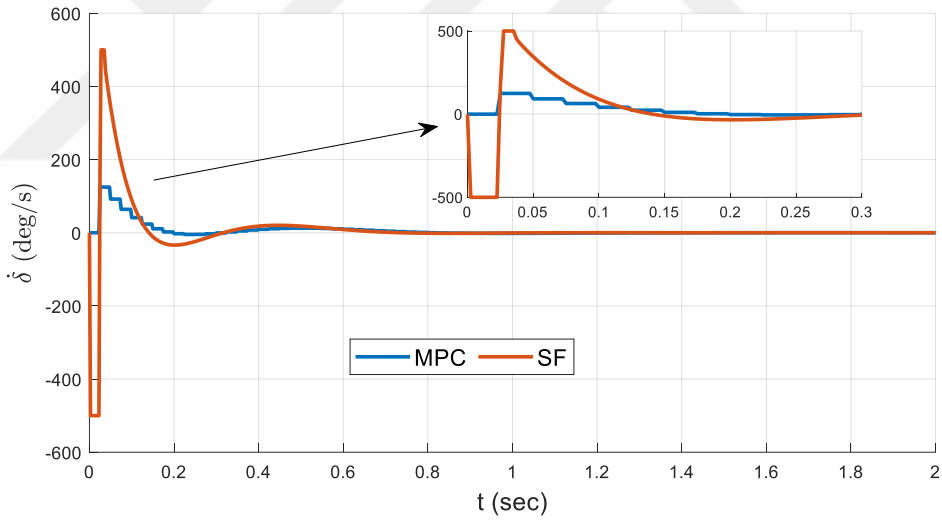

Figure 5.44. Angle of attack results for $x_0 = [5\ 15]$

For $x_0 = [5\ 15]$ case, MPC outperforms SF in terms of rise time and undershoot characteristic whereas SF controller has better settling time and overshoot behavior. There is an undershoot behavior in the SF response initially which can be seen in the open loop response given in Figure 5.28 (b).

When the controller tries to follow a setpoint value above 5 degrees, an undershoot behavior occurs due to the system's tendency to return to zero. In addition, SF makes sharp movement in control action and control rate is saturated which can be seen in Figure 5.44.

Table 5.24. Performance Metrics of MPC and SF for Different ICs

	$\boldsymbol{x_0 = [0\ 0]}$		$\boldsymbol{x_0 = [5\ 15]}$	
	MPC	**SF**	**MPC**	**SF**
Tracking Error (TE, deg)	146.2	127.0	93.93	125.3
Control Expenditure (CE, deg)	925.9	910.9	974.9	928.9
Control Rate Expenditure (CRE, deg/s)	799.6	890.6	781.1	2435.0

Performance metrics are also calculated to compare the results numerically and given in Table 5.24. SF has lower TE about % 13 and higher CRE about 11 % than MPC in zero initial case. For the second initial condition ($x_0 = [5\ 15]$), MPC has much better performance in terms of TE and CRE whereas CE values are similar.

The tracking performance results of all noise and controller combinations studied for linear system are summarized in Figure 5.45 and Figure 5.46. MPC appears to be more successful than SF, especially at nonzero initial conditions. As stated before, this is because the SF is designed at zero initial condition and MPC has a prediction model which increases the robustness of MPC for different initial conditions. The fact that MPC is better in terms of CRE in both cases is related to the presence of constraints in MPC design. The main disadvantage of MPC is having much overshoot than SF.

This results from the integral action added to MPC which is used to resolve the steady state error in case of model uncertainties.

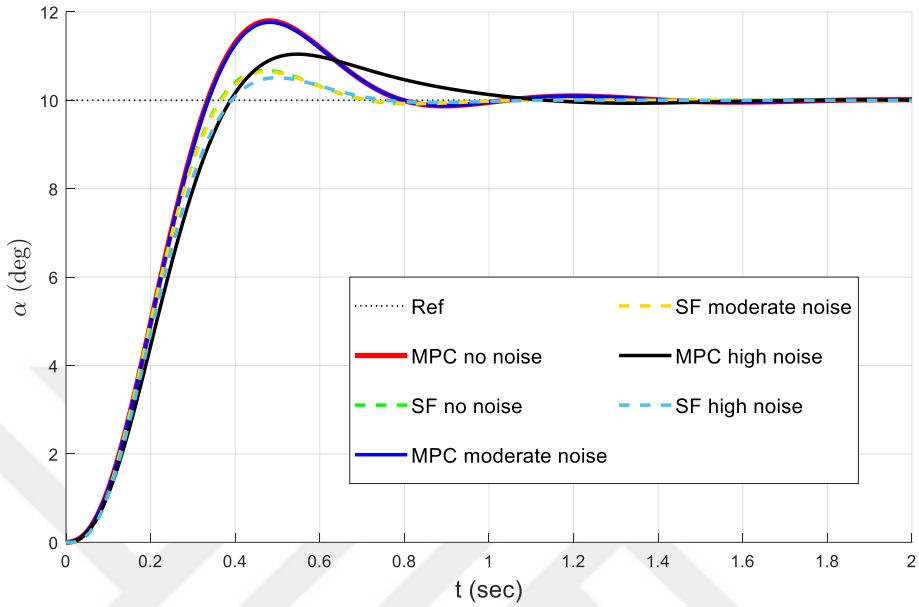

Figure 5.45. Angle of attack results for $x_0 = [0\ 0]$

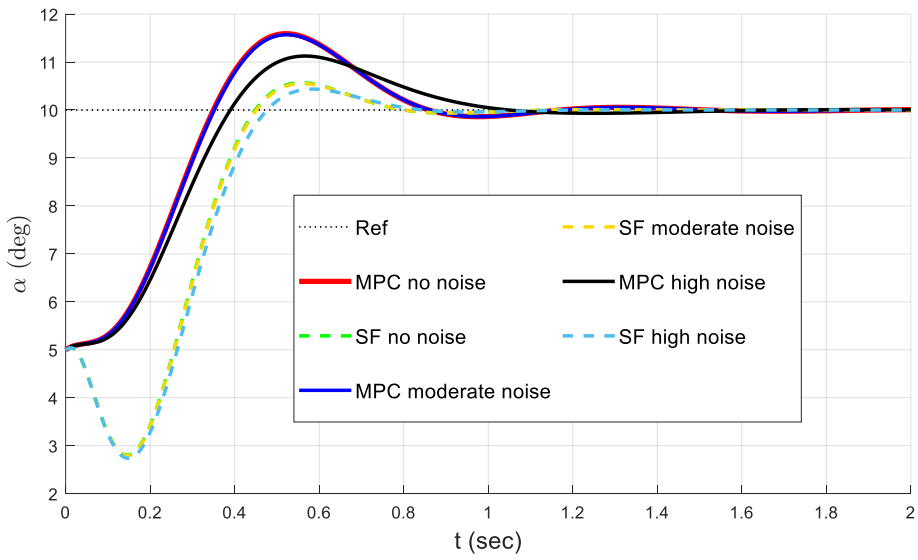

Figure 5.46. Angle of attack results for $x_0 = [5\ 15]$

5.2.2. Control Performance Comparison for Non-Linear Missile Model

In this section, 3 control methods that is non-linear MPC, linear MPC and State Feedback will be compared. In all methods, nonlinear system model given by Eqn. (5-6) is used as true system model. The description of the methods is as follows.

1. **Non-liner MPC (NMPC)**
   True system is controlled by MPC using the non-linear system model discovered by SINDY.

2. **Linear MPC (MPC)**
   True system is controlled by the MPC using the linearized system model that is obtained using non-linear SINDY model.

3. **State Feedback (SF)**
   True system is controlled by the state feedback using the linearized system model that is obtained using non-linear SINDY model.

With this comparison, the performance of MPC and SF in the control of a nonlinear system will be examined. In addition, the performances of using linear and nonlinear prediction models in MPC will be analyzed. The true model and the previously discovered models for clean and noisy measurements are given in Table 5.25.

Table 5.25. Discovered models using SINDY

	True model	**Model-4 (Clean Measurement)**	**Model-5 (Moderate Noise)**	**Model-6 (High Noise)**
	$\dot{x}_1$			
x_1	-0.4382	-0.4495	-0.4454	-0.3981
x_2	0.5392	0.5392	0.5368	0.5085
u	-0.0243	0	0	0
${x_1}^2$	-0.2	-0.190	0	0
${x_1}^3$	4.5	4.927	5.7781	5.4889
${x_1}^2 x_2$	-1.2	-1.197	-1.1508	-0.9221
${x_1}^2 u$	100	98.77	95.9496	91.9266
	$\dot{x}_2$			
x_1	-122.5085	-122.5085	-122.9884	-119.7355
x_2	-1.0823	-1.0823	-1.0666	-0.9822
u	102.7949	102.7949	102.5359	99.3816
${x_1}^2$	-120	-120.0000	-117.9593	110.1007
${x_1}^3$	-30	-30.0000	0	0
$x_2 u^2$	20	20.0000	20.0004	0

MPC and State Feedback (SF) design parameters are given in Table 5.26 and Table 5.27 respectively.

Table 5.26. MPC design parameters for linear system

MPC Design Parameters	**Values**
Sample Time (Ts)	0.025
Prediction Horizon (Hp)	35
Control Horizon (Hm)	10
Output Weight (Q)	1.0
Input Rate Weight (R)	2.0
Input Constraints	[-15, 15] deg
Input Rate Constraints	[-250, 250] deg/s

Table 5.27. SF design parameters

SF Design Parameters	Values
Sample Time (Ts)	0.0025
Desired CL Damping Ratio (ζ)	0.55
Desired CL Natural Frequency (ω_n)	1.5 x ($\omega_n of\ open\ loop$)

5.2.2.1. Control of Non-Linear Missile Model Discovered from Clean Data

The Model-4 in Table 5.25 obtained using SINDY is used as a prediction model in NPMC method whereas linearized version is used for MPC and SF design. The results for initial condition $x_0 = [0\ 0]$ are given in Figure 5.47 through Figure 5.50. Both controllers are tuned to be close to each other in zero initial condition in terms of tracking performance for better comparison.

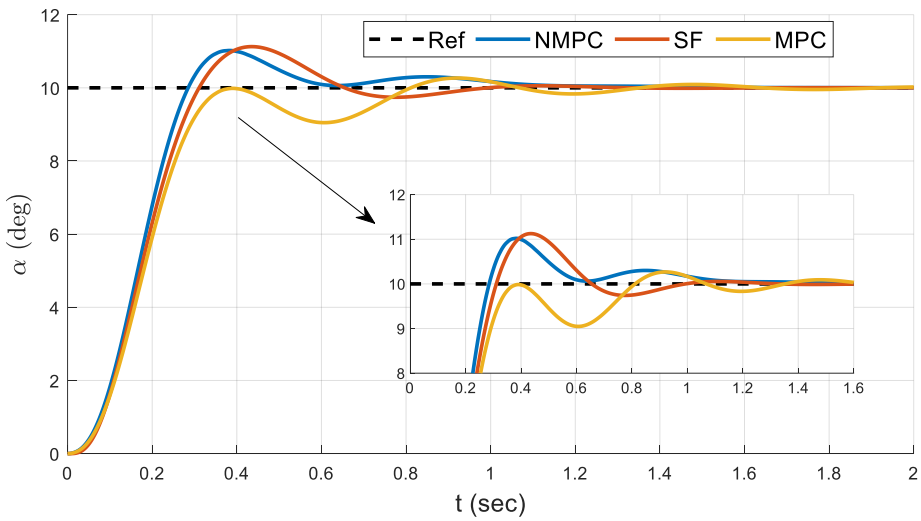

Figure 5.47. Angle of attack results for $x_0 = [0\ 0]$

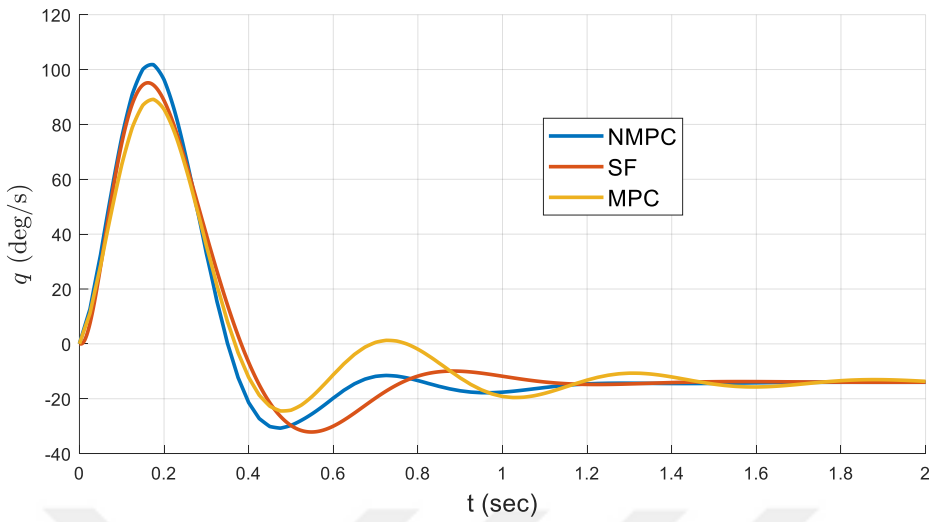

Figure 5.48. Pitch rate results for $x_0 = [0\ 0]$

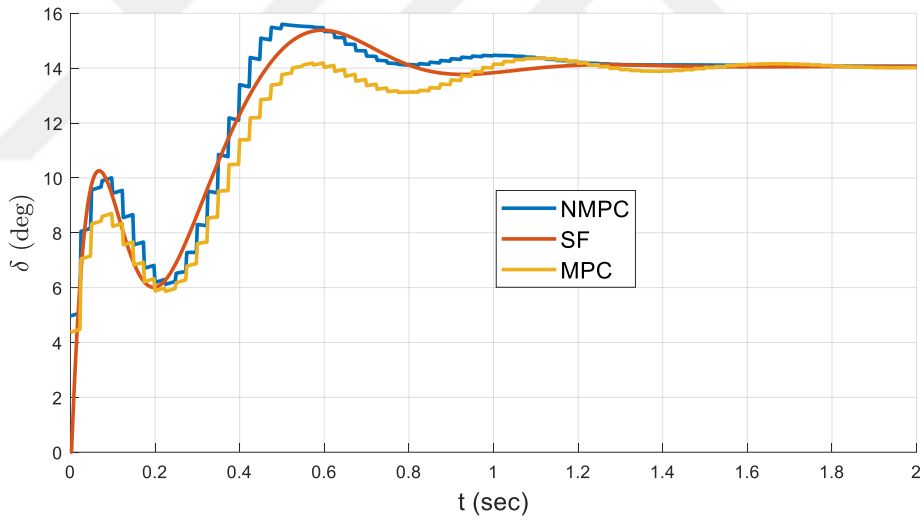

Figure 5.49. Delta results for $x_0 = [0\ 0]$

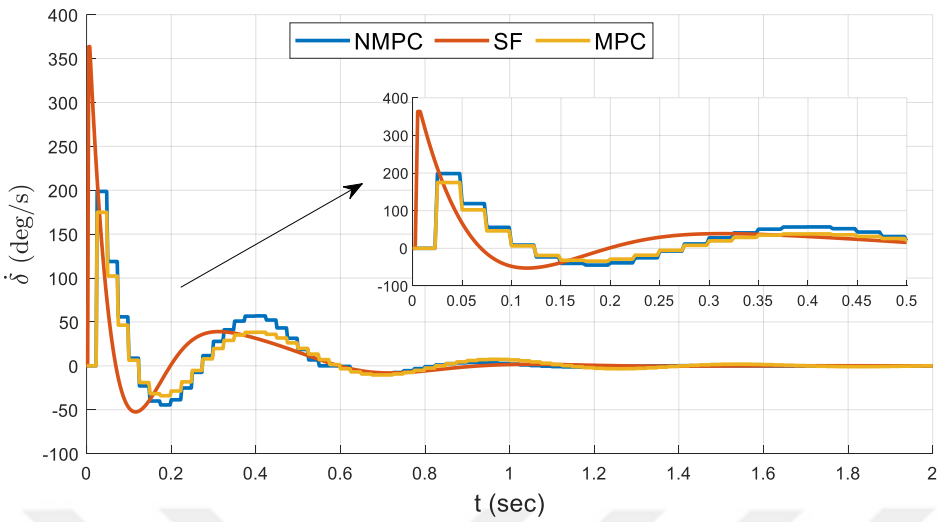

Figure 5.50. Delta dot results for $x_0 = [0\ 0]$

For zero initial condition case, it is seen that NMPC is slightly better than SF in terms α tracking. SF's tracking response is satisfactory as well. On the other hand, MPC exhibits some oscillations that die out shortly and has moderate set point tracking. The comparisons in terms of control inputs do not give very distinctive information. The only difference is that SF requires slightly more $\dot{\delta}$ than the others at the beginning of the simulation.

The results for initial condition $x_0 = [15\ 5]$ are given in Figure 5.51 through Figure 5.54.

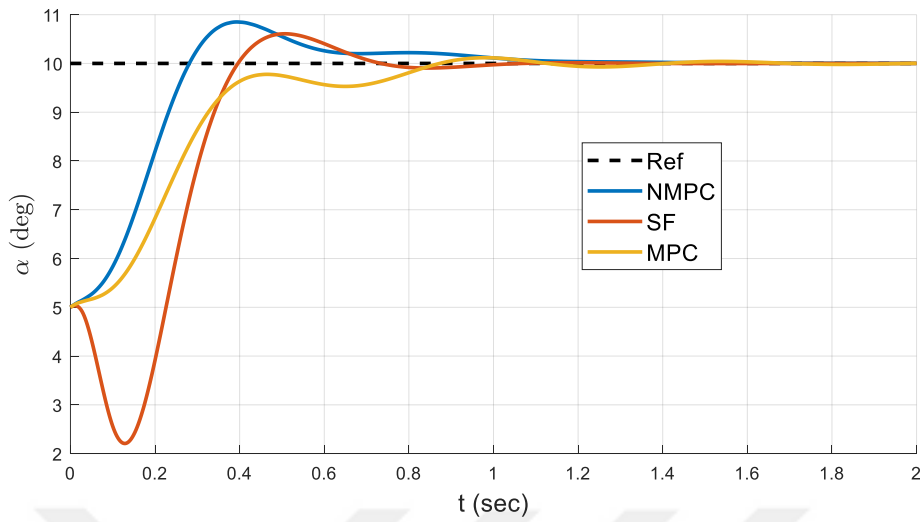

Figure 5.51. Angle of attack results for $x_0 = [5\ 15]$

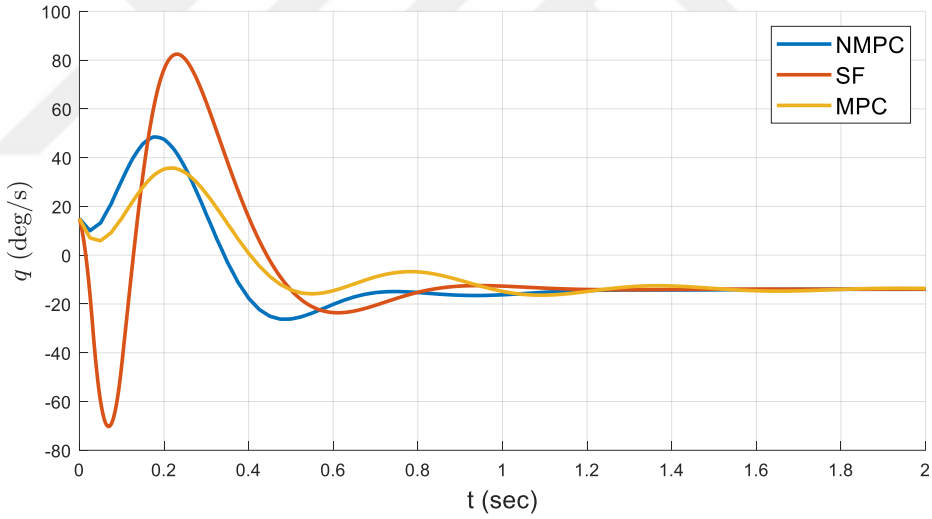

Figure 5.52. Pitch rate results for $x_0 = [5\ 15]$

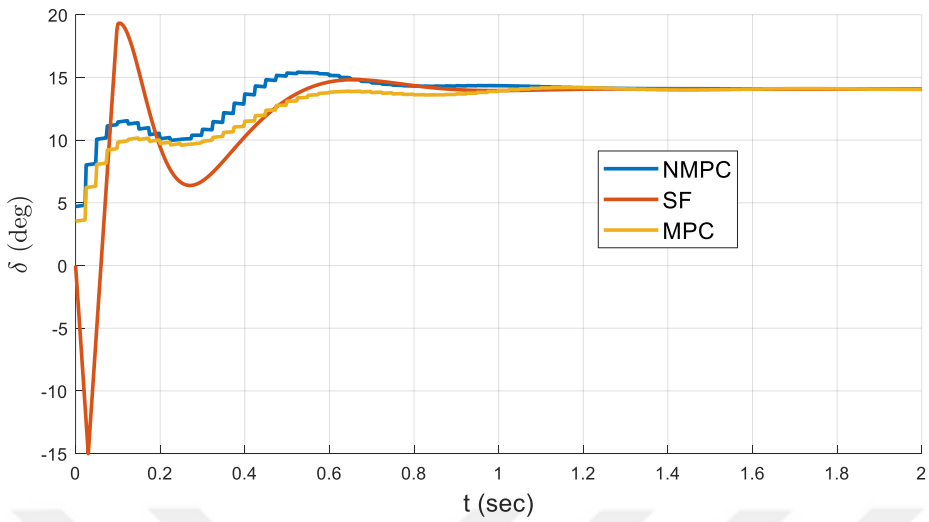

Figure 5.53. Delta results for $x_0 = [5\ 15]$

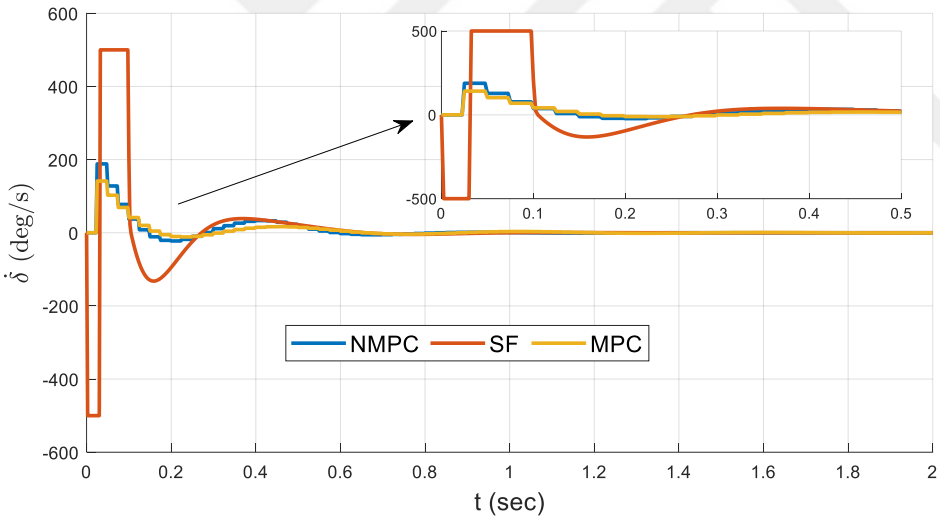

Figure 5.54. Delta dot results for $x_0 = [5\ 15]$

For $x_0 = [15\ 5]$ case, NMPC outperforms both SF and MPC in terms of set point tracking. Rise time of NMPC is highly better than the others. There is an undershoot behavior in the SF response initially whereas MPC has some degree of oscillations in

α tracking. On the other hand, SF makes sharp movements in control action and control rate is saturated which can be seen in Figure 5.54.

Table 5.28. Performance Metrics for Different ICs

	$x_0 = [0\ 0]$			$x_0 = [5\ 15]$		
	NMPC	**SF**	**MPC**	**NMPC**	**SF**	**MPC**
Tracking Error (TE, deg)	102.2	110.7	122.6	53.9	111.7	77.9
Control Expenditure (CE, deg)	1068.3	1068.4	1036.5	1115.9	1104.3	1077.8
Control Rate Expenditure (CRE, deg/s)	1394.2	1438.9	1315.8	1056.5	4108.9	889.7

Performance metrics are also calculated to compare the results numerically and given in Table 5.28. For zero initial condition case, CE values are all similar whereas MPC has lowest CRE. In terms of TE, NMPC has the best performance as stated before. MPC has nearly 10% and 20% higher tracking error than SF and NMPC respectively.

For the second initial condition ($x_0 = [5\ 15]$), tracking error of NMPC and MPC is much better than SF. All methods are similar in terms of CE. For CRE, MPC has the best performance again whereas SF reaches the operating limits of the system for short time interval.

To summarize the effect of initial conditions on the performance, NMPC and MPC appear to be more successful than SF, especially at nonzero initial conditions. As stated before, this results from the fact that SF is designed at zero initial condition and MPC type controllers have a prediction model which increases the robustness of MPC for different initial conditions. Also, presence of constraints in MPC makes it better than SF in terms of CRE.

As can be seen, use of linear and non-linear models in MPC has also effects on performance. Comparing the NMPC and MPC results, it was observed that the use of non-linear model improved the set point tracking performance as expected. This is because the non-linear model represents the real system model more accurately and its predictions are more successful than the linear one. On the other hand, MPC model has the lowest CRE in all cases.

5.2.2.2. Control of Non-Linear Missile Model Discovered from Noisy Data

The Model-6 in Table 5.25 obtained using SINDY is used as a prediction model in NPMC method whereas linearized version is used for MPC and SF design. Remember that Model-6 was discovered using SINDY with high level of noisy measurements. The results for initial condition $x_0 = [0\ 0]$ are given in Figure 5.55 through Figure 5.58. Both controllers are tuned to be close to each other in zero initial condition in terms of tracking performance for better comparison.

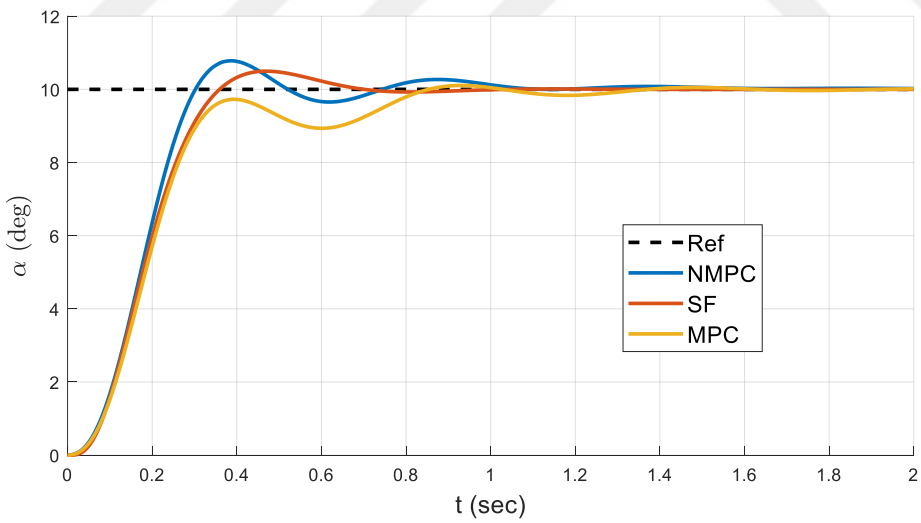

Figure 5.55. Angle of attack results for $x_0 = [0\ 0]$

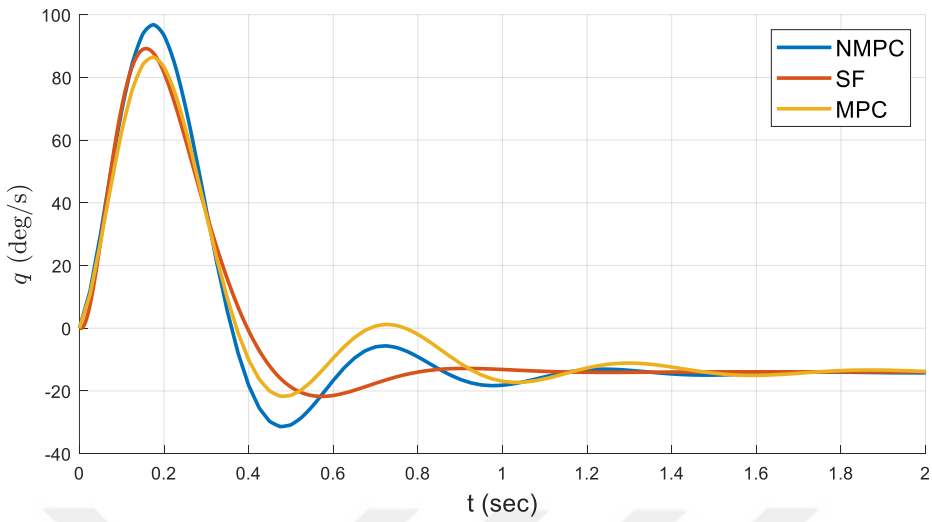

Figure 5.56. Pitch rate results for $x_0 = [0\ 0]$

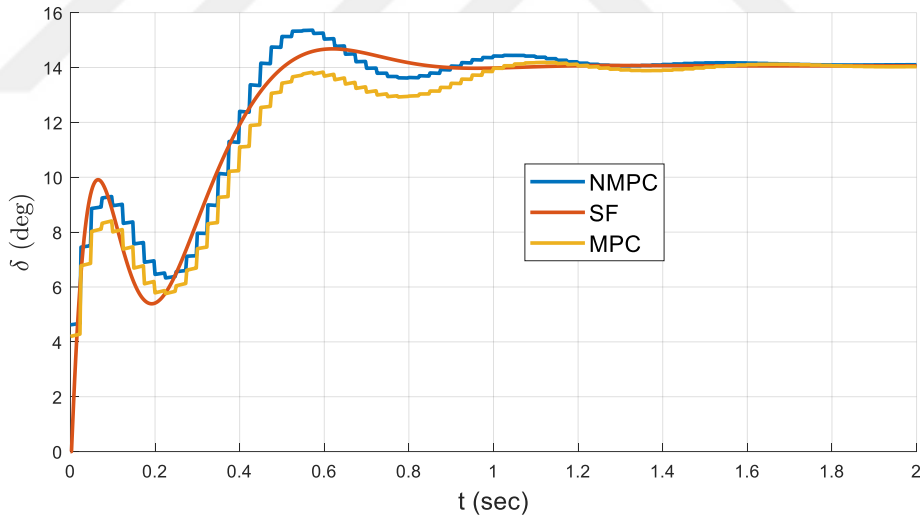

Figure 5.57. Delta results for $x_0 = [0\ 0]$

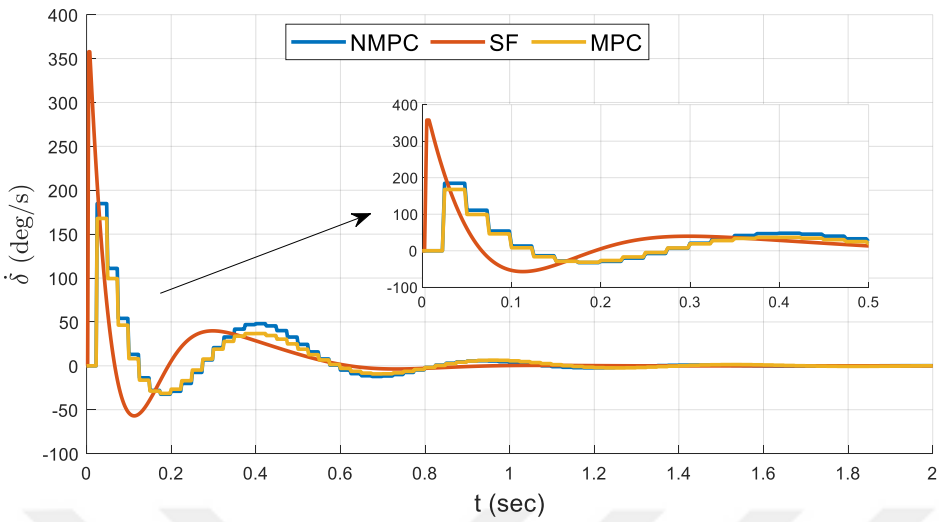

Figure 5.58. Delta dot results for $x_0 = [0\ 0]$

For zero initial condition case, it is seen that NMPC and SF's tracking response is satisfactory. NMPC has better rise time than SF, however overshoot and settling time of SF controller is better than NMPC. On the other hand, MPC has slightly longer time to reach the set point and exhibits some oscillations that die out shortly. The comparisons in terms of control inputs do not give very distinctive information. The only difference is that SF requires slightly more $\dot{\delta}$ than the others at the beginning of the simulation.

The results for initial condition $x_0 = [15\ 5]$ are given in Figure 5.59 through Figure 5.62

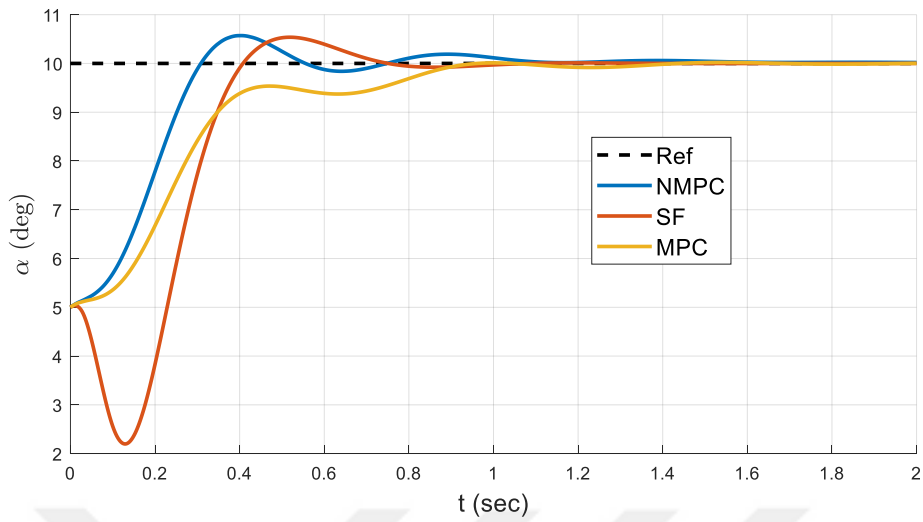

Figure 5.59. Angle of attack results for $x_0 = [5\ 15]$

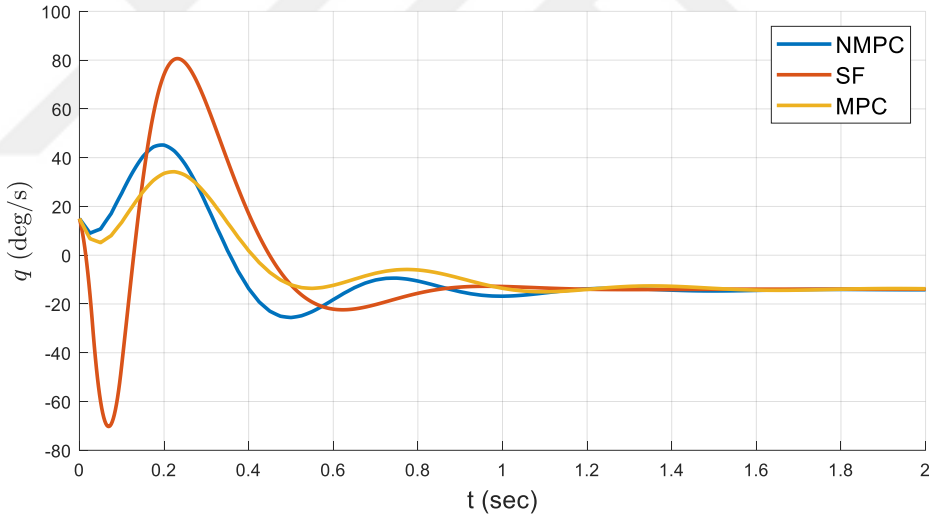

Figure 5.60. Pitch rate results for $x_0 = [5\ 15]$

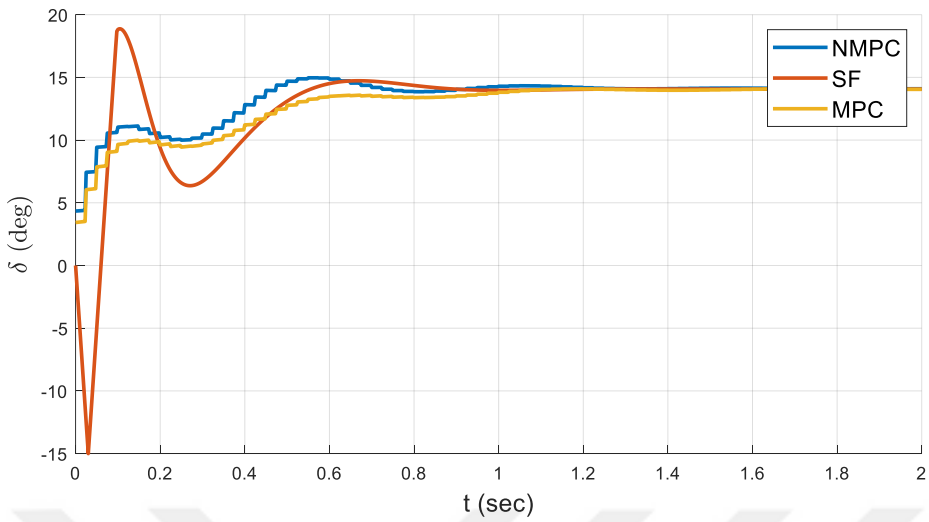

Figure 5.61. Delta results for $x_0 = [5\ 15]$

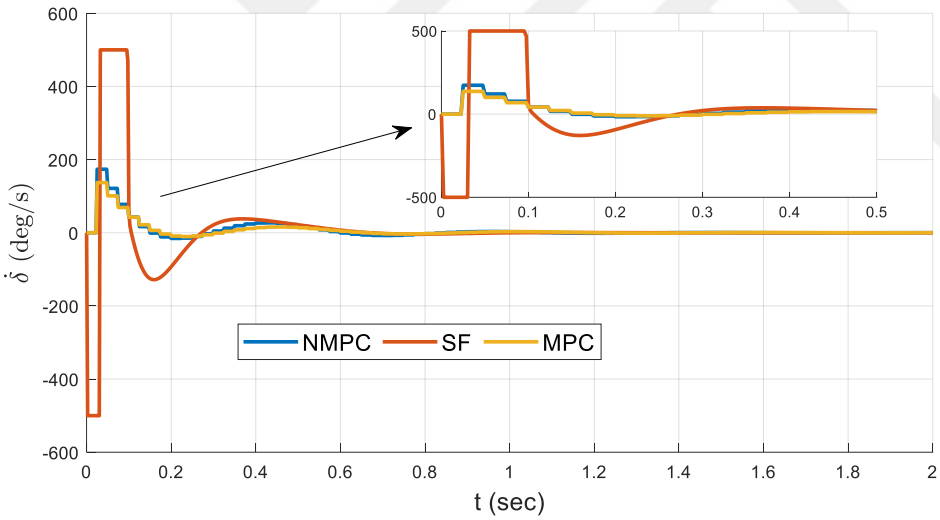

Figure 5.62. Delta dot results for $x_0 = [5\ 15]$

For $x_0 = [15\ 5]$ case, NMPC is better than SF in terms of set point tracking. Rise time of NMPC is highly better than the others. There is an undershoot behavior in the SF response initially whereas MPC has longer time to reach set point in α tracking. SF

has the best settling time between the studied controllers. On the other hand, SF makes sharp movements in control action and control rate is saturated which can be seen in Figure 5.62.

Table 5.29. Performance Metrics for Different ICs

	$x_0 = [0\ 0]$			$x_0 = [5\ 15]$		
	NMPC	**SF**	**MPC**	**NMPC**	**SF**	**MPC**
Tracking Error (TE, deg)	111.6	111.6	128.3	62.0	112.6	85.2
Control Expenditure (CE, deg)	1078.4	1064.6	1020.9	1125.8	1100.5	1062.4
Control Rate Expenditure (CRE, deg/s)	1413.6	1406.3	1236.1	1103.7	4047.0	854.4

Performance metrics are also calculated to compare the results numerically and given in Table 5.29. For zero initial condition case, CE values are all similar whereas MPC has lowest CRE. In terms of TE, NMPC and SF have very similar performance. MPC has nearly 10% higher tracking error than SF and NMPC.

For the second initial condition ($x_0 = [5\ 15]$), tracking error of NMPC and MPC is much better than SF. All methods are similar in terms of CE. For CRE, MPC has the best performance again whereas SF reaches the operating limits of the system for short time interval and has larger CRE.

To summarize the effect of initial conditions on the performance, NMPC and MPC appear to be more successful than SF, especially at nonzero initial conditions. On the other hand, SF controller has very promising performance at zero initial condition case. As stated before, this results from the fact that SF is designed at zero initial

condition and MPC type controllers have a prediction model which increases the robustness of MPC for different initial conditions. Also, presence of constraints in MPC makes it better than SF in terms of CRE.

As can be seen, use of linear and non-linear models in MPC has also effects on performance. Similar to the case of clean measurements at previous section, comparing the NMPC and MPC results show that the use of non-linear model improved the set point tracking performance as expected. This is because the non-linear model represents the real system model more accurately and its predictions are more successful than the linear one. On the other hand, MPC model has the lowest CRE in all cases.

CHAPTER 6

DISCUSSION

The proposed SINDY-SAIC algorithm determined the important dynamics of the longitudinal missile system accurately for clean, moderate and high level of noise cases. In case of clean measurement of states, SINDY-SAIC could find the coefficients of the true model with great accuracy whereas for noisy data, all the important dynamics of the system was captured with at most 10% error in the coefficients.

Calculation of state derivatives using sliding window approach significantly increased the robustness of SINDY-SAIC to noise.

In addition, the proposed algorithm eliminated the need for threshold parameters tuning and presence of AIC model selection enables to select the most sparse solutions among many others.

Furthermore, MPC and state feedback controllers were designed using discovered models. All controller's performances such as tracking, control expenditure and control rate expenditure were compared. For linear missile system, MPC appears to be more successful than SF, especially at nonzero initial conditions. This is because MPC uses the prediction model to overcome initial condition changes. Also, MPC requires less control rate due to the presence of constraints inherently.

For non-linear missile system, NMPC and SF performed similarly for zero initial condition case whereas MPC has slightly longer time to reach the set point and exhibits some oscillations. In non-zero initial condition, NMPC is better than SF. MPC and SF are similar in terms of set point tracking. All controllers tracked the set point successfully and exhibit stable behavior under uncertainties. Therefore, an appropriate controller can be selected according to the controller requirements.

This study motivates several future investigations and extensions such as:

- Measurement data obtained from real flight tests could be used to check the robustness of the SINDY-SAIC algorithm.

- Hardware implementation of the algorithm and the controllers could be done on cost effective platforms such as CPUs, GPUs, or FPGAs.

- It is possible to use SINDY-SAIC online since its convergence rate is very high. Especially with linear SINDY, an approximate linear model could be built quickly, and then more exact nonlinear model could be estimated in parallel with increasing amount of data online.

- In addition, if there are known terms, functions, and constraints in the dynamic model of the system, this knowledge could also be included in the SINDY-SAIC algorithm to increase accuracy and speed.

- The required full-state measurements were assumed to be available in this study. Instead, state estimation and mapping techniques could be used to convert measurements to appropriate basis for better generalization.

- Nonlinear integral action was added to MPC to avoid steady state errors in case of model uncertainties. This resulted in slight overshoot in the response. Different nonlinear functions for integral action could be further analyzed.

REFERENCES

[1] A. Punjani and P. Abbeel, "Deep learning helicopter dynamics models," in *IEEE International Conference on Robotics and Automation (ICRA)*, 2015, vol. 20, pp. 3223–3230.

[2] Y. Kang, S. Chen, X. Wang, and Y. Cao, "Deep Convolutional Identifier for Dynamic Modeling and Adaptive Control of Unmanned Helicopter," in *IEEE Transactions on Neural Networks and Learning Systems*, 2019, vol. 30, no. 2, pp. 524–538.

[3] D. Rolnick and M. Tegmark, "The power of deeper networks for expressing natural functions," *6th Int. Conf. Learn. Represent. ICLR*, pp. 1–14, 2018.

[4] H. W. Lin, M. Tegmark, and D. Rolnick, "Why does deep and cheap learning work so well?," *J. Stat. Phys.*, vol. 168, no. 6, pp. 1223–1247, 2017.

[5] M. Raissi, P. Perdikaris, and G. E. Karniadakis, "Physics Informed Deep Learning (Part II): Data-driven Discovery of Nonlinear Partial Differential Equations," no. Part II, pp. 1–19, 2017.

[6] E. Kilic, M. Dolen, A. B. Koku, H. Caliskan, and T. Balkan, "Accurate pressure prediction of a servo-valve controlled hydraulic system," *Mechatronics*, vol. 22 (7), pp. 997–1014, 2012.

[7] E. Kilic, M. Dolen, H. Caliskan, A. B. Koku, and T. Balkan, "Pressure prediction on a variable-speed pump controlled hydraulic system using structured recurrent neural networks," *Control Eng. Pract.*, vol. 26, pp. 51–71, 2014.

[8] B. O. Koopman, "Hamiltonian Systems and Transformations in Hilbert Space," *Mathematics*, vol. 17, pp. 315–318, 1931.

[9] M. Budišić, R. Mohr, and I. Mezić, "Applied Koopmanism," *Chaos*, vol. 22, no. 4, 2012.

[10] I. Mezić, "Spectral properties of dynamical systems, model reduction and decompositions," *Nonlinear Dyn.*, vol. 41, no. 1–3, pp. 309–325, 2005.

[11] M. Korda and I. Mezić, "Linear predictors for nonlinear dynamical systems: Koopman operator meets model predictive control," *Automatica*, vol. 93, pp. 149–160, 2018.

[12] J. P. Boyd, "Chebyshev & Fourier Series," *Chebyshev Fourier Spectr. Methods*, pp. 19–60, 2000.

[13] H. Wendland, "Meshless Galerkin methods using radial basis functions," *Math. Comput.*, vol. 68, no. 228, pp. 1521–1532, 1999.

[14] B. Lusch, J. N. Kutz, and S. L. Brunton, "Deep learning for universal linear

embeddings of nonlinear dynamics," *Nat. Commun.*, vol. 9, no. 1, 2018.

[15] M. Quade, M. Abel, J. Nathan Kutz, and S. L. Brunton, "Sparse identification of nonlinear dynamics for rapid model recovery," *Chaos*, vol. 28, no. 6, pp. 1–10, 2018.

[16] S. L. Brunton, J. L. Proctor, and J. Nathan Kutz, "Supporting Information for: Discovering governing equations from data: Sparse identification of nonlinear dynamical systems," *Nat. Commun.*, vol. 8, no. 1, pp. 1–38, 2017.

[17] H. Schaeffer, "Learning partial differential equations via data discovery and sparse optimization," *Proc. R. Soc. A Math. Phys. Eng. Sci.*, vol. 473, no. 2197, 2017.

[18] S. L. Brunton, J. L. Proctor, J. N. Kutz, and W. Bialek, "Discovering governing equations from data by sparse identification of nonlinear dynamical systems," *Proc. Natl. Acad. Sci. U. S. A.*, vol. 113, no. 15, pp. 3932–3937, 2016.

[19] K. Kaheman, J. N. Kutz, and S. L. Brunton, "SINDy-PI: A robust algorithm for parallel implicit sparse identification of nonlinear dynamics: SINDy-PI," *Proc. R. Soc. A Math. Phys. Eng. Sci.*, vol. 476, no. 2242, 2020.

[20] N. M. Mangan, S. L. Brunton, J. L. Proctor, and J. N. Kutz, "Inferring Biological Networks by Sparse Identification of Nonlinear Dynamics," *IEEE Trans. Mol. Biol. Multi-Scale Commun.*, vol. 2, no. 1, pp. 52–63, 2016.

[21] L. Boninsegna, F. Nüske, and C. Clementi, "Sparse learning of stochastic dynamical equations," *J. Chem. Phys.*, vol. 148, no. 24, 2018.

[22] H. Akaike, "Information Theory and an Extension of the Maximum Likelihood Principle," *2nd Int. Symp. Inf. Theory*, vol. 90, no. 29, pp. 267–281, 1973.

[23] H. Akaike, "A New Look at the Statistical Model Identification," *IEEE Trans. Automat. Contr.*, vol. 19, no. 6, pp. 716–723, 1974.

[24] L. I. Rudin, S. Osher, and E. Fatemi, "Nonlinear total variation based noise removal algorithms," *Phys. D*, vol. 60, no. 1–4, pp. 259–268, 1992.

[25] S. L. Brunton and J. N. Kutz, *Data Driven Science & Engineering - Machine Learning, Dynamical Systems, and Control*. Lauren Cowles,Cambridge, 2017.

[26] E. Kaiser, J. N. Kutz, and S. L. Brunton, "Sparse identification of nonlinear dynamics for model predictive control in the low-data limit," *Proc. R. Soc. A Math. Phys. Eng. Sci.*, vol. 474, no. 2219, 2018.

[27] H. Zhu, "On Information and Sufficiency," *Ann. Stat.*, pp. 1–5, 1997.

[28] S. Kullback, *Information theory and statistics*. Dover Publications, 1968.

[29] C. M. Hurvich and C. L. Tsai, "Regression and time series model selection in

small samples," *Biometrika*, vol. 76, no. 2, pp. 297–307, 1989.

[30] J. M. Maciejowski, *Predictive Control with Constraints*. Prentice Hall, 2000.

[31] R. H. Bishop, *Model Based Predictive Control-A Practical Approach*. CRC Press LLC, 2005.

[32] K. R. Muske and T. A. Badgwell, "Disturbance modeling for offset-free linear model predictive control," *J. Process Control*, vol. 12, no. 5, pp. 617–632, 2002.

[33] C. V Rao, S. J. Wright, and J. B. Rawlings, "Application of interior-point methods to model predictive control," vol. 99, no. 3, pp. 723–758, 1998.

[34] Y. Cao, "Nonlinear Model Predictive Control Using Automatic Differentiation," *IFAC Proc. Vol.*, vol. 16, pp. 1037–1042, 2005.

[35] R. M. Howard, "Dynamics of Flight: Stability and Control; Third Edition," *J. Guid. Control. Dyn.*, vol. 20, no. 4, pp. 839–840, 1997.

[36] K. Ogata, *Modern Control Engineering*, 4th ed., vol. 39, no. 12. Prentice Hall, New Jersey, 2002.